Metal complexes of organic molecules containing multiple bonds.

by

Andrew Knighton Johnson.

A thesis presented for the degree of

Doctor of Philosophy

in the

University of Aston in Birmingham

November 1974.

Summary.

The kinetics of the rearrangement of benzaldoxime to benzamide, catalysed by nickel acetate tetrahydrate in digol, are reported. The process is exothermic. Apparatus designed to study the rearrangement at a constant temperature and an infrared spectroscopic technique for the detection of benzamide are described.

It is found that the production of benzamide occurs in two, consecutive, psuedo-first order steps. Kinetic isotope studies reveal the first step to involve a nickel dependent cleavage of the carbon-hydrogen bond of benzaldoxime. The second step is observed to be essentially nickel independent and is suggested to be the organic rearrangement of an intermediate, postulated to be a benzimidate. It is thought that benzaldoxime exists in its anti (β) configuration prior to rearrangement. A number of related experiments are cited.

A kinetic investigation of the production of the deep-blue solution (blau), found to arise under certain conditions, in aqueous solutions of potassium tetrachloroplatinite and acetonitrile, is presented. The reaction is accompanied by the release of acid. Apparatus designed to enable the reaction to be studied titratiometrically and spectrophotometrically, at constant pH and temperature is described.

A preliminary study of the ligand substitution reactions of the tetrachloroplatinite(II) ion in this system reveals the normal two-term rate law to be obeyed.

The production of the blau is found to depend upon an initial sequence of substitution reactions of platinum(II), followed by several less clearly defined processes, which are believed to include the oxidation of platinum(II) to

platinum(IV), the hydrolysis of acetonitrile and the chelation of the resultant acetamido anion. The blau is suggested to be dihydroxybis(acetamido)platinum(IV) involved in a set of complex equilibria.

A preliminary investigation of the behaviour of cyanoacetamide towards several transition metal ions is included as an interesting area for further research.

Statement.

The work presented in this thesis was undertaken between 1970 and 1974 at the University of Aston in Birmingham. It has been done independently and has not been submitted for any other degree.

A.K.Johnson.

Acknowledgments.

I wish to express my gratitude to Dr.J.D.Miller for his overall guidance throughout the period of this research.

In addition, I am indebted to the many research students and members of the academic staff within the department, whose stimulating suggestions often proved invaluable.

I should also like to thank Mr.E.J.Hartland for the preparation of the nuclear magnetic resonance spectra, Mr.M.C. Perry for the preparation of the infrared spectra and the members of the Glassblowing Workshop for their patience and skill in the construction of several difficult items of glassware.

Finally, my special thanks are due to the Scientific Research Council for financing this work.

Contents.

Abbreviations.

acen	bisacetylacetone-ethylenediamine
ca.	approximately
DH	dimethylglyoximato
M	molar
n.m.r.	nuclear magnetic resonance
OAc	acetate
OF	formate
Ph	phenyl
P.T.F.E.	polytetrafluoroethylene
R	alkyl
R.T.	room temperature
sh	shoulder

Symbols.

$\Delta H^{\ddagger}$	enthalpy of activation
$\Delta S^{\ddagger}$	entropy of activation
E^{o}	redox potential
μ	ionic strength

Units.

Kinetic and thermodynamic parameters are expressed in units of the calorie. It is noted that 1 calorie = 4.184 joule.

1. Introduction.

The chemistry of organic molecules may be profoundly altered by the presence of metal ions. The coordination of a ligand to a metal ion may result in an entirely new reaction for that ligand. More usually the existing chemical properties of the ligand are subtly modified. However, there exists no 'a priori' means of predicting the precise nature or extent of such changes.

The coordination of a ligand to a positively charged metal ion would be expected to result in a degree of polarization of that ligand. However, the nature of the change in electronic distribution would be anticipated to depend upon the type of coordinate bond involved. If a typical sigma bond is formed, involving the donation of electrons from the ligand to the metal ion, a decrease in the electron density on the ligand might be expected. If however, in addition, pi bonding occurs, involving the donation of electrons from the metal ion to the ligand, the situation will be more complex. The change in the electron density on the ligand will then be determined by the relative importance of these two types of bonding. If pi bonding, of this type, is predominant an increase in the electron density on the ligand may arise.

The polarizing influence of a metal ion upon a ligand would be anticipated to be greatest in the region of the coordinate bond. In the case of small molecules therefore, it is expected that coordination will affect significant changes in the electron density over the majority of the ligand. Indeed, it is found that, given the type of bonding involved, the polarization concept is quite useful in

rationalizing the changes in reactivity of small molecules upon coordination.

Where the coordinate bond primarily involves normal sigma bonding the resultant electron deficiency of the ligand would be anticipated to enhance its electrophilic behaviour. Thus the electrophilic halogenation of aromatic compounds, catalysed by a number of Lewis acids[1], including ferric chloride, may be envisaged to arise as a result of the polarization of the coordinated diatomic halogen molecule, according to the scheme 1.1 for chlorine.

$$FeCl_3 + Cl_2 \rightleftharpoons Cl\text{-}ClFeCl_3 \qquad 1.1$$

The electron deficient chlorine atom, thus produced, is considered to be the reactive species.

A considerable number of reactions involving coordinated alkenes are known[2,3]. An important industrial example of these is the catalytic manufacture of acetaldehyde from ethylene, in the presence of the tetrachloropalladite(II) ion and cupric chloride (Wacker Process). The reactive species is believed to be the complex $PdCl_2(OH)(C_2H_4)^-$ in which the electron deficient ethylene ligand undergoes nucleophilic attack by the adjacent hydroxide ligand[4,5,6]. The bonding of ethylene in the related complex $PtCl_3(C_2H_4)^-$ has been demonstrated to predominantly involve sigma donation[7], consistent with an overall electron deficiency of this ligand.

In those cases where pi bonding, from the metal ion to the ligand, is predominant in the coordinate bond the resultant electron richness of the ligand would be expected to enhance its nucleophilic behaviour. Such a situation often arises with carbon monoxide and is the basis for many

useful organometallic syntheses[8]. Probably the most important of these is the catalytic manufacture of propionaldehyde from ethylene, carbon monoxide and molecular hydrogen, in the presence of cobalt carbonyl (Oxo Process). The mechanisms of these hydroformylation reactions are believed to involve a hydride migration to the coordinated alkene, yielding a coordinated alkyl group, followed by an alkyl migration to a coordinated carbon monoxide ligand[9], illustrated by the scheme 1.2.

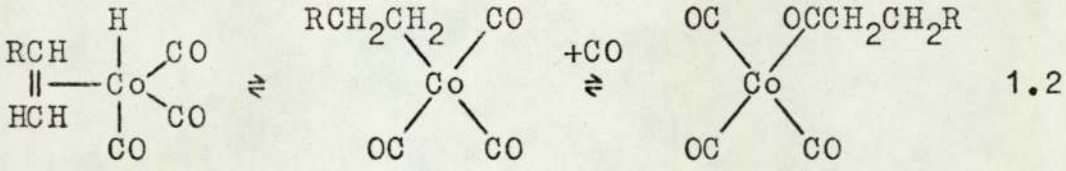

1.2

The result of the coordination of a ligand to a metal ion may not only be to cause a degree of electronic distortion of that ligand and to favour a subsequent reaction. In a great many instances relatively drastic electronic rearrangements within the metal complex may occur. These may be manifested in the disruption of the ligand, the participation of the metal ion and ligand in a redox reaction, or a combination of both.

For instance, the deprotonation of the ligand may arise, illustrated lucidly by the marked increase in acidity of water upon coordination[10]. The electrophilicity of a coordinated ligand is expected to be substantially decreased by deprotonation[11]. In this context the behaviour of molecular hydrogen, notably in the presence of certain transition metal ions occupying the right hand side of each transition series, is of interest. Coordination may result either in the heterolytic cleavage[12,13], or in the oxidative addition[14] of the hydrogen molecule to produce metal hydride

species. The hydride ligand may essentially be envisaged as deprotonated molecular hydrogen and would therefore be anticipated to show nucleophilic behaviour towards coordinated alkenes. In fact a substantial number of metal hydride complexes are observed to catalyse the homogeneous hydrogenation of both alkenes and alkynes[8,9,15,16]. The hydrogenation of other unsaturated groups has also been reported[8,17].

The oxidative addition of certain ligands to several coordinatively unsaturated d^8 complexes represent novel examples of ligand disruption[18]. Possibly the most intriguing of these is that of the decarbonylation of certain aldehydes and acyl halides by the complex $RhCl(PPh_3)_3$ to yield alkanes and alkenes[19], represented in the scheme 1.3.

$$\begin{array}{ccc} & RhCl(PPh_3)_3 & \\ + RCH_2CH_2CHO \swarrow & & \searrow + RCH_2CH_2COCl \\ RhCl(CO)(PPh_3)_2 + RCH_2CH_3 & & RhCl(CO)(PPh_3)_2 + RCH_2{=}CH_2 + HCl \end{array} \qquad 1.3$$

The driving force in these reactions is obtained from the stability of the complex $RhCl(CO)(PPh_3)_2$.

The limiting case of ligand polarization may be considered to arise when an actual electron transfer between the metal ion and the ligand occurs. Examples of such metal ion redox reactions are widespread[20].

If the coordinate bond primarily involves normal sigma bonding an electron transfer from the ligand to the metal ion may arise. The resultant oxidation of the ligand may be catalytic if the presence of molecular oxygen enables the reoxidation of the metal ion to occur. The copper(II) ion is found to be particularly effective in this respect[21,22],

presumably due to the small standard electrode potential, $E^{o}(Cu^{2+}/Cu^{+})$, of ca. -0.19 Volt[23].

If the metal ion favours adduct formation with molecular oxygen, in which the coordinate bond involves a predominant pi contribution, an electron transfer from the metal ion to the oxygen ligand may occur[24]. The superoxide ion, thus generated, can initiate the oxidation of suitable organic molecules more effectively than molecular oxygen itself. Iron(II) and cobalt(II) are often found to activate molecular oxygen in this manner[25]. Such processes are presumably the basis for respiration.

Metal ion-ligand redox reactions often result in the production of free radicals[26]. The decomposition of hydrogen peroxide in the presence of certain metal ions[25,27], leads to the formation of both hydroxyl (·OH) and peroxo ($\cdot O_2H$) radicals which may subsequently initiate a wide variety of free radical reactions in the presence of suitable organic species. One example of such behaviour is that of Fenton's reagent[28] which consists of a trace of iron(II) and hydrogen peroxide. The overall reaction is exhibited in equation 1.4.

$$Fe^{2+} + 2H_2O_2 \longrightarrow Fe^{3+} + O_2H + OH^{-} + H_2O \qquad 1.4$$

The polarization of a ligand by a metal ion is a useful qualitative concept in the consideration of changes in ligand reactivity upon coordination. However, a simple valence bond treatment of the coordinate bond is unrealistic and would be expected to exaggerate the extent of electronic distortion of the ligand.

This is well illustrated by the electrophilic substitution reactions of certain coordinated aromatic ligands in which the

reactive centre is removed from the coordinate bond. For instance, the coordination of aniline to chromium(III) might be predicted to deactivate this ligand towards electrophilic attack at the ortho and para positions on the aromatic ring. However, the bromination of aniline in the presence of chromic chloride produces 2,4,6-tribromoaniline in the normal manner[29]. It is generally found that the coordination of such aromatic ligands to a metal ion does not alter the pattern of electrophilic substitution significantly[30], although some reduction in rate may be expected.

In a great many cases the polarization of a ligand is not the principle basis upon which the facilitation of a subsequent reaction depends. The essential function of the metal ion may be to organize the ligands within its coordination sphere such that a specific reaction is then stereochemically favoured.

Under this heading are the various types of template syntheses. These may involve the combination of two or more ligands within the coordination sphere of the metal ion, illustrated by the numerous examples of oligomerization reactions[8]. For instance, certain nickel complexes may induce the tricyclization of acetylene to yield benzene[31], according to the scheme 1.5.

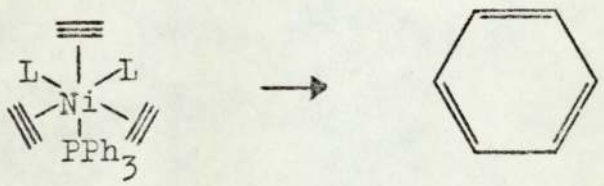

1.5

Alternatively, the addition of suitable external reagents to the coordinated ligands may be accomplished, often to produce large macrocycles[32,33]. The ability of metal ions to

impose particular geometric orientations upon macrocyclic ligands is of distinct relevance to many biological processes[32,34].

The reactivity of complex organic molecules, containing several potential donor atoms, would be anticipated to depend upon their mode of coordination. The decarboxylation of certain γ-carboxyl-β-keto acids is catalysed by the presence of small amounts of suitable metal ions[35], probably according to the scheme 1.6.

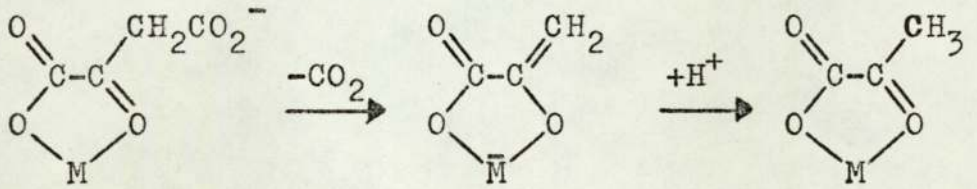

1.6

At high concentration of metal ion the reaction is inhibited, due to the participation of the normally labile carboxyl group in chelation.

The scope of ligand reactivity is enormous and it is not the purpose of this introduction to attempt a comprehensive review of the subject. It is seen that the facilitation of a ligand reaction upon coordination may depend on a number of factors. These include the polarization of the ligand, the stereochemical requirements of the reaction and any electronic rearrangements within the complex. In order to gain a useful understanding of the function of a metal ion in the facilitation of a ligand reaction it is necessary to examine the kinetic and thermodynamic aspects of such processes.

The fundamental changes that allow coordination to influence the kinetic and thermodynamic factors governing a ligand reaction are the variations in the ease of attainment of suitable transition states and the variations in the free

energies of the reactants, intermediates and products. For solution reactions the ease of attainment of the transition state may principally be affected by both alterations in the enthalpy of activation ($\Delta H^{\ddagger}$) and the entropy of activation ($\Delta S^{\ddagger}$). Substantial changes in these quantities will result in measurable differences between the reaction profile for the free ligand and that for the coordinated ligand. Ideally, an interpretation of the mechanistic function of the metal ion requires a knowledge of these differences. Where this is not possible detailed kinetic information upon the reaction of the coordinated ligand is required.

The kinetic studies presented in this thesis are intended to be essentially autonomous. Accordingly, each is assigned a separate chapter, which includes a pertinent literature review as an introduction. Chapter 3 presents an investigation of the nickel(II) catalysed rearrangement of benzaldoxime to benzamide. It is believed that the polarization of the imine bond, by nickel(II), is an important feature of this reaction. Chapter 5 deals with the various processes that arise in aqueous systems of the tetrachloroplatinite(II) ion and acetonitrile. The ultimate product in this system is a platinum(IV) species containing the hydrolysed nitrile ligand. It is thought that the polarization of the nitrile bond, by platinum(IV), facilitates the hydrolysis of acetonitrile and is one important factor in a complex series of processes. In fact, it is the initial processes in this system, concerned with the substitution reactions of platinum(II), that are best understood and form the bulk of chapter 5. In order to gain a thorough understanding of the initial aspects of the overall reaction, an investigation of the substitution reactions of

the tetrachloroplatinite(II) ion in aqueous solution, both in the absence and presence of acetonitrile, was undertaken. This work is reported in chapter 4.

2. Experimentation.

2.1. Physical studies.

Ultraviolet and visible spectroscopy. Solution spectra were recorded on a Pye Unicam SP 1800, used in conjunction with an AR 25 linear recording unit.

Infrared spectroscopy. Solid state spectra were recorded on a Perkin Elmer 457 grating instrument, as either a nujol mull, or more usually a potassium bromide disc. Solution spectra were run on the same model, using a matched pair of Beckmann R.I.C. F-05 detachable cells.

Nuclear magnetic resonance spectroscopy. For general analysis a Perkin Elmer R10 was employed. High resolution and variable temperature studies were undertaken with a Varian HA 100D.

Mass spectroscopy. An A.E.I. MS9 was employed.

Elemental analysis. All samples were submitted to Dr.F.B. Strauss (Microanalytical Laboratory, 10, Carlton Road, Oxford OX2 7SA.) or Alfred Bernhardt (Mikroanalytisches Laboratorium, 5251 Elbach uber Engelskirchen, Fritz-Pregl-Straße 14-16, West Germany.).

Differential scanning calorimetry. Undertaken by RAPRA (Shawbury, Shrewsbury SY4 4NR.).

Melting point apparatus. All melting points were determined with a Gallenkamp MF-370 and are uncorrected.

Computation. Unless otherwise stated all computer programs were written in algol and run on an I.C.L. 1905A computer at the Computer Centre, University of Aston, Gosta Green, Birmingham B4 7ET. George 3 job presentation was used.

2.2. Experimental techniques.

2.2.1. The nickel(II) catalysed Beckmann rearrangement.

2.2.1.1. Apparatus.

The apparatus was designed to enable a kinetic study of the strongly exothermic, nickel(II) catalysed, isomerization of benzaldoxime to benzamide to be undertaken at a constant temperature. It is constructed of glass and shown in figure 2.1. diagramatically.

The cylindrical inner vessel V, which contains a suitable solvent, is serviced by a ground glass conical joint G_1 (B19). The surrounding outer jacket J, which holds the solution under study, is serviced by three ground glass conical joints G_2 (B14), G_3 and G_4 (both B10). G_4 holds a thermometer and G_3 provides a sampling outlet through a suitable suba seal. G_1 and G_2 are fitted with appropriate water condensers. The operating capacity of J is ca. 200mls. and the contents are stirred magnetically.

The entire apparatus is clamped in the thermostatted silicone oil bath assembly shown diagramatically in figure 2.2.

The vacuum flask F, containing the silicone oil, is mounted securely on a specially constructed scaffolding. Thermostatting of the flask contents is achieved by the hot wire relay R, coupled to a mercury contact thermometer T and a heating element E. The motor M_1 drives a stirrer S and ensures efficient stirring of the oil. A magnetic stirring assembly is provided by the motor M_2 and a horseshoe magnet H, positioned under the flask. The operator is protected from hot oil splashes by a sliding perspex shield, fitted to the scaffolding.

Under run conditions, described in section 2.2.1.2., the

oil bath is set to a temperature slightly above the boiling point of the solvent in the inner vessel, which is observed to reflux gently. Thus the reaction solution, in the jacket, makes good thermal contact with an effective heat sink and local temperature variations, due to the exothermic reaction, are quickly dissipated. To maximize the efficiency of the apparatus it is designed such that the jacket thickness is as small as possible (ca. 1cm.).

The system is found to operate satisfactorily in practice and enables the temperature of the reaction solution to be held to within $\pm 0.25^{\circ}C$.

2.2.1.2. Procedure.

The oil bath is brought up to temperature with mechanical stirring, which must be continually adjusted as the oil thins to avoid splashing.

200mls. of a solution of α-benzaldoxime in purified 2,2'-dihydroxydiethylether (digol) is made up to the required concentration and transferred to the jacket. A suitable solvent is introduced into the inner vessel to the same level as that of the reaction solution. The services are fitted to the apparatus, which is immersed centrally in the oil bath. The jacket contents are magnetically stirred and after ca. 20mins. the inner solvent is seen to reflux gently. A known quantity of finely ground catalyst is weighed into a small glass receptacle, which is then introduced into the jacket solution, thus initiating the run.

After each run, the jacket, receptacle and magnetic follower (P.T.F.E.) are cleaned with chromic acid.

It is found in practice that for a given inner solvent of boiling point T_s, the temperature of study may be varied

over the range T_s to ca. T_s + 12°C, by suitably adjusting the temperature of the oil bath. Thus it is possible to study the rearrangement at six different temperatures using only four solvents, according to table 2.1.

Table 2.1.

Reaction temp.(°C)	Inner solvent in V	B.pt.(°C)
160.5	Isopropylbenzene	152.4
168.5	1,3,5-trimethylbenzene	164.7
176.5	"	
184.0	1,2-dichlorobenzene	180.5
191.5	"	
200.0	Decahydronaphthalene	195.7

Digol was chosen as the reaction medium for the reasons discussed in section 3.2.2. and initially was redistilled before use[36]. However, since this treatment appeared to have no significant effect upon the reproducibility of a particular run it was abandoned and the solvent used as supplied (section 2.2.1.4.).

2.2.1.3. Sampling and detection.

Immediately prior to the introduction of the catalyst a small aliquot (ca. 0.5ml.) is taken from the reaction solution with a 2ml. syringe and 20cm. needle inserted through the suba seal in G_3 (figure 2.1.). After the addition of catalyst further aliquots are removed at suitable intervals of time. Aliquots are quickly quenched by transference to clean semi-micro test tubes, which are immediately corked to avoid possible contamination. After each sample is taken the syringe and needle are washed with ethanol and ether. Acetone is avoided since traces could interfere with the subsequent

infrared analysis of the aliquots.

In the early runs the syringe needle was left in the reaction solution as a permanent sampling outlet. However, spectroscopic analysis of the solution revealed the presence of benzamide, in significant quantity, prior to the addition of catalyst. It was subsequently discovered that the stainless steel needle catalysed the rearrangement, a fact probably due to its nickel content, since iron appears to have no catalytic effect upon the reaction[65].

The detection of benzamide is accomplished by infrared spectroscopy. A pair of matched solution cells, of path length 0.05cm., are used. Since digol is hygroscopic these are constructed with silver chloride windows. All liquids are introduced into the cells with a 2ml. syringe, taking care to avoid the inclusion of air bubbles, which affect the absorbance reading. Spectra of samples are run against a solvent reference, over the region between $2000cm^{-1}$. and $1500cm^{-1}$., to ensure a good baseline. Initially the spectrometer is zeroed with nothing in either beam. A standard 0.1M solution of benzamide in digol is run and the spectrometer gain adjusted, if necessary, until the absorbance at $1675cm^{-1}$., corrected for baseline, corresponds to the value obtained from the calibration graph shown in figure 3.2. (chapter 3). The initial aliquot is run to confirm that no absorbing species are present prior to the introdution of catalyst. Subsequently all aliquots are run. After each analysis the syringe and sample cell are flushed through with ethanol and ether and dried in a stream of warm, dry nitrogen gas. All spectra are recorded on absorbance paper. The peak height and baseline are read directly unless the former is greater than 0.6, in which case the $\log_{10}$ of the

transmittance is evaluated.

The cells are kept in a sealed container and used in a darkened room to reduce the photosensitized decomposition of the silver chloride windows. Periodically they are dismantled, cleaned thoroughly with water, ethanol and ether, reassembled and rematched. At no stage were the cell windows reground, due to the difficulty experienced in the grinding of silver chloride plates, which can often lead to surface damage and severe darkening.

2.2.1.4. Equipment.

Spectrometer. Perkin Elmer grating infrared; model 457. Used on a medium scan mode and with a normal slit width.

Solution cells. Beckmann R.I.C. F-05.

Vacuum flask. Day Impax (Dilvac). Constructed to order from pyrex; diameter ca. 20cm.; depth ca. 20cm.

Relay. A.E.I. Sunvic hot wire; type H.V.R.

Contact thermometer. Gallenkamp; mercury filled; cat. no. TM-480; $0^{\circ}C$ to $200^{\circ}C$.

Heating element. Bray; model no. EH165791; 500 Watts.

Stirrer motors. Kestner; model no. B4840/41. (M_1).
Pickstone. (M_2).

Silicone oil. Hopkin and Williams; type MS200/100cs.

Digol. B.D.H. purified; boiling range $241^{\circ}C$ to $248^{\circ}C$.

Figure 2.1.

Reaction vessel used in the study of the nickel(II) catalysed rearrangement of benzaldoxime to benzamide (side view)

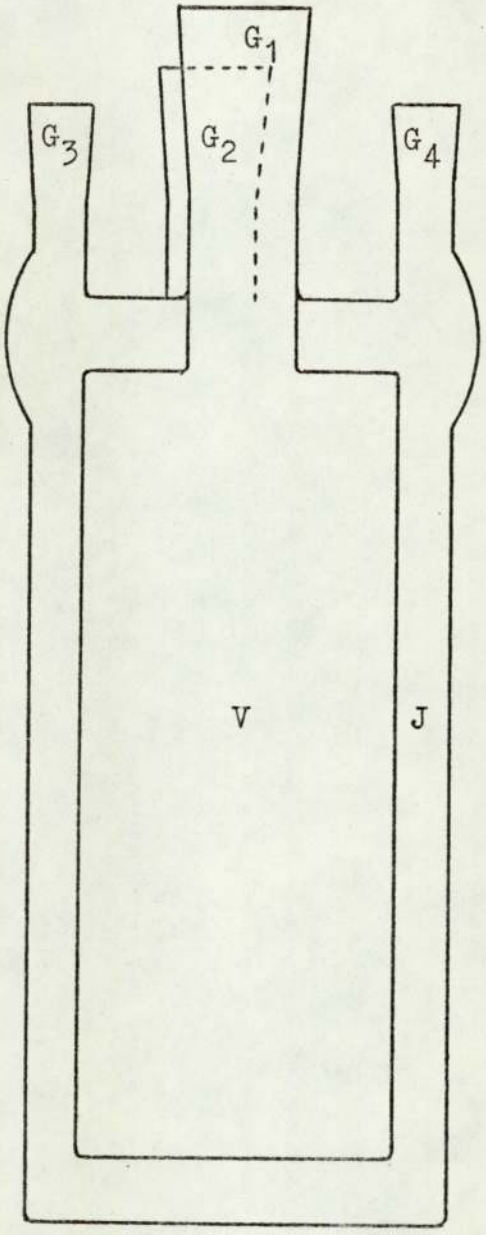

Figure 2.2.

Oil bath assembly used in the study of the nickel(II) catalysed rearrangement of benzaldoxime to benzamide (side view)

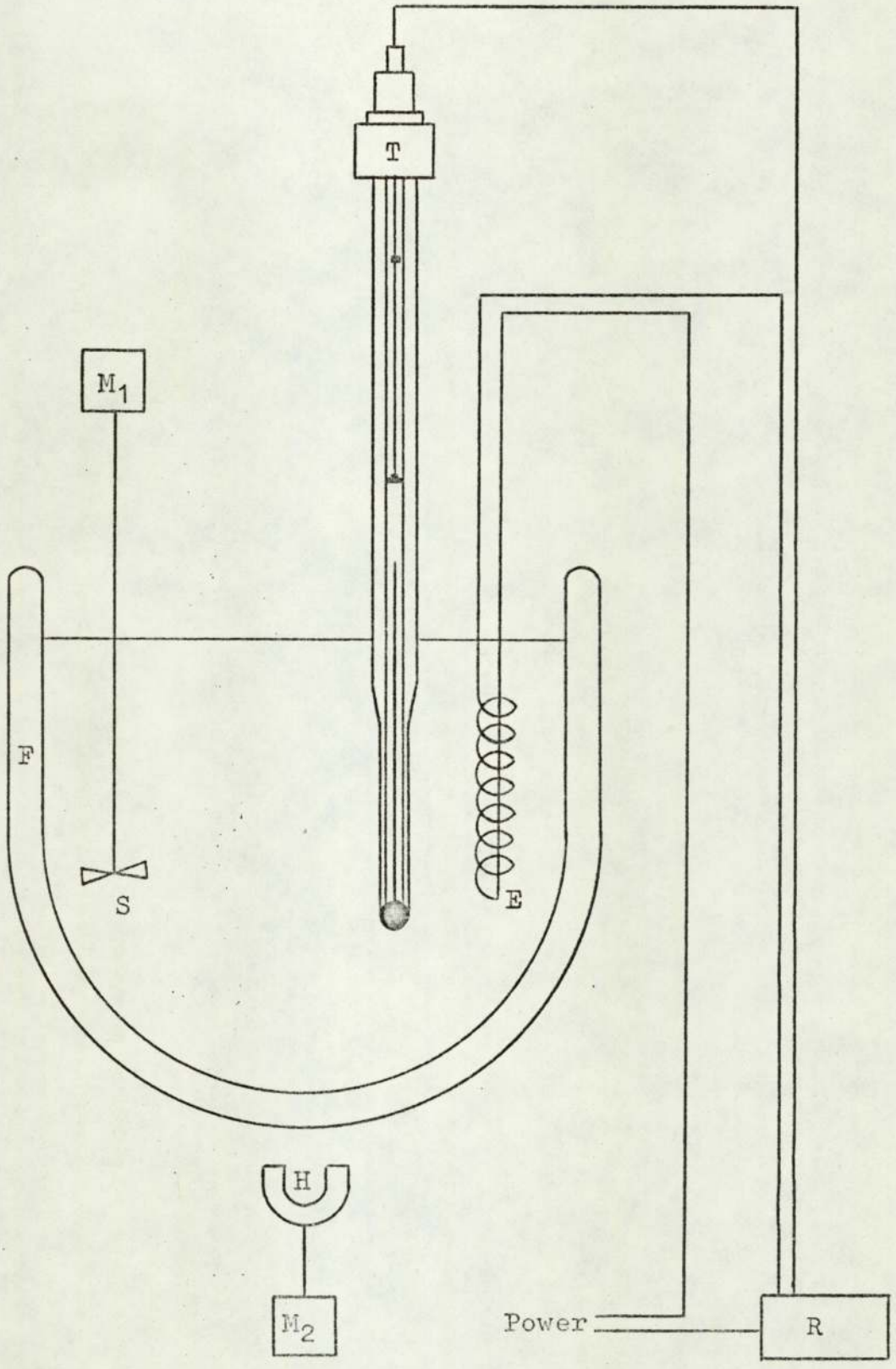

2.2.2. Aqueous systems of potassium tetrachloroplatinite and acetonitrile.

The blue solution produced under the appropriate conditions in these systems will be referred to as the blau. Evidence for the nature of this material was obtained both from the kinetic investigation of its production and from a variety of physical studies performed on solid products isolated from solution. This will be cited in subsequent sections.

Two different methods were employed to enable the production of the blau to be followed spectrophotometrically at constant pH. The first technique, described in section 2.2.2.1., was found to be unsatisfactory for the reasons outlined in section 5.2.3. (chapter 5). However, it is included since it provided a basis from which the technique, described in section 2.2.2.2., was developed.

2.2.2.1. Method involving the use of buffers.

The reaction is followed in a 4ml. sample cell situated in the thermostatted cell housing of the spectrophotometer. Thermostatting is achieved by means of a constant temperature bath and a circulating pump.

Standard solutions of potassium dihydrogen phosphate (0.3M) and sodium hydroxide (0.3M) are made up. The necessary quantities of buffer and base are mixed to attain the required pH. The solution is then halved. One half is diluted by a factor of three with distilled water and the other is similarly treated with acetonitrile and distilled water to produce a solution that is 1.0M in acetonitrile. These two solutions may now be mixed to produce a reaction solution of the required acetonitrile concentration. 2.9mls. of such a

solution is transferred to both the sample and reference cells, positioned in the cell housing. The cell contents are brought up to temperature (ca. 15mins.). The spectrophotometer is zeroed at the required wavelength and set for a fixed wavelength run[37]. 0.1ml. of distilled water is added to the reference cell, with a micrometer screw syringe assembly, and 0.1ml. of a fresh solution of potassium tetrachloroplatinite is similarly introduced into the sample cell, thus initiating the run. The buffer is able to withstand the ca. 3% volume change involved in this procedure.

The reaction involves molecular oxygen and calculations revealed that for a solution volume of 3mls. there is sufficient atmospheric oxygen present to ensure complete oxidation of platinum(II) to platinum(IV), for concentrations of potassium tetrachloroplatinite of up to 0.001M. Thus evaporation of acetonitrile and solvent can be minimized by stoppering the cells.

2.2.2.2. Method incorporating the use of the autotitrator.

2.2.2.2.1. Apparatus.

The system developed to meet the requirements discussed in section 5.2.3. is shown schematically in figure 2.3.

The pH of the solution is monitered by the pH meter M, used in conjunction with glass and saturated potassium chloride electrodes. The pH meter is coupled to an autotitrator controller A, which operates a delivery unit D, holding a suitable burette filled with an appropriate solution of potassium hydroxide.

Spectrophotometric studies are undertaken by circulating the reaction solution through a silica flow cell Q, with a peristaltic pump P_2. Silicone rubber tubing is used with the

pump and is kept well lubricated with silicone oil. The flow circuit is completed with polypropylene tubing and two narrow glass tubes immersed in the solution. The spectrophotometer is operated on a fixed wavelength scan and drives a suitable recording unit.

The reaction vessel W is made of glass and shown diagramatically in figure 2.4. The cylindrical inner vessel U, which holds the solution under study, is serviced by four conical joints C_1, C_2, C_3, and C_4. C_1 is designed to fit a rubber bung (size 31), which holds the electrodes in position in the solution. C_2 is made to fit another bung (size 23), which contains the tubes of the peristaltic flow circuit and a mercury thermometer. C_3 is a C14 ground glass joint and provides an inlet for the burette of the delivery unit, whilst C_4 holds a B14 condenser. The operating capacity of U is ca. 200mls. and the contents are stirred magnetically. Under run conditions the ratio of the solution volume to the vessel volume is high. This helps to minimize loss of solvent and acetonitrile.

The vessel and flow cell contents are kept at constant temperature by pumping water from a thermostatted water bath B, with a circulating pump P_1, through the surrounding jacket K and the cell housing H respectively. A calibration graph of bath temperature against solution temperature is not shown since it was established that several factors influence this relationship. These are, the circulating pump speed, the peristaltic pump speed and the magnetic stirring speed.

2.2.2.2.2. Procedure.

The experimental technique is essentially the same for all the kinetic studies mentioned in section 2.2.2.2.4.

Therefore a generalized procedure is described below. Wherever specific differences arise they are mentioned in the relevant section.

The thermostatting assembly is switched on. The burette is washed through with potassium hydroxide solution and filled. The peristaltic flow circuit is flushed through with distilled water and the silicone tubing relubricated. The fixed wavelength run mode is selected on the spectrophotometer[37]. The pH meter is calibrated with a suitable buffer. The required volume of distilled water is introduced into the vessel and the electrodes and all other services fitted. The appropriate volumes of acetonitrile solution (1.0M) and lithium perchlorate solution (1.0M), to maintain the ionic strength, are added. The pH of the solution is adjusted to the required value by suitable addition of perchloric acid or potassium hydroxide and the autotitrator set to this on the 'standby' mode. The burette is zeroed. The spectrophotometer is zeroed with solvent in a silica reference cell. The vessel contents are brought up to temperature. Once a steady temperature is attained 2mls. of a freshly prepared solution of potassium tetrachloroplatinite are pipetted into the vessel, such that the final volume is 200mls. Immediately the autotitrator is set to the 'run' mode and the fixed wavelength scan started on the spectrophotometer, thus initiating the run.

The vessel and flow cell are regularly cleaned with chromic acid. Periodically the silicone rubber and polypropylene tubing are replaced.

2.2.2.2.3. Further considerations.

In the use of the autotitrator controller assembly, to keep the pH constant, two competing factors are of importance

in determining the concentration of base added. Firstly, the addition of one drop of base to the reaction solution should not alter the pH drastically. Secondly, the total volume of base added should be a small percentage of the total solution volume.

It was decided that a 5% volume change was the maximum which could be tolerated over the complete reaction. Thus the concentration of base added is dependent on the starting concentration of potassium tetrachloroplatinite. In the work with the blau this is 0.0004M, for which a base concentration of 0.02M is found to be satisfactory.

2.2.2.2.4. Scope of the method.

The system was primarily designed to investigate the kinetics of the production of the blau spectrophotometrically. However, it is also suitable for spectrophotometric studies of the kinetics of the ligand substitution reactions of the tetrachloroplatinite(II) ion in aqueous solution, both in the presence and absence of acetonitrile. Furthermore, since the system incorporates an autotitrator assembly it is possible to follow the kinetics of acid release, in those reactions in which this occurs. In the former investigation this proved to be of considerable importance.

2.2.2.2.5. Equipment.

Spectrophotometer. Pye Unicam SP 1800. Used with an AR 25 linear recording unit.

pH meter. E.I.L. direct reading; model 23A. Used with a glass electrode; type G.H.S. 23.

pH control. Pye autotitrator controller; cat. no. 11603. Used with a solenoid operated delivery unit on the slow channel, incorporating a 10ml. burette, calibrated in 0.02ml. divisions.

Peristaltic pump. Watson Marlow H.R. flow inducer; type H.R.E.; serial no. 12328.

Thermostat bath. Townson Mercer; mercury contact control; cat. no. X27; serial no. 711040.

Circulating pump. Stuart Turner; model no. 12CT 68182. Used with variac control.

Magnetic stirrer. Baird Tatlock; model no. Y136562/204.

Figure 2.3.

Apparatus used in the study of aqueous systems of the tetrachloroplatinite(II) ion and acetonitrile (schematic).

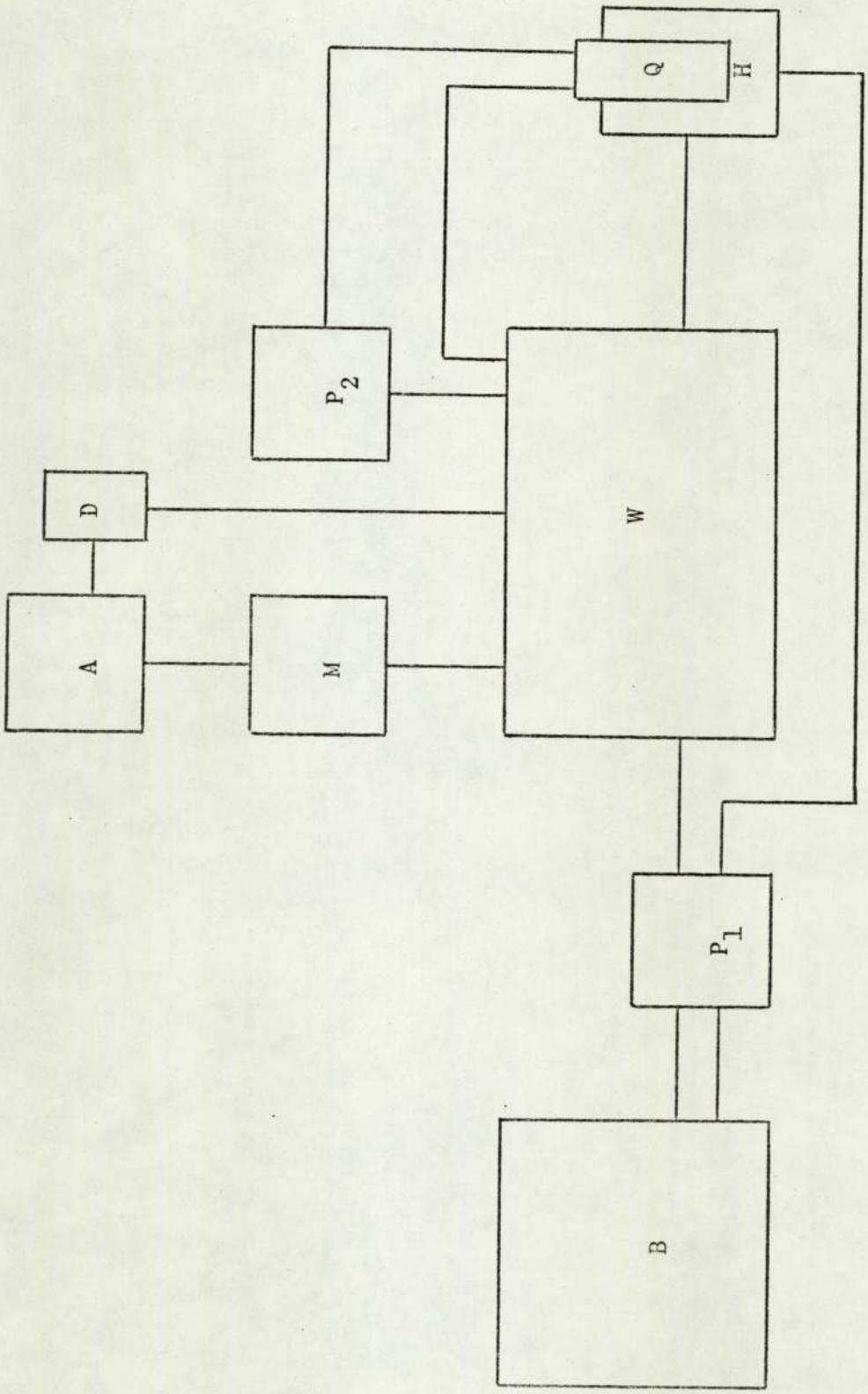

Figure 2.4.

Reaction vessel used in the study of aqueous systems of the tetrachloroplatinite(II) ion and acetonitrile (side view).

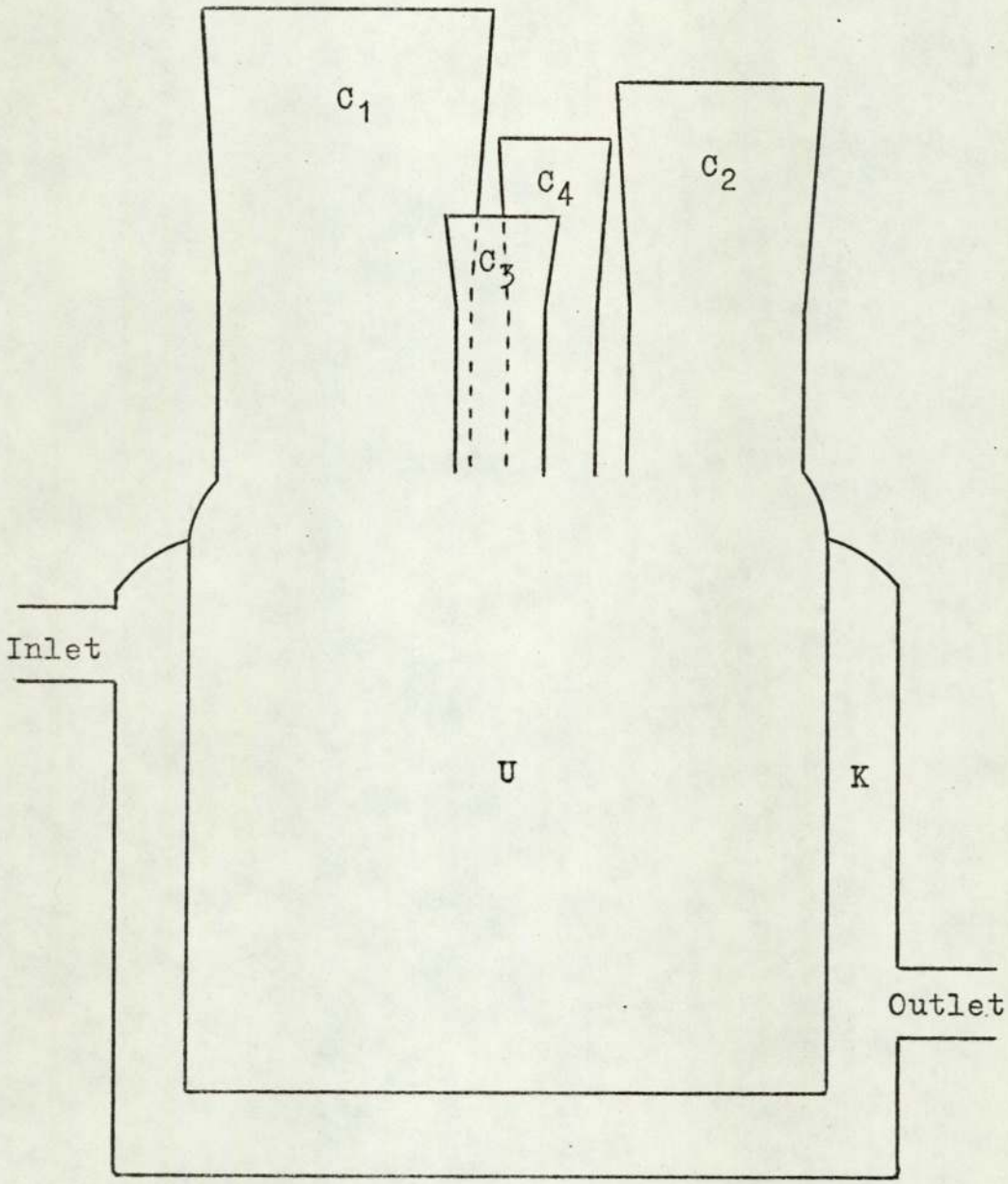

2.3. Preparation of compounds.

2.3.1. α-benzaldoxime.

Attempts to employ the method of Pearson and Bruton for ketoximes[38] were largely unsuccessful.

A method, concerned principally with the bulk production of α-benzaldoxime, was developed from that described by Vogel[39] and is presented below.

To a solution of 56gms. of sodium hydroxide in 160mls. of distilled water, contained in a 1litre conical flask, 80mls. of reagent grade benzaldehyde is added slowly, whilst cooling in an external ice bath. To this mixture either 60gms. of hydroxylamine hydrogen chloride or 70gms. of hydroxylamine hydrogen sulphate is added in small portions, such that the temperature is kept below 10°C, and with frequent vigorous shaking. During this process a solid may form, however, ultimately a homogeneous solution is produced. This is left to stand in the ice bath whereupon a solid, crystalline mass of the sodium salt of the oxime gradually separates out. The solid is transferred to a 2litre beaker and stirred vigorously with ca. 750mls. of distilled water until a white, translucent, alkaline solution is produced. Small lumps of solid carbon dioxide are then added, to liberate the oxime from its sodium salt, until the solution becomes colourless. The crude oxime is filtered on a suitable buchner at the pump, washed with several aliquots of cold, distilled water and then dissolved in ca. 75mls. of diethylether. The ethereal solution is transferred to a separating funnel, shaken over the minimum necessary quantity of anhydrous magnesium sulphate powder to remove traces of water and then filtered to remove any residual salts. The ether is removed on a steam bath to produce a light

brown, viscous oil, which is then vacuum distilled at 12mm. pressure. The colourless fraction, boiling at 123°C, is collected. Upon cooling this forms a solid, crystalline mass of α-benzaldoxime.

Analysis for C_6H_5CHNOH.

Found	C69.7%	H5.6%	N11.4%.
Calculated	C69.4%	H5.8%	N11.6%.

The advantage of using solid carbon dioxide in this synthesis is twofold. Firstly, it is a convenient source of the gas and secondly, it lowers the temperature of the solution such that the low melting α-benzaldoxime precipitates out as an easily manageable solid.

Both p-methoxy-α-benzaldoxime and p-nitro-α-benzaldoxime are prepared, from their respective aldehydes, by this method. However, purification is achieved by recrystallization. p-methoxy-α-benzaldoxime is thus isolated from cyclohexane as long, white needles, of melting point 131-133°C (reported[40a] 133°C) and p-nitro-α-benzaldoxime from benzene as long, buff needles, of melting point 180-183°C (reported[40b] 182-184°C).

2.3.2. Deuterated α-benzaldoxime.

The synthesis is a multi-stage process. Firstly, the ylide benzal-bis-pyridiniumbromide is prepared[41]. This is then hydrolysed in deuterium oxide to produce deuterated benzaldehyde[42] (C_6H_5CDO). The aldehyde is then subjected to a modified procedure, based on that of section 2.3.1., to yield the deuterated oxime (C_6H_5CDNOH).

The method was developed in order to obtain the maximum yield of product. Therefore purification of intermediate compounds is not attempted. The procedure is outlined below.

20gms. of benzalbromide and 15mls. of pyridine are warmed

on a steam bath, in a 250ml. round bottomed flask equipped with a water condenser, for ca. 1hr. The resultant deep red, crystalline mass of benzal-bis-pyridiniumbromide is filtered on a suitable buchner at the pump, washed with several aliquots of diethylether and vacuum dried overnight. The salt is then dissolved in the minimum of suitably buffered deuterium oxide[42] and left to stand overnight. The solution is then refluxed for ca. 3hrs. and the liberated pyridine neutrilized by acidification with hydrobromic acid. The deuterated aldehyde is steam distilled, extracted with diethylether and the ethereal solution dried over the minimum of anhydrous calcium sulphate powder. The solution is filtered and the ether removed on a steam bath, leaving ca. 15mls. of deuterated benzaldehyde (yield ca. 55%).

The aldehyde is treated in the manner described in section 2.3.1. except that initially it is added to the required volume of distilled water and cooled in an external ice/sodium chloride bath to ca. -5°C, without the addition of sodium hydroxide. Subsequently ca. 10% of the total sodium hydroxide is introduced, quickly followed by a similar quantity of the hydroxylamine salt, with vigorous shaking. This process is reiterated slowly, keeping the temperature at ca. -5°C, until all of the reagents are added. In order to maximize the yield of product an ether extraction is performed on the aqueous phase, after the addition of solid carbon dioxide and filtration. All ethereal solutions are combined and the oxime purified as before.

The n.m.r. spectrum of this material is compared to that of α-benzaldoxime in figure 2.5. The C-H resonance is seen to be considerably reduced. Integration of the spectrum enables

the extent of isotopic substitution to be estimated as 60%. This is probably accurate to within a few percent. The i.r. spectrum shows an absorption at 2205cm^{-1}., assignable to the C-D stretch.

2.3.3. β-benzaldoxime.

This compound was prepared, from its α-isomer, by the method of Vogel[39]. Melting point 128.5-130°C (reported[39] 130°C)

2.3.4. Benzimidates.

Benzimidates may be prepared, as the hydrogen chloride salt, by a number of methods[43,44].

The synthesis of alkylbenzimidate hydrogen chloride salts may be accomplished by the action of dry hydrogen chloride gas upon benzonitrile and a suitable alcohol, under stringent anhydrous conditions. All reagents are therefore thoroughly dried before use. Digol is redistilled from a suspension containing calcium oxide. 2-methoxyethanol and benzonitrile are kept over oven dried (100°C) molecular sieve (type 5A).

Equimolar proportions of benzonitrile (25mls.) and digol (23mls.) or 2-methoxyethanol (20mls.) are mixed in a 250ml. round bottomed flask. The mixture is cooled in an ice/sodium chloride bath and dry hydrogen chloride gas bubbled gently through for ca. 20mins. The flask is stoppered, fitted with a drying tube containing fresh, anhydrous calcium chloride grains and the contents allowed to stand. After several days a white, solid mass develops. This is dissolved in the minimum of absolute ethanol, filtered and dry diethylether added to the filtrate. The hydrogen chloride salt of the benzimidate separates out as a white precipitate and is filtered on a buchner at the pump, washed with dry ether and kept under a vacuum over silica gel.

Analysis for $C_6H_5C(NH_2Cl)OCH_2CH_2OCH_2CH_2OH$.

Found	C53.7%	H6.0%	N7.4%	Cl19.6%.
Calculated	C53.8%	H6.5%	N5.7%	Cl14.4%.

The high nitrogen and chlorine content of this sample is probably indicative of some disubstitution, due to the possession of two alcoholic groups by digol.

Analysis for $C_6H_5C(NH_2Cl)OCH_2CH_2OCH_3$.

Found	C54.8%	H6.5%	N6.8%	Cl16.7%.
Calculated	C55.7%	H6.5%	N6.5%	Cl16.5%.

2.3.5. Nickel complexes.

Complexes of the general formula NiL_4X_2, where L is benzaldoxime or p-methoxybenzaldoxime and X is chloride or iodide, were prepared. Attempts to synthesize the analogous p-nitrobenzaldoxime complexes were unsuccessful.

The method of Heiber and Leutart[45,46] may be followed with slight modification. For the recrystallization of iodide complexes a mixed solvent system, equal volumes of chloroform and cyclohexane, is found to be superior to pure chloroform.

An alternative preparation may also be employed. The appropriate nickel halide is gently heated with ca. a 20:1 molar excess of the ligand, in an open dish, until a viscous homogeneous solution is produced. Care must be taken since vigorous heating will cause a rapid exothermic reaction to occur, undoubtedly the nickel catalysed rearrangement of the oxime to the amide. Thus continual stirring with a glass rod is necessary. The solution is poured into a large excess of equal volumes of diethylether and cyclohexane and left to stand. Crystalline products usually separate out overnight and are filtered on a number 4 sinter at the pump, washed with ether and vacuum dried.

Analysis for $Ni(C_6H_5CHNOH)_4Cl_2$.

Found C55.4% H5.2% N9.3%.

Calculated C54.7% H4.6% N9.1%.

Analysis for $Ni(C_6H_5CHNOH)_4I_2$.

Found C42.1% H3.6% N7.0%.

Calculated C42.2% H3.5% N7.0%.

Analysis for $Ni(CH_3OC_6H_4CHNOH)_4Cl_2$.

Found C49.9% H5.0% N7.2%.

Calculated C52.3% H4.9% N7.6%.

Analysis for $Ni(CH_3OC_6H_4CHNOH)_4I_2$.

Found C42.5% H4.1% N6.4%.

Calculated C41.9% H3.9% N6.1%.

The melting point characteristics of these complexes are unusual and consequently they were subjected to a differential scanning calorimetric analysis the results of which are reported in section 6.1. (chapter 6).

The complexes dichlorobis(triphenylphosphine)nickel(II) of decomposition point 245-248°C (reported 247-250°C) and diiodobis(triphenylphosphine)nickel(II) of decomposition point 218-222°C (reported 218-220°C) were prepared according to the method of Venanzi[47].

Bis(dimethylglyoximato)nickel(II) was prepared in the manner usual for gravimetric analysis[48]. Decomposition point 245-247°C (reported[49] 248°C).

(Bisacetylacetone-ethylenediamine)nickel(II) was prepared by the method of McCarthy et al[50]. Melting point 193-196°C (reported 195-196°C).

2.3.6. Platinum complexes.

Cis-dichlorobis(triphenylphosphine)platinum(II) was prepared by the method of Malatesta et al[51]. The corresponding

palladium complex was prepared in an identical fashion.

Cis-dichlorobis(acetonitrile)platinum(II) was prepared along the general lines described by Golovnya et al[52].

Dichlorobis(acetamido)platinum(IV) was prepared by the method of Brown et al[53].

Dihydroxybis(acetamido)platinum(IV) was synthesized in solution by treating an aqueous suspension of cis-dichlorobis(acetonitrile)platinum(II) with an excess of silver nitrate[54].

Solutions of the blau were produced using the apparatus described in section 2.2.2.2. at concentrations of 0.0004M in potassium tetrachloroplatinite and 0.1M in acetonitrile and pH 7. Usually several duplicate reaction solutions were combined and solid products isolated by the following method.

Solvent is removed from the bulk solution by rotary evaporation under reduced pressure until ca. 1% remains. About 20mls. of ethanol is added and any undissolved solids removed by filtration. To the filtrate is added ca. 500mls. of diethylether whereupon a blue precipitate develops. The suspension is allowed to stand and the excess solvent decanted off. The remainder is slowly filtered at the pump on a number 4 sinter. The dark blue precipitate is washed with several aliquots of diethylether and dried in a vacuum desiccator over silica gel.

Elemental analysis of this material demonstrated the retention of potassium chloride and probably ethanol as well. A tentative formulation is given below.

Analysis for $Pt(CH_3CONH)_2(OH)_2.CH_3CH_2OH.K_{9.9}Cl_{8.9}$.

Found C6.5% H0.9% N2.5% K35.4% Cl29.3% Pt18.0%.

Calculated C6.6% H1.4% N2.6% K35.4% Cl28.9% Pt17.9%.

A discussion of the nature of the species in dilute solution is deferred until section 5.4.5.

Figure 2.5.

Comparison of the n.m.r. spectra of α-benzaldoxime and deuterated α-benzaldoxime (in carbon tetrachloride).

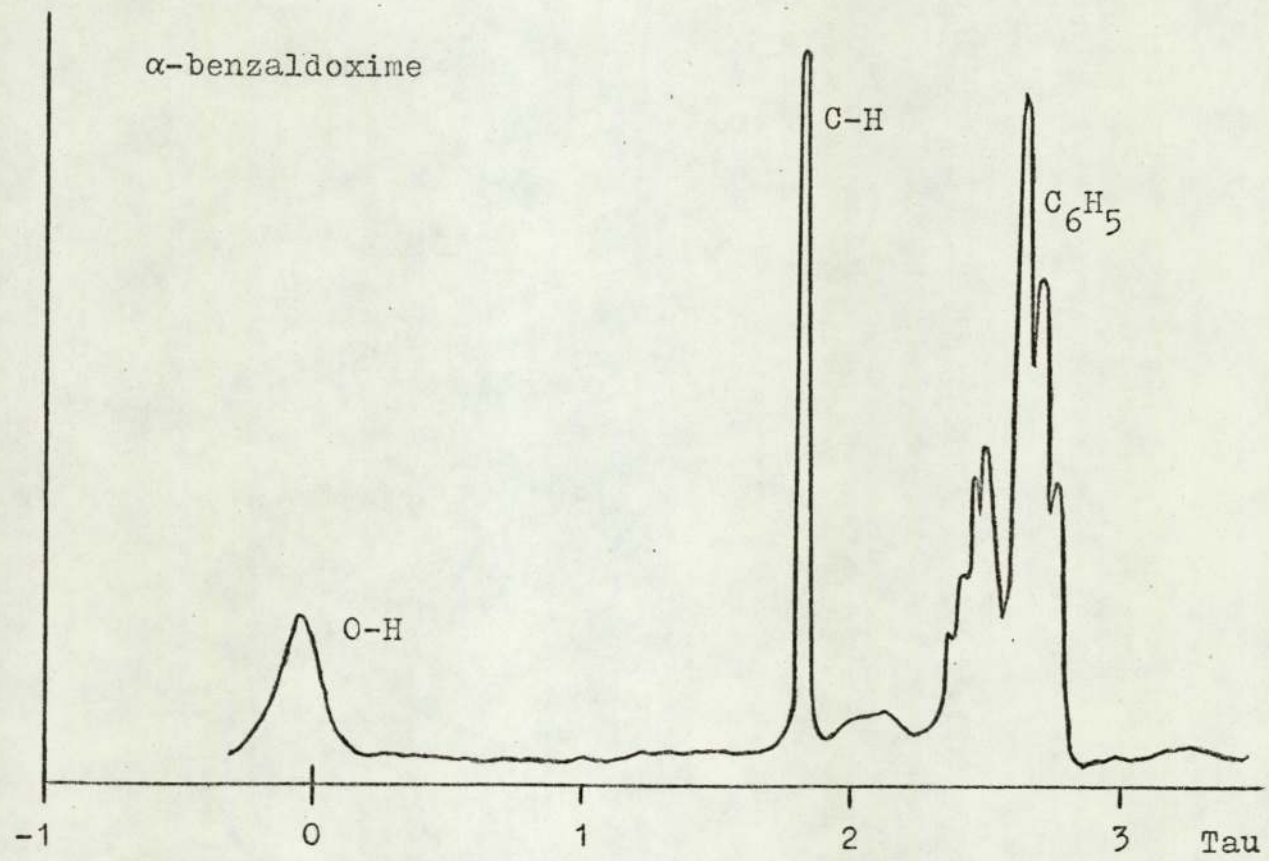

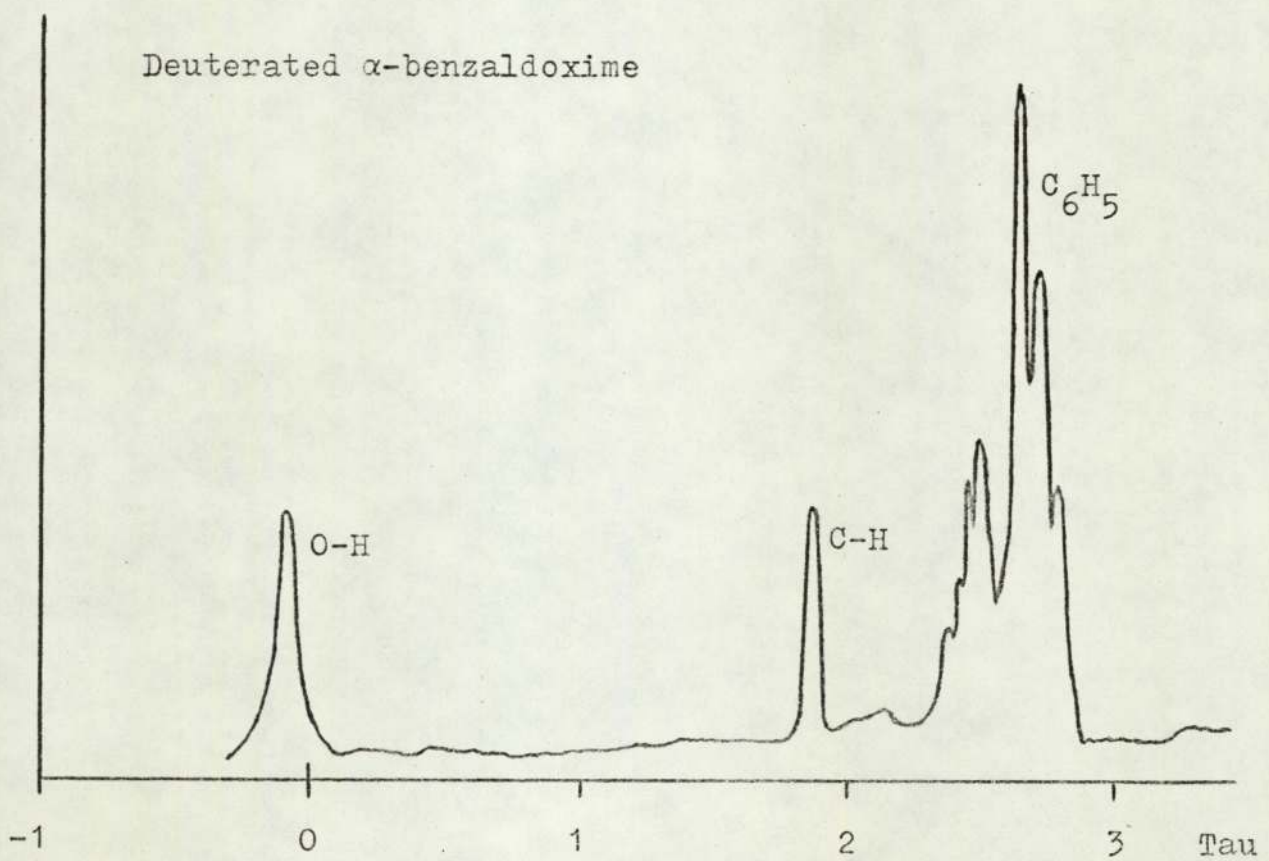

3. An investigation of the nickel(II) catalysed rearrangement of benzaldoxime to benzamide.

3.1. Introduction.

The Beckmann rearrangement of ketoximes (I) to N-substituted amides (II) is probably the most familiar example of that class of organic reactions in which an alkyl or aryl group migrates from a carbon atom to an electron deficient nitrogen atom[55,56].

The rearrangement is effected by a variety of acidic reagents including sulphuric acid, phosphorous pentoxide, sulphur trioxide and phosphorous pentachloride, although milder conditions are usually required for the rearrangement of aldoximes[57].

The conversion is believed to involve the migration of that group trans to the hydroxide group of the oxime, as shown by the scheme 3.1.

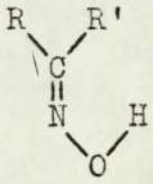

I

II

3.1.

Furthermore, isotopic exchange studies[55], in $H_2{}^{18}O$, have revealed that a direct interchange of the alkyl and hydroxide groups does not take place, and that the carbonyl oxygen of the amide is derived from the solvent medium.

The rearrangement of both ketoximes and aldoximes to amides, in the presence of metals or metal salts, is well established.

As early as 1897 Comstock[58] observed that the heating of benzaldoxime with cuprous chloride, in benzene or toluene,

produced benzamide, although breakdown to benzaldehyde often occurred.

Yamaguchi[59,60] undertook the hydrogenation of both ketoximes and aldoximes, on a reduced copper catalyst, at elevated temperature (ca. 200°C) and discovered amides to be present amongst other products.

The heterogeneous hydrogenation of four aldoximes was also attempted by Paul[61,62], using raney nickel as a catalyst. Amides were produced in quite high yields, although ketoximes were found to undergo hydrogenation.

Later Paul, Buisson and Joseph[63] developed a nickel-boron catalyst for hydrogenation, which was superior to raney nickel to fatigue, however, again they noted its ability to isomerize 2-furancarboxaldoxime to 2-furancarboxamide in high yield, even at room temperature.

The initial method of Paul[61] was employed by Caldwell and Jones[64] for the isomerization of the oximes of tetrahydrocitral, citronellal and citral. Although primarily interested in the use of the catalyst for the synthesis of the previously uncharacterized amides of these compounds, they remarked that the ethylinic linkage appeared to have a deleterious effect upon the function of the catalyst, since the reaction occurred quite satisfactorily with the oxime of tetrahydrocitral (yield of amide ca. 70%), moderately so with that of citronellal (ca. 50%) and rather poorly with that of citral itself (ca. 40%).

The first comprehensive study of the metal catalysed rearrangement under homogeneous conditions was undertaken by Field, Hughmark, Holroyd and Marshall[65]. A wide selection of potential catalysts were evaluated under heterogeneous conditions, with the intention of selecting the most promising

for a homogeneous study. They discovered the rearrangement to be catalysed by a number of nickel and copper compounds and even cobaltic oxide. Other compounds of copper and cobalt were unproductive, as were compounds of iron, silver and mercury. The blue, high melting solid, obtained during the attempted rearrangement with cupric acetate monohydrate, was probably the complex reported by Hieber and Leutart[45]. As a result of this work they chose nickel acetate tetrahydrate for a homogeneous study in xylene. This catalyst system was found to be exceptionally versatile and effected the isomerization of a wide range of aldoximes, usually in good yields. Thus the oxime of citronellal was isomerized in 71% yield to the amide (cf. Caldwell and Jones[64]).

Although the synthetic possibilities of the metal catalysed rearrangement of aldoximes to amides are by now well documented, the mechanistic aspects of the isomerizations have, as yet, generally remained a matter of qualitative speculation[66].

Bryson and Dwyer[67], who characterized a number of metal ion complexes of 2-furancarboxaldoxime, observed the formation of 2-furancarboxamide, during the preparation of certain nickel and copper complexes. They found that treatment of tris(2-furancarboxaldoxime)nickel(II), in a variety of ways, resulted in the production of bis(2-furancarboxaldoxime)nickel(II and a mixture of 2-furancarboxaldoxime and 2-furancarboxamide. In addition, they discovered that heating a suspension of the bis-complex in benzene, with a large excess of the oxime, produced the amide catalytically, apparently by the successive formation and decomposition of tetrakis(2-furancarboxaldoxime) nickel(II).

Since it is generally the β-aldoxime that forms metal ion complexes, via coordination through the nitrogen atom[46,68,69], they concluded that the isomerization involved a trans Beckmann rearrangement and that the α-aldoxime (III) was converted to the β-aldoxime (IV), as a prerequisite to amide formation.

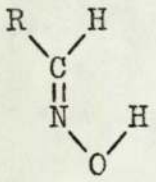

III

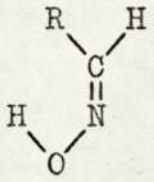

IV

Yamaguchi suggested the function of copper, in his rearrangement, to be essentially that of weakening the N-O bond of the oxime, by the formation of a suitable complex salt.

This view was developed by Paul[62], who envisaged the rearrangement to be assisted by the overall electron deficiency of the oxime, arising as a result of its interaction with nickel.

Other coordination centres are believed to behave in a similar manner. Hoffenberg and Hauser[70] proposed that the stable complex β-p-chlorobenzaldoxime-N-borontrifluoride (V), when heated (ca. 150°C), was converted to the reactive species β-p-chlorobenzaldoxime-O-borontrifluoride (VI), which could subsequently undergo either dehydration to produce p-chlorobenzonitrile or a Beckmann rearrangement to yield p-chlorobenzamide, illustrated by the scheme 3.2.

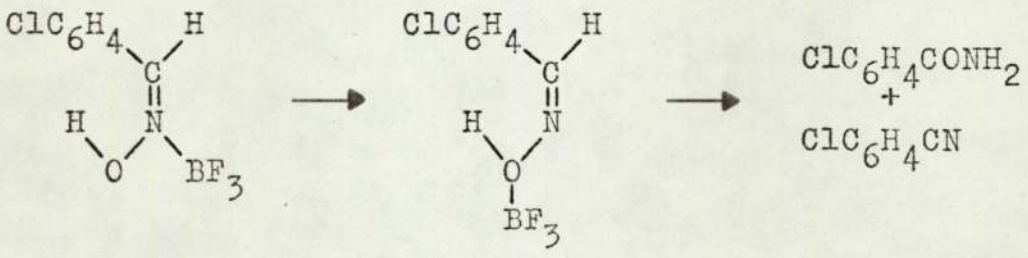

3.2

V VI

They concluded that the formation of the amide could possibly be a result of nitrile hydrolysis and therefore that the reaction might not constitute a true example of the Beckmann rearrangement. Furthermore, they suggested that nitriles might also be intermediates in the rearrangement of aldoximes to amides with polyphosphoric acid[71], since this reagent had been shown to convert nitriles to amides[72].

Although the dehydration of aldoximes to nitriles is well established[57], for those reagents normally employed to effect the Beckmann rearrangement of ketoximes, it appears unlikely that such a process occurs during the nickel catalysed isomerization of aldoximes.

Thus neither Field et al[65], nor Bryson and Dwyer[67], could find any evidence to suggest that nitrile intermediates were involved in their reactions.

It would appear likely, therefore, that certain basic differences exist between the nature of the rearrangement with transition metal catalysts and that with other coordination centres. However, it should be noted that the coordination of an aldoxime to a metal ion may, in fact, be achieved through the oxygen atom of the aldoxime, in certain special cases[68,69].

The function of the transition metal catalysts in these isomerizations is not well understood. It was the purpose of this study to undertake a kinetic investigation of a suitably representative reaction, so that the mechanistic role of the metal, in facilitating rearrangement, could be elucidated.

This work is reported in the following sections of chapter 3.

3.2. Initial studies.

In the following sections no attempt is made to distinguish between α and β benzaldoxime. A discussion of the isomeric form of benzaldoxime, prior to rearrangement to benzamide, is deferred until section 3.4.5.

3.2.1. Studies in aromatic solvents.

Field et al[65] showed that the conversion of benzaldoxime to benzamide could be achieved, under heterogeneous conditions, with a number of nickel compounds. It was of interest, therefore, to investigate the potential catalytic use of a selection of nickel compounds, under homogeneous conditions, with a view to choosing the most promising for a kinetic study. Accordingly benzaldoxime was refluxed in xylene (ca. 140°C) in the presence of a series of nickel compounds. A summary of the results is presented in table 3.1.

Table 3.1.

Compound	Concentration		Reflux	Observations
	Compound	Oxime	time	
$Ni(DH)_2$	0.08M	0.6M	15hrs.	Dark red solution, no benzamide.
Ni(acen)	0.08M	0.6M	15hrs.	Dark brown solution, no benzamide.
$NiCl_2(PPh_3)_2$	0.012M	0.2M	11hrs.	Non-homogeneous, no benzamide.
$NiCl_2 6H_2O$	0.012M	0.2M	11hrs.	Non-homogeneous, no benzamide.
$Ni(OF)_2 2H_2O$	0.012M	0.2M	5hrs.	Non-homogeneous, no benzamide.
$Ni(OAc)_2 4H_2O$	0.012M	0.2M	5hrs.	Light green to light brown solution, gave benzamide on cooling (yield ca.85%).

Table 3.1. reveals those complexes containing tightly bound, multidentate ligands to be ineffective as catalysts. In addition, compounds containing the chloride ion do not appear to have any catalytic effect. Rather incongruously nickel acetate tetrahydrate is seen to effect rearrangement satisfactorily, whereas nickel formate dihydrate appears to be ineffective. In the subsequent kinetic studies (section 3.3.) and related experiments (section 3.4.) evidence is cited by which these observations may be rationalized.

Work with a selection of metal acetates in xylene revealed that zinc acetate dihydrate also catalysed the rearrangement, although both manganese acetate dihydrate and cobalt acetate tetrahydrate were ineffective. Nickel acetate tetrahydrate was found to effect rearrangement in xylene under an atmosphere of nitrogen, suggesting molecular oxygen to have no involvement in the reaction. Since this latter nickel compound appeared the most effective catalyst in xylene a qualitative study of the rearrangement, in a series of refluxing aromatic solvents, was undertaken with this catalyst. The solvents chosen were, in sequence of increasing boiling point, toluene (111°C), xylene (140°C), 1,3,5-trimethylbenzene (165°C) and tetrahydronaphthalene (207°C). Both the time for reaction completion and the overall conversion of benzaldoxime to benzamide were found to decrease with respect to this sequence. Thus benzamide was produced in ca. 40% yield after about half an hour in tetrahydronaphthalene and in ca. 85% yield after several hours in xylene. This behaviour implies the presence of a side reaction of high activation energy, a possibility inferred by Field et al[65] and supported here by subsequent work reported in section 3.3.5.

Attempts to perform the reaction in tetrahydronaphthalene at a fixed temperature below the boiling point, using a small oven assembly, failed. The temperature rose sharply upon the introduction of the catalyst. The exothermic nature of the reaction is well established for a variety of heterogeneous catalysts[62,65], although it was not observed apparently for nickel acetate tetrahydrate[65].

Suprisingly this compound was found to be almost insoluble in any of the pure aromatic solvents mentioned above, although its solubility increased in the presence of benzaldoxime. Furthermore, the rearrangement product, benzamide, was observed to separate out as a liquid in the higher boiling point solvents especially tetrahydronaphthalene, during refluxing. Indeed, xylene was selected by Field et al[65] since it is an excellent solvent for the recrystallization of amides.

Thus it was clear that aromatic solvents were not satisfactory reaction media for a kinetic study of the nickel acetate tetrahydrate catalysed isomerization of benzaldoxime to benzamide, since homogeneous conditions were not ideally fulfilled.

3.2.2. Studies in digol.

A preliminary investigation revealed that the rearrangement could be achieved in digol under homogeneous conditions. Moreover, the concentration of benzamide in solution can be monitered effectively by infrared spectroscopy in this solvent. Benzamide has a characteristic spectrum between 1700cm^{-1}. and 1500cm^{-1}., shown in figure 3.1., a region in which digol does not absorb. The work in aromatic solvents had indicated that quite high temperatures were necessary for the production of benzamide to occur at a convenient rate.

Since the boiling range of digol is 241-248°C it can be used for studies over an elevated temperature range.

The rearrangement in digol was initially investigated at high temperature by employing a thermostatted silicone oil bath, similar to the one finally developed and described in section 2.2.1.1. It was found that the exothermic nature of the rearrangement rendered impossible attempts to maintain a constant temperature throughout the duration of the reaction. Attempts to control this, by performing the reaction in a vessel equipped with a cooling coil, failed. The temperatures involved (ca. 150-200°C) prevented the use of tap water as a coolant, due to its relatively low boiling point. Ideally such a coolant should be employed near the temperature of study. A flow system involving the circulation of a liquid at these elevated temperatures was impractical. The system employed had to possess good thermal transfer characteristics, which were easily controllable. For this reason the oven assembly was discarded.

The system finally developed to meet the requirements of the kinetic study derived inspiration from the fact that the temperature of a reaction undertaken in a refluxing solvent is automatically fixed at the boiling point of the solution. The heat produced during an exothermic reaction, under such conditions, is merely utilized to reflux the solvent more vigorously.

Possible solvent effects on the rearrangement precluded the use of a range of solvents, each under reflux, to vary the temperature of study. However, the idea of a refluxing solvent system led to the construction of the apparatus noted previously in section 2.2.1.1.

Figure 3.1.

Infrared spectrum of a 0.1M solution of benzamide in digol (cell path length 0.05cm.).

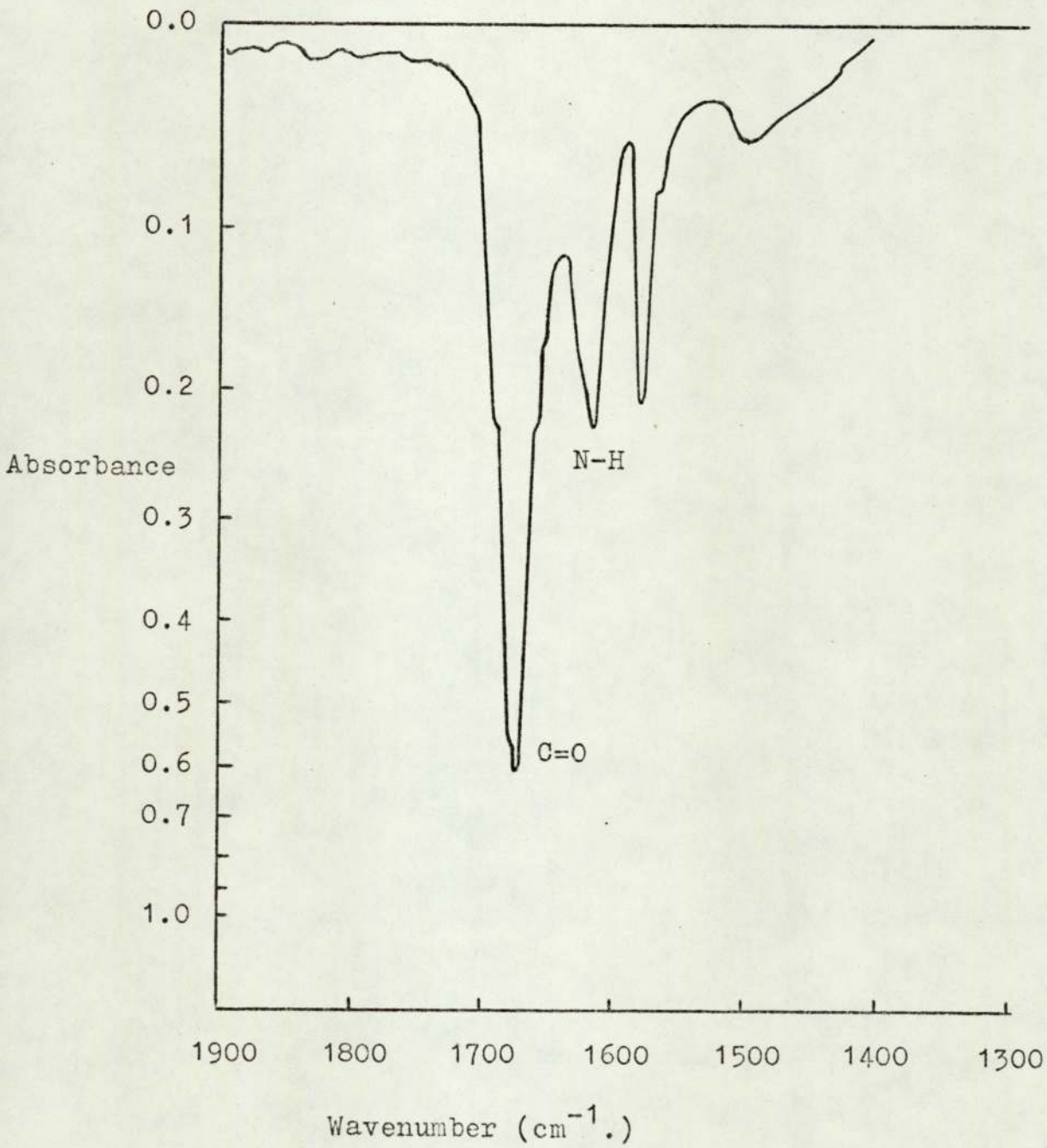

3.3. Kinetics of the nickel acetate tetrahydrate catalysed rearrangement of benzaldoxime to benzamide.

The infrared spectrum of a 0.1M solution of benzamide in digol is shown in figure 3.1. and exhibits a characteristic absorption at 1675cm^{-1}., due to the carbonyl stretch. The two less intense absorptions at 1615cm^{-1}. and 1575cm^{-1}. can reasonably be assigned to the N-H bend and the aromatic C-C stretch respectively[73]. A 0.2M solution of benzaldoxime in digol has no discernible spectrum in the region between 2000cm^{-1}. and 1500cm^{-1}., revealing the low intensity of the C=N absorption. A plot of benzamide concentration against absorbance at 1675cm^{-1}., with a suitable baseline correction, is shown for a series of benzamide solutions in digol in figure 3.2. and reveals Beer's law to be obeyed. Thus the concentration of benzamide can be followed kinetically, during the rearrangement, as a function of the absorbance at 1675cm^{-1}.

Firstly, it was established that reproducible results could be obtained. Figure 3.3. shows two plots of the corrected absorbance at 1675cm^{-1}. against time under identical conditions. It is seen that the curves exhibit the 'S' shaped character often indicative of product formation in two, consecutive, first order steps[74].

For the consecutive process

$$A \xrightarrow{l} B \xrightarrow{m} C \qquad 3.3.$$

it may be shown that

$$c = c_{\infty}\left(1 + \frac{l}{(m-l)}e^{-mt} - \frac{m}{(m-l)}e^{-lt}\right) \qquad 3.4.$$

where $c = [C]$ at time t, and $c_{\infty} = [C]$ at infinite time.

It was found that the experimental plots could be fitted

satisfactorily to equation 3.4. using the least squares computer program SEQUEXP shown in appendix 1. Values of the two psuedo-first order rate constants and the absorbance at infinite time were obtained.

Since equation 3.4. is demonstrably symmetrical neither rate constant can be unambiguously associated with the first or second step in the consecutive sequence. For this reason, in tables 3.2., 3.3., 3.4. and 3.5. shown later, no attempt is made, until section 3.3.4., to assign the two observed rate constants to particular steps in the reaction.

The overall conversion of benzaldoxime to benzamide is tabulated in terms of the fractional yield, F, defined as the ratio of the absorbance at infinite time to the absorbance of a 0.2M solution of benzamide in digol, calculated from figure 3.2.

3.3.1. Variation of the concentration of benzaldoxime.

Runs were performed at a catalyst concentration of 0.012M and 184°C.

Table 3.2. reveals both rate constants (k_a and k_b) and the fractional yield to be essentially independent of the reagent concentration.

Table 3.2.

[Oxime]	$k_a(min^{-1})$	$k_b(min^{-1})$	F
0.1M	0.0236	0.0395	0.505
0.2M	0.0230	0.0380	0.569
0.3M	0.0254	0.0406	0.553

3.3.2. Variation of the concentration of catalyst.

Runs were performed at a benzaldoxime concentration of 0.2M and 184°C.

Table 3.3. shows k_a to be considerably enhanced and k_b to be slightly reduced as the catalyst concentration is increased. The fractional yield of benzamide remains effectively constant.

Table 3.3.

[Catalyst]	$k_a(min^{-1})$	$k_b(min^{-1})$	F
0.004M	0.00940	0.0419	0.580
0.008M	0.0159	0.0391	0.573
0.012M	0.0230	0.0380	0.569
0.016M	0.0282	0.0305	0.595
0.020M	0.0365	0.0281	0.606
0.024M	0.0446	0.0314	0.594

3.3.3. Variation of the temperature.

Runs were performed at concentrations of 0.2M in benzaldoxime and 0.012M in catalyst.

An inspection of table 3.4. reveals k_a to be only moderately temperature dependent, whereas k_b is seen to be highly so. Consistent with the work in aromatic solvents (section 3.2.1.), the fractional yield of benzamide is observed to diminish with increasing temperature.

Table 3.4.

Temp.(°C)	$k_a(min^{-1})$	$k_b(min^{-1})$	F
160.5	0.00828	0.00522	0.749
168.5*	0.0132	0.0124	0.685
176.5*	0.0191	0.0192	0.639
184.0	0.0230	0.0380	0.569
191.5	0.0303	0.0603	0.537
200.0	0.0435	0.124	0.483

In appendix 4 it is shown that under conditions in which the two rate constants governing a consecutive reaction approach the same value they can no longer be determined accurately. Those cases in which this phenomenon was apparent are marked throughout the text with an asterisk (*).

An Arrhenius plot of the data in table 3.4. is shown in figure 3.4., from which an activation energy of 15.8 Kcal.mol^{-1} is calculated for k_a and 31.0 Kcal.mol^{-1} for k_b.

3.3.4. The rearrangement of deuterated benzaldoxime.

The isomerization of benzaldoxime to benzamide must involve the cleavage of the C-H bond in the reagent at some stage. Therefore, it was of considerable interest to ascertain whether a kinetic isotope effect could be observed for either rate constant in the rearrangement of deuterated benzaldoxime.

Two runs were undertaken at a catalyst concentration of 0.012M and 189°C. The first contained a 0.2M solution of deuterated benzaldoxime, of isotopic substitution ca. 60% (section 2.3.2.), and the second a 0.2M solution of benzaldoxime itself. The experimental plot for the partially deuterated run was corrected for 100% isotopic substitution by using the second as a control.

Table 3.5. reveals k_a to exhibit a kinetic isotope effect and k_b to remain essentially unaltered.

Table 3.5.

Reagent	k_a(min^{-1})	k_b(min^{-1})	F
C_6H_5CDNOH	0.0189	0.0537	0.525
C_6H_5CHNOH	0.0299	0.0558	0.538

The infrared spectrum of a 2M solution of deuterated

benzaldoxime in digol exhibits a C-D absorption at 2205cm^{-1} and is shown in figure 3.5. It is therefore possible to follow kinetically the disappearance of this peak during the rearrangement. Since the independence of either rate constant on the reagent concentration is established (table 3.2.), it was possible to undertake the reaction at a deuterated benzaldoxime concentration of 2M. The catalyst concentration was 0.012M and the temperature 189°C as before.

Figure 3.6. shows the C-D cleavage to follow first order kinetics. Therefore, it must follow that C-H cleavage is the first step in the consecutive sequence. Furthermore, tables 3.3. and 3.5. reveal this step to be strongly catalyst dependent. Calculation of the psuedo first order rate constant from figure 3.6. gives a value of 0.0176min^{-1}, which is in reasonable agreement with k_a from table 3.5. for the rearrangement of deuterated benzaldoxime.

The systematic errors in the determination of k_a, k_b and F are suggested to be within ±5%, from the reproducibility runs undertaken, including that depicted in figure 3.3. The standard deviation of the rate constant associated with C-D cleavage is calculated to be within ±5%, from figure 3.6. and the approximate formula given in appendix 5.

3.3.5. The side reaction.

Under the conditions of study not all the benzaldoxime is converted to benzamide, however, the catalyst is still active since the introduction of further benzaldoxime is found to cause additional rearrangement. Thus the presence of at least one side reaction is suggested. Such processes can, in principle, occur at a number of positions in the reaction sequence. Experiments cited in section 3.4.5. show the thermal

decomposition of benzaldoxime[61] to be unlikely. The kinetics preclude the possibility that benzamide undergoes a subsequent reaction and imply the first step in the consecutive sequence to be purely C-H cleavage, although this could arguably produce a reactive species, which might then undergo a rapid parallel reaction with suitable species in solution.

If either of the consecutive steps involves a parallel reaction then its associated observed rate constant will be composite and it may be shown that

$$k_{obs} = k_m + k_s \qquad 3.5.$$

where k_{obs} refers to the observed rate constant and k_m and k_s are the rate constants of the main and side reactions respectively.

Assuming neither the main nor side reaction to be composite

$$k_{obs} = A_m e^{-E_m/RT} + A_s e^{-E_s/RT} \qquad 3.6.$$

where A_m and A_s are the pre-exponential factors and E_m and E_s are the activation energies of the main and side reactions respectively.

Therefore

$$-\frac{d(\ln k_{obs})}{d(1/T)} = \frac{E_m k_m + E_s k_s}{R(k_m+k_s)} \qquad 3.7.$$

If the composite rate constant gives a linear Arrhenius plot

$$E_{obs} = \frac{E_m k_m + E_s k_s}{(k_m+k_s)} \qquad 3.8.$$

If only one of the consecutive steps, irrespective of

which, involves a parallel reaction

$$F = \frac{k_m}{(k_m+k_s)} \qquad 3.9.$$

Let

$$\bar{E} = E_s - E_m \qquad 3.10.$$

From equations 3.8., 3.9. and 3.10. it may be shown that

$$E_{obs} = E_m + \bar{E}(1-F) \qquad 3.11.$$

and consequently that

$$F/(1-F) = (A_m/A_s)e^{\bar{E}/RT} \qquad 3.12.$$

A plot of $\log_{10}(F/(1-F))$ against $1/T$ is shown for equation 3.12. in figure 3.7., from which a value of 10.6 Kcal.mol^{-1} is calculated for $\bar{E}$.

If both consecutive steps involve a parallel reaction equation 3.12 will be of the form

$$F/(K-F) = (A_m/A_s)e^{\bar{E}/RT}$$

where K is a collection of appropriate rate constants of the same form as equation 3.9. and is therefore temperature dependent. Since figure 3.7. is observed to show no significant curvature it appears probable that only one of the consecutive steps involves a pronounced parallel reaction.

Using the data of table 3.4., equation 3.11 may be employed to predict the deviation expected for either Arrhenius plot from linearity. From such a treatment it may be shown that the extra contribution, over the temperature range, is 2.8 Kcal.mol^{-} This means that the gradient of the Arrhenius plot for k_a at

160.5°C should differ by ca. 18% from that at 200°C, if branching occurs in this step. Such a deviation would almost certainly be observed. However, in the case of the Arrhenius plot for k_b the corresponding discrepancy is only ca. 9% which is within the standard deviation (see below).

An inspection of figure 3.4. reveals neither Arrhenius plot to exhibit a systematic curvature. Thus it seems likely that the side reaction occurs in the second step of the consecutive reaction.

Equations 3.5. and 3.9. may be used to calculate values for the rate constants of the main and side reactions at a given temperature. Table 3.6. shows the values thus obtained at 184°C, using graphically corrected values for the composite rate constant k_b and the fractional conversion F from figures 3.4. and 3.7. respectively.

Table 3.6.

Rate constant	Value (min^{-1})
k_m	0.0214
k_s	0.0152

The activation energies of the main and side reactions may be estimated from equation 3.11. However, since it is easily shown that

$$k_{obs}F = A_m e^{-E_m/RT}$$

and $$k_{obs}(1-F) = A_s e^{-E_s/RT}$$

Arrhenius plots may be undertaken in the usual manner. These plots are shown in figure 3.8., from which activation energies of 27.7 Kcal.mol^{-1} and 39.1 Kcal.mol^{-1} are calculated for the main and side reactions respectively.

The standard deviations of the activation energies reported here are calculated to be within ±10%, from figures 3.4. and 3.8. and the approximate formula given in appendix 5. The principle contribution to these rather large values may be attributed to the inherent errors associated with the determination of k_a and k_b, under those conditions in which they approach the same value (appendix 4). Inspection of table 3.4. and figure 3.4. confirms that it is precisely under these conditions that substantial discrepancies in the Arrhenius plots are found.

3.3.6. Interpretation of the results.

It is clear that the first step is nickel dependent and involves the cleavage of the C-H bond in the reagent. This implies the reacting species to be a nickel complex of benzaldoxime. If such a complex is produced it must be present in small concentration, otherwise the first step would not be a psuedo-first order process and the consecutive scheme would not hold. It seems probable that C-H cleavage is followed by the rapid production of a relatively stable intermediate, which has a slight affinity for the catalyst. The second step would appear to involve parallel organic reactions of the intermediate to produce benzamide and at least one side product.

The following general reaction mechanism is therefore proposed.

$$\mathrm{Ni + Ox} \overset{K_1}{\rightleftharpoons} \mathrm{NiOx}$$

$$\mathrm{NiOx} \xrightarrow{k_1} \mathrm{NiI}$$

$$\mathrm{Ni + I} \overset{K_2}{\rightleftharpoons} \mathrm{NiI}$$

$$\mathrm{I} \xrightarrow{k_2} \mathrm{Am}$$

$$\mathrm{I} \xrightarrow{k_3} \mathrm{S}$$

where Ni refers to the catalytic species, Ox to benzaldoxime, I to the intermediate, Am to benzamide and S to the side product(s).

The assumptions are made that the concentration of catalytic species remains constant and that the equilibrium constants K_1 and K_2 are small.

We have that

$$K_1 = \frac{[NiOx]}{[Ni][Ox]} \qquad 3.13.$$

and $$K_2 = \frac{[NiI]}{[Ni][I]} \qquad 3.14.$$

Let

$$a = [NiOx] + [Ox]$$

and $$b = [NiI] + [I]$$

From 3.13. and 3.14. and collecting the constant terms

$$a = [NiOx]/\alpha \qquad 3.15.$$

and $$b = [I]/\beta \qquad 3.16.$$

We have that

$$\frac{da}{dt} = -k_1 \, NiOx$$

From 3.15.

$$\frac{da}{dt} = -k_1 \alpha a$$

Integration of this gives

$$a = a_o e^{-k_1 \alpha t} \qquad 3.17.$$

Also we have that

$$\frac{db}{dt} = k_1[NiOx] - (k_2+k_3)[I]$$

From 3.15., 3.16. and 3.17.

$$\frac{db}{dt} = k_1\alpha a_o e^{-k_1\alpha t} - (k_2+k_3)\beta b$$

This equation is of the same mathematical form as that for two consecutive reactions[74]. Integration produces the equation

$$b = \frac{k_1\alpha a_o}{(k_2+k_3)\beta - k_1\alpha}(e^{-k_1\alpha t} - e^{-(k_2+k_3)\beta t}) \qquad 3.18.$$

We have that

$$a_o = a + b + [Am] + [S]$$

and $[Am]/[S] = k_2/k_3$

Therefore from 3.17. and 3.18.

$$[Am] = \frac{a_o k_2}{(k_2+k_3)}\left(1 + \frac{k_1\alpha}{(k_2+k_3)\beta - k_1\alpha}e^{-(k_2+k_3)\beta t} - \frac{(k_2+k_3)\beta}{(k_2+k_3)\beta - k_1\alpha}e^{-k_1\alpha t}\right.$$

This equation is of the same form as equation 3.4. which describes the formation of product in two consecutive first order steps.

The observed catalyst dependent rate constant, k_a, may be related to the kinetic parameters of the general reaction mechanism by the expression

$$k_a = \frac{k_1K_1[Ni]}{(1+K_1[Ni])}$$

and the observed slightly inversely catalyst dependent rate

constant, k_b, may be expressed as

$$k_b = \frac{(k_2+k_3)}{(1+K_2[Ni])}$$

Since K_1 and K_2 are assumed to be small these expressions approximate to

$$k_a = k_1K_1[Ni] \qquad 3.19.$$

and $$k_b = k_2+k_3 \qquad 3.20.$$

A plot of k_a against catalyst concentration is shown for equation 3.19. in figure 3.9. and exhibits a reasonable straight line dependence. The standard deviation of the slope is calculated to be within ±7%, using the approximate formula of appendix 5.

Figure 3.2.

Plot of absorbance at $1675cm^{-1}$. against the concentration of benzamide, for a series of solutions in digol.

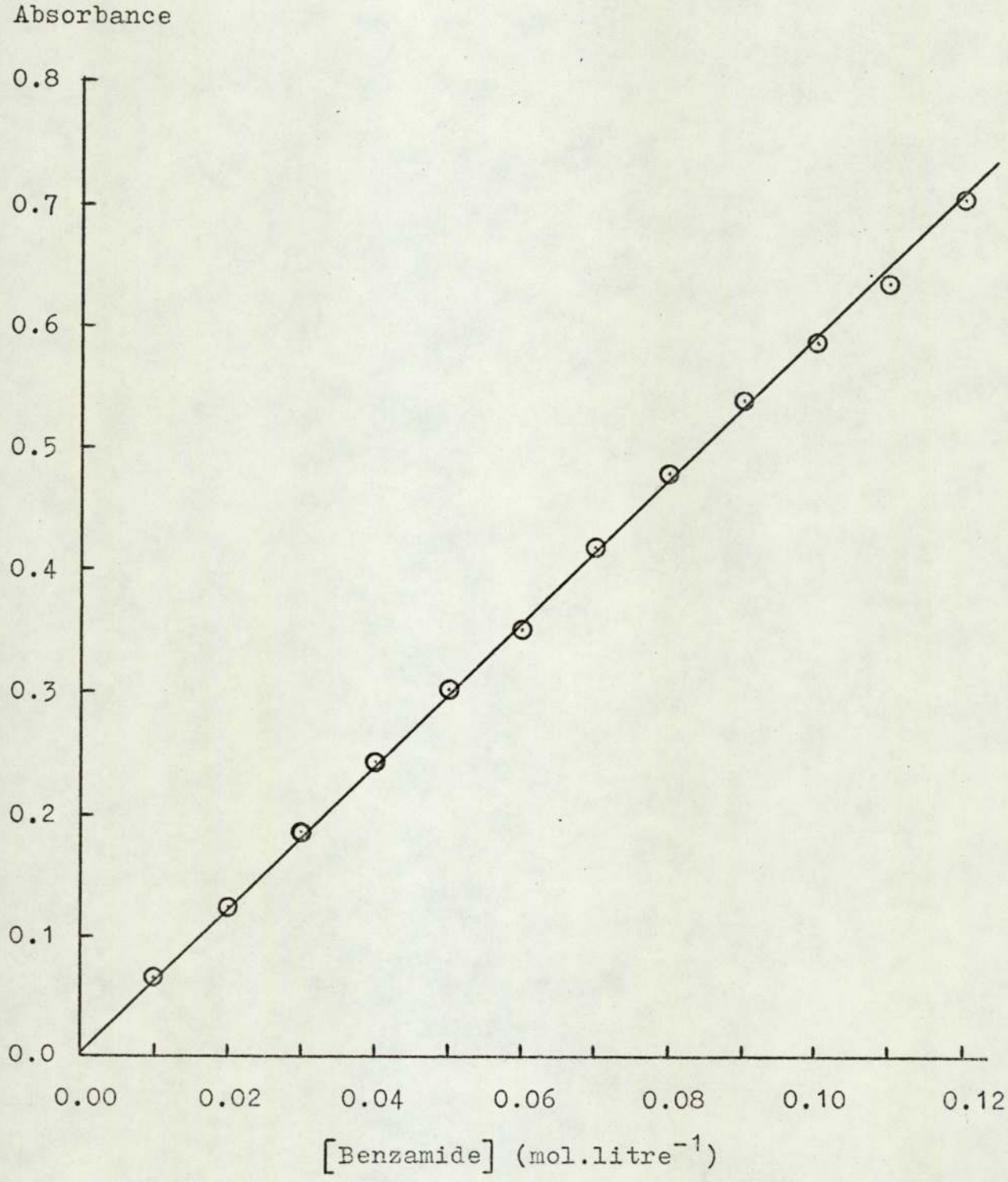

Figure 3.3.

Two plots of the absorbance at 1675cm^{-1} against time at concentrations of 0.2M benzaldoxime and 0.012M nickel acetate tetrahydrate and at 184^{o}C.

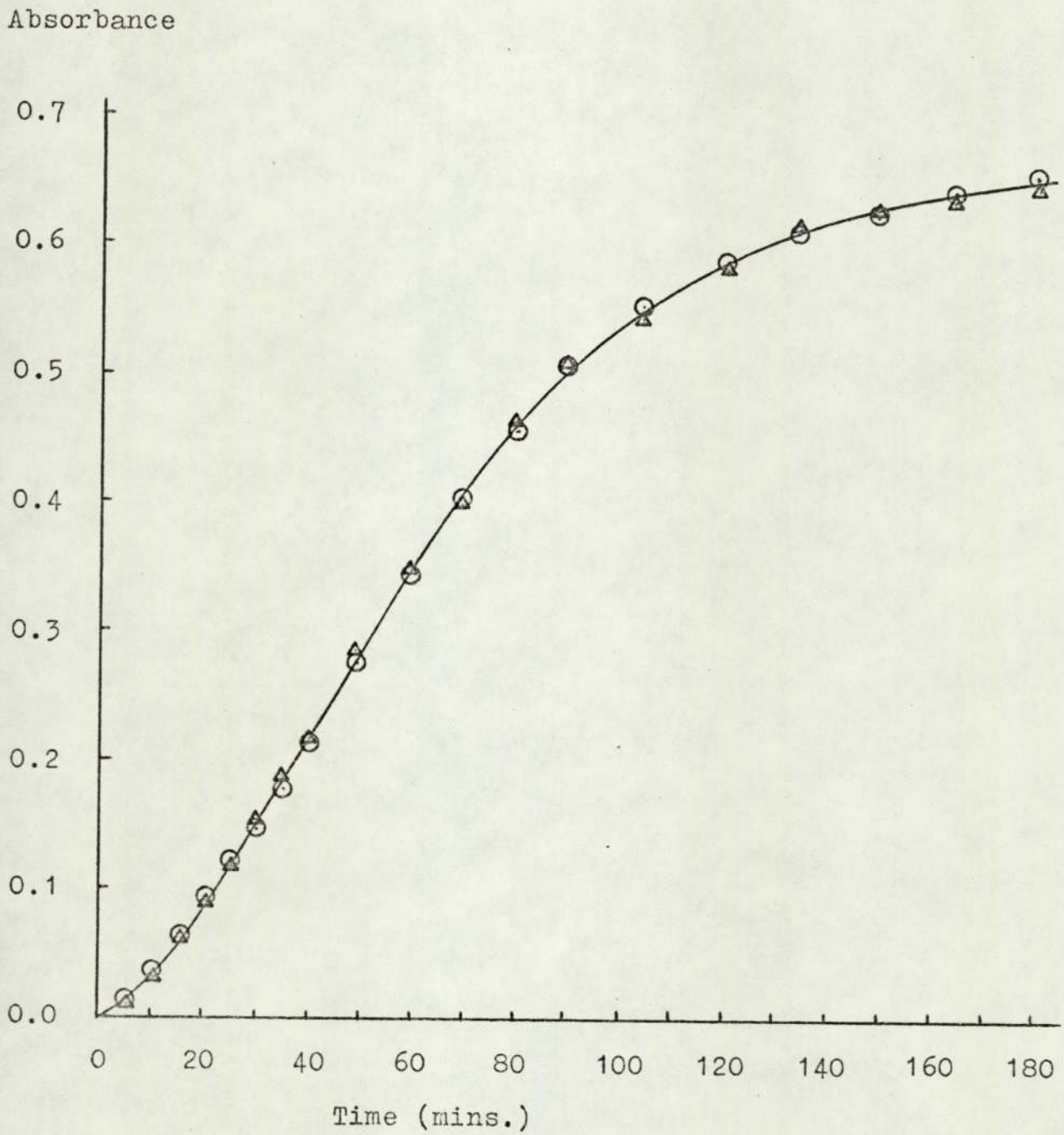

Figure 3.4.

Plots of $\log_{10}k_a$ and $\log_{10}k_b$ against 1/T at concentrations of 0.2M benzaldoxime and 0.012M nickel acetate tetrahydrate.

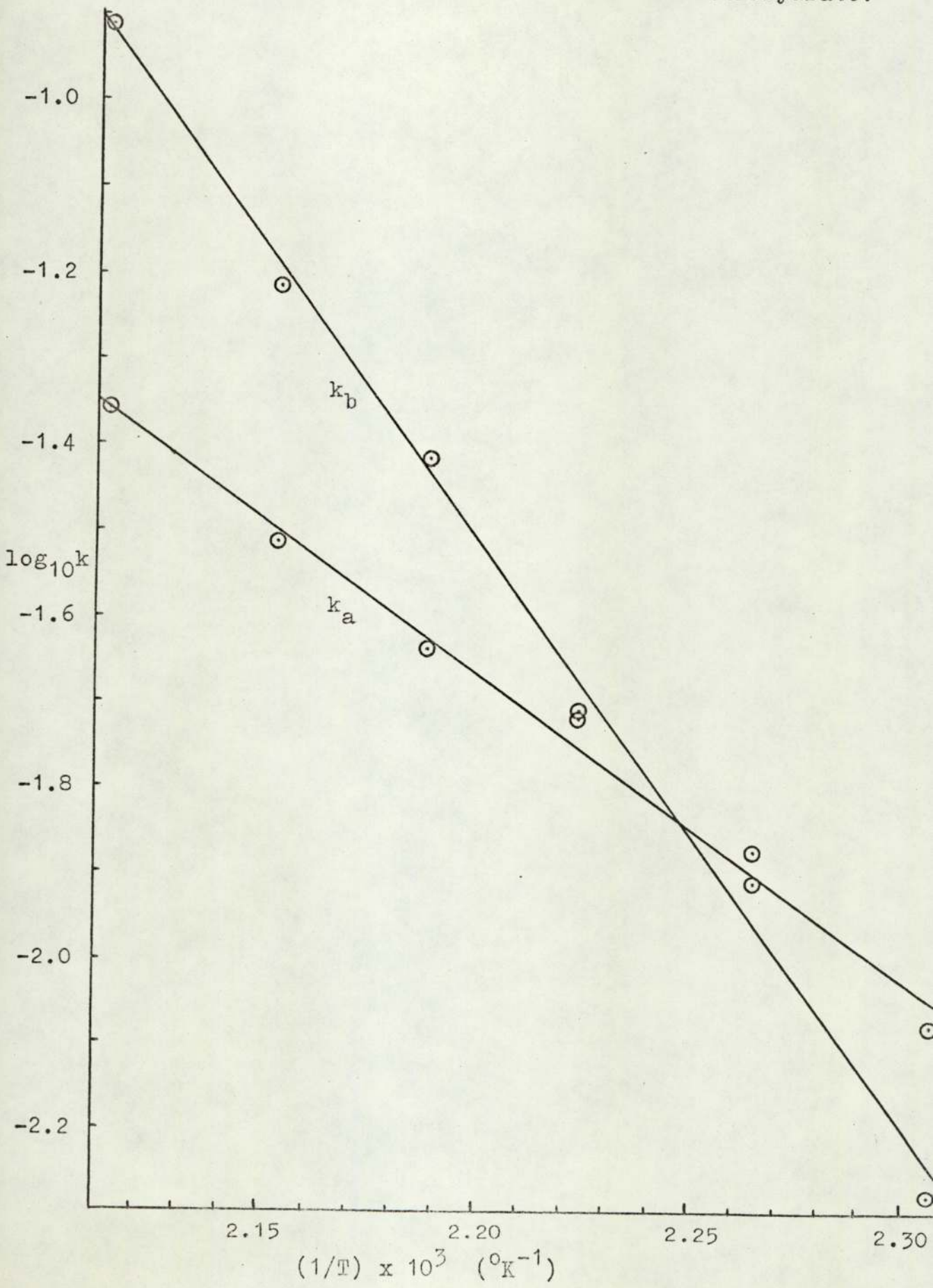

Figure 3.5.

Infrared spectrum of a 2M solution of deuterated α-benzaldoxime in digol (cell path length 0.05cm.).

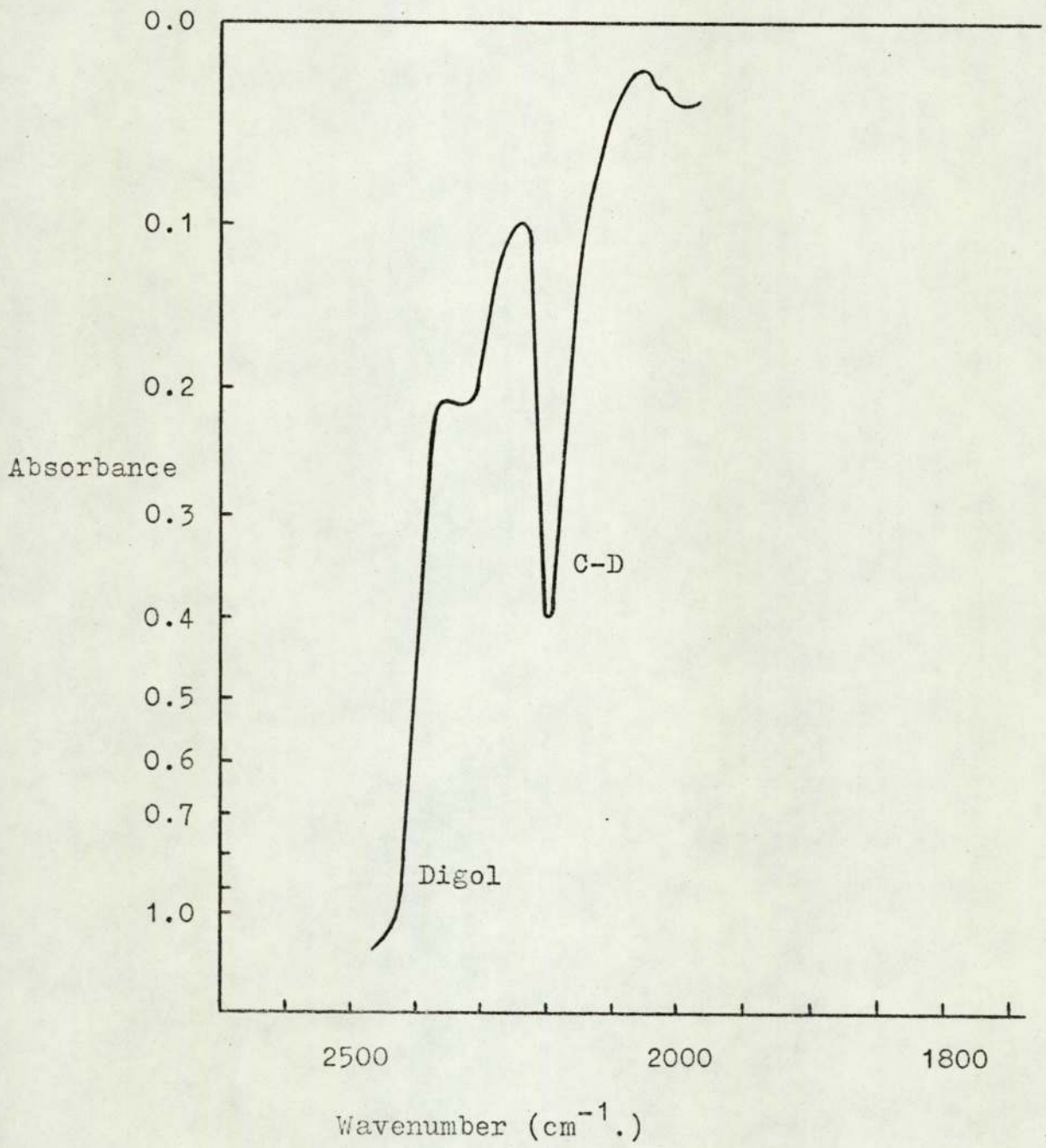

Figure 3.6.

Plot of $\log_{10}$(Absorbance of C-D peak) against time.

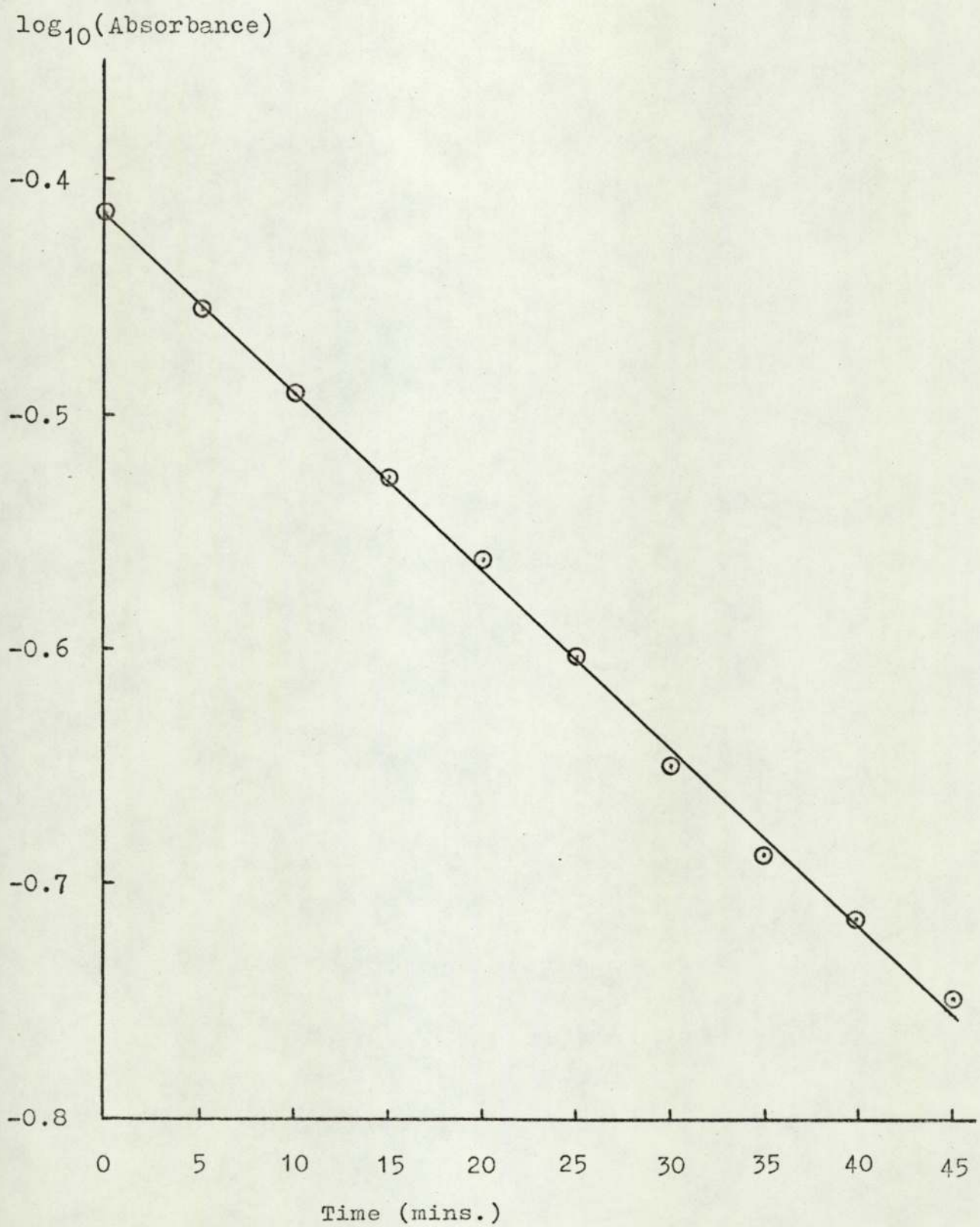

Figure 3.7.

Plot of $\log_{10}(F/(1-F))$ against 1/T at concentrations of 0.2M benzaldoxime and 0.012M nickel acetate tetrahydrate.

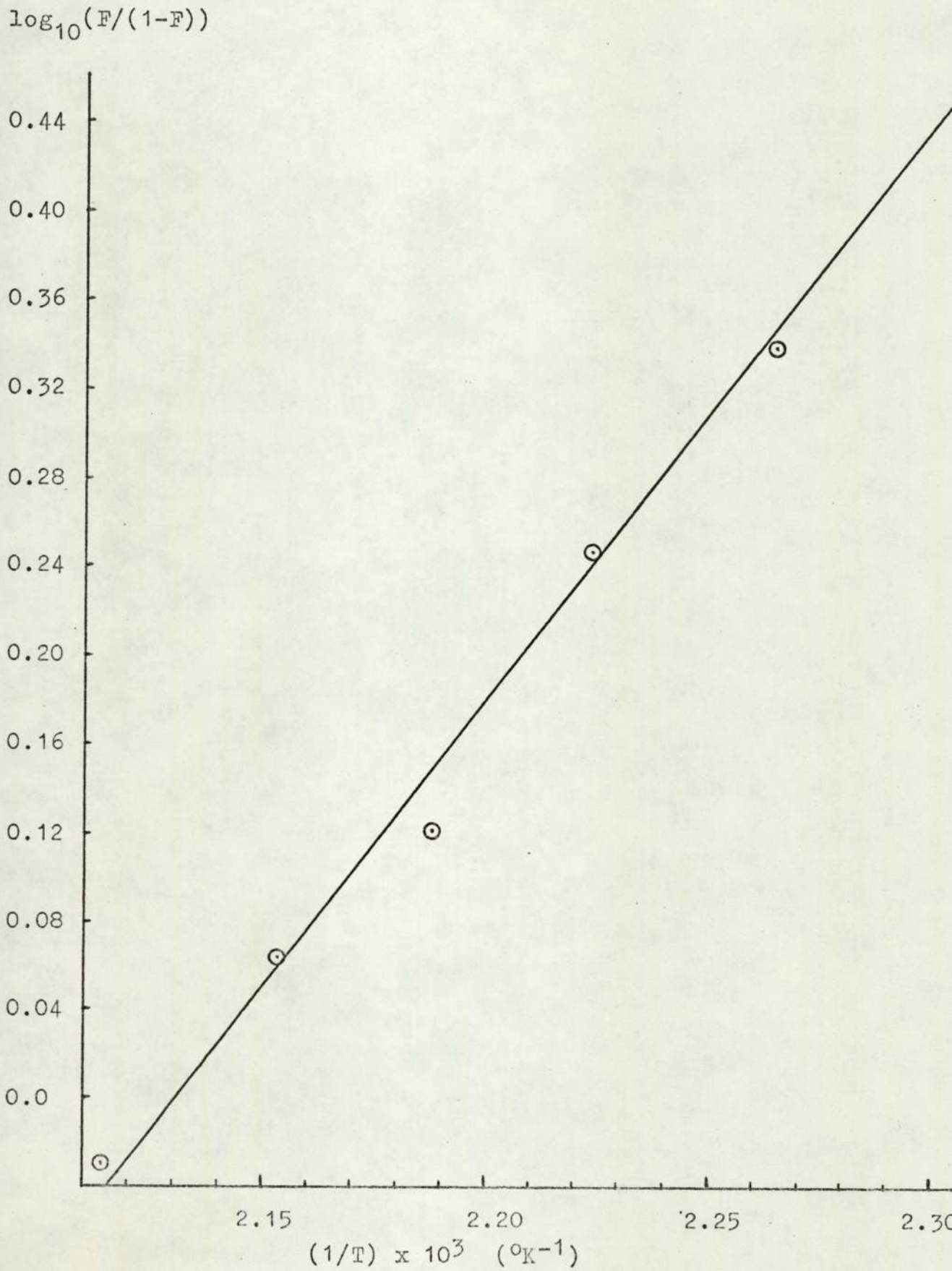

Figure 3.8.

Plots of $\log_{10}(F.k_b)$ and $\log_{10}((1-F).k_b)$ against 1/T at concentrations of 0.2M benzaldoxime and 0.012M nickel acetate tetrahydrate.

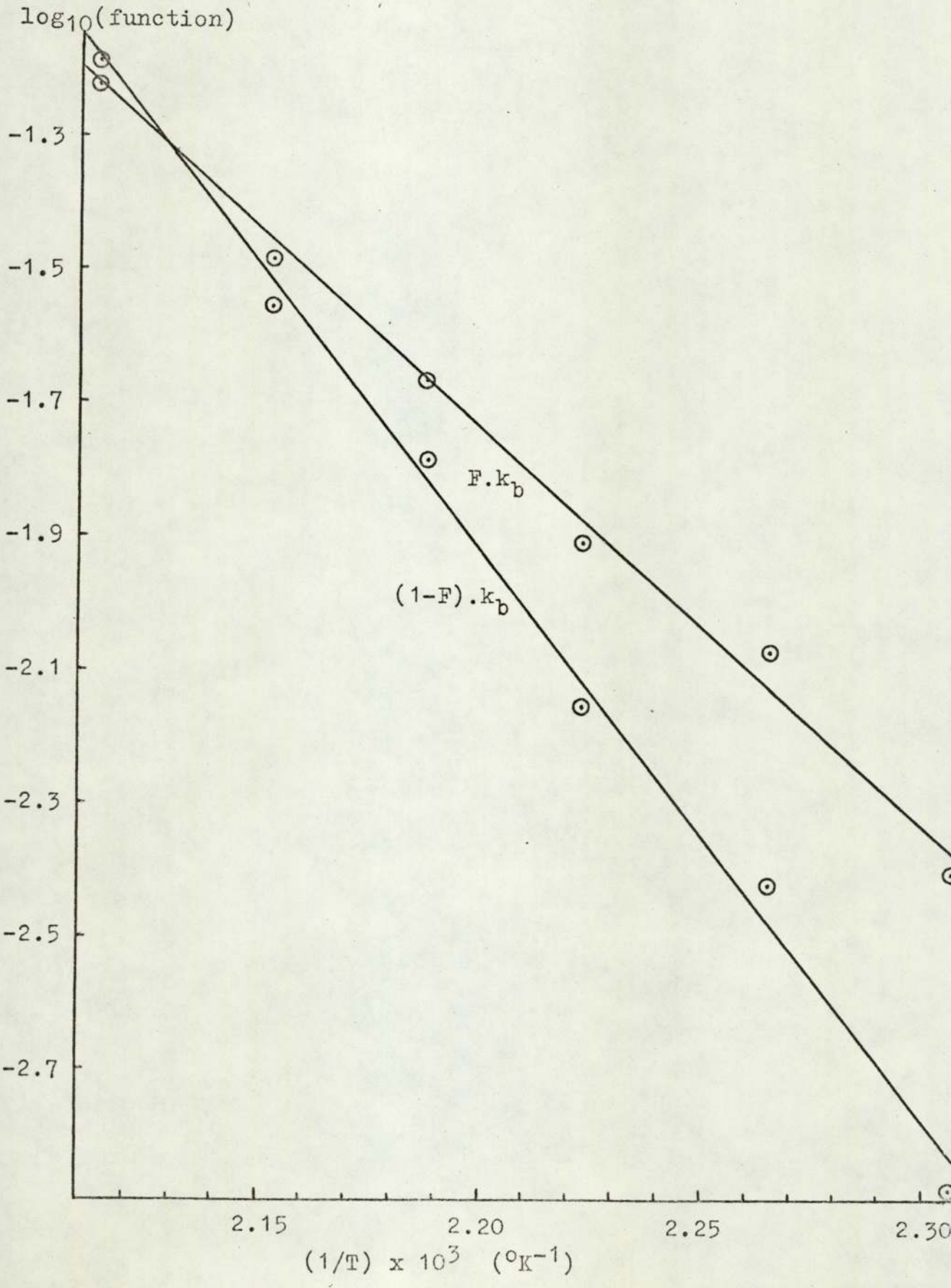

Figure 3.9.

Plot of k_a against the concentration of nickel acetate tetrahydrate at a concentration of 0.2M benzaldoxime and 184°C.

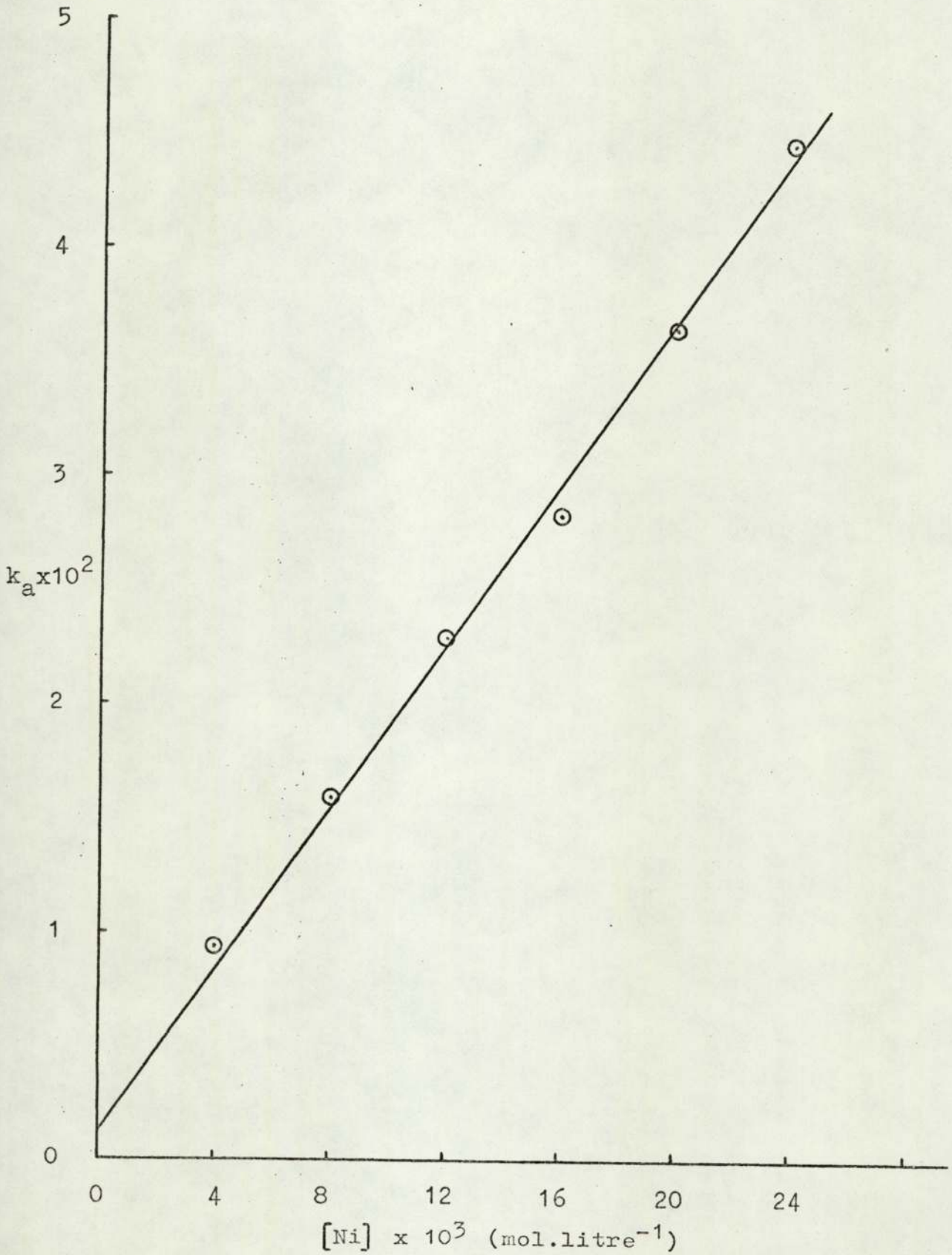

3.4. Related studies.

3.4.1. Additional catalysts.

A number of nickel compounds were found to effect the isomerization of benzaldoxime to benzamide in digol. These included dichlorobis(triphenylphosphine)nickel(II), diiodobis-(triphenylphosphine)nickel(II), dichlorotetrakis(benzaldoxime)-nickel(II), diiodotetrakis(benzaldoxime)nickel(II), nickel chloride hexahydrate and anhydrous nickel chloride.

In addition, both zinc acetate dihydrate and zinc chloride were found to be effective catalysts, although somewhat less efficient than their nickel analogues. A slight catalytic effect was shown by dichlorobis(triphenylphosphine)platinum(II), however, dichlorobis(triphenylphosphine)palladium(II) was found to be ineffective and produced a fine, grey suspension, probably of palladium metal. The heterogeneous catalytic action of stainless steel has been previously noted (section 2.2.1.3.)

No thorough attempt was made to investigate the kinetics of rearrangement with these catalysts for several reasons. Firstly, those complexes containing the iodide ligand produced reaction solutions that were subsequently discovered to damage the silver chloride windows of the solution cells during the spectroscopic analysis, probably as a result of chloride-iodide exchange. Secondly, phosphine complexes were found to dissolve only slowly in the reaction medium. Thirdly, those compounds containing chloride were found to catalyse the reaction rather slowly. Moreover, in the case of nickel chloride hexahydrate, the measurement of the carbonyl peak at $1675cm^{-1}$. was hindered by the release of water absorbing at $1655cm^{-1}$. No constant correction could be introduced since it

was apparent that the water gradually evaporated. For this reason kinetic runs with added water were also impractical, although benzamide is undoubtedly produced under such conditions as divulged by the growth of the characteristic aromatic absorption at 1575cm^{-1}.

In spite of these complications a careful study was undertaken for several catalysts at a concentration of 0.012M, a reagent concentration of 0.2M and at 184°C.

The experimental plots obtained, although far from ideal, exhibited similar 'S' shaped profiles to those shown in figure 3.3. and were fitted to equation 3.4. using the least squares computer program SEQUEXP as before (appendix 1). The values of the two pseudo-first order rate constants and the fractional conversion thus obtained are shown in table 3.7.

Table 3.7.

Catalyst	$k_a(min^{-1})$	$k_b(min^{-1})$	F
$Ni(PPh_3)_2Cl_2$	0.00693	0.0336	0.646
$Ni(PPh_3)_2I_2$ ‡	0.114	0.0443	0.612
$Ni(C_6H_5CHNOH)_4Cl_2$ ‡	0.0104	0.0208	0.675
$Ni(C_6H_5CHNOH)_4I_2$	0.0592	0.0404	0.670
$NiCl_2 6H_2O$ ‡	0.0154	0.0211	0.587
$Zn(OAc)_2 2H_2O$ *	0.00938	0.00930	0.248
$Ni(OAc)_2 4H_2O$	0.0230	0.0380	0.569

The data for nickel acetate tetrahydrate is included for the purpose of comparison. A suitable correction is applied to F for those catalysts containing benzaldoxime as a ligand.

The data of table 3.7. is clearly insufficient for a detailed interpretation to be attempted. Furthermore, for

*cf. section 3.3.3.

those catalysts marked with a double dagger the computer fits were rather poor and consequently the observed rate constants are unreliable. Nevertheless, even with these limitations in mind, certain trends are indicated.

The essentially catalyst independent rate constant and the fractional conversion to benzamide seem relatively unaffected by the catalyst type, although those catalysts containing chloride and zinc acetate dihydrate appear somewhat inconsistent. The latter compound was observed to produce a turbid, beige reaction mixture and may therefore be rather different from its nickel analogue. A possible explanation of the anomolous behaviour in the presence of chloride ion is discussed in section 3.4.2. The catalyst dependent rate constant is clearly influenced by the nature of the catalyst, as might be expected. Iodide complexes appear superior to their chloride counterparts and to nickel acetate tetrahydrate.

A suprising fact emerges from this study. Whereas the compounds dichlorobis(triphenylphosphine)nickel(II) and nickel chloride hexahydrate are seen to catalyse the rearrangement in digol, they are ineffective in aromatic solvents such as xylene (section 3.2.1.). This observation reveals a basic difference between the rearrangement in digol and that in xylene and implies that nickel acetate tetrahydrate possesses some feature, not shared by these chloride compounds, that enables it to effect rearrangement in aromatic solvents.

Field et al[65] reported that acetic acid was apparently necessary for their reaction to take place successfully. This remark was upheld in this study by the refluxing of a 0.2M solution of benzaldoxime in xylene, with a mixture of 0.012M nickel chloride hexahydrate and 0.024M sodium acetate.

Benzamide was produced in high yield. Furthermore, the rearrangement occurred satisfactorily, albeit rather slowly, if the sodium acetate was replaced by acetic or propionic acid. However, if formic acid was used no trace of benzamide could be discerned, even after 12hrs. of reflux, followed by several weeks of standing at room temperature.

These experiments demonstrate that the acetate group plays an important role in the rearrangement in xylene but is not necessary in digol. Presumably this reflects the ability of digol to undertake a similar function to that of the acetate group.

The kinetics of section 3.3.suggest that the essential role of the catalyst is to facilitate cleavage of the C-H bond in benzaldoxime. Arguably this would produce an electron deficient carbon atom, susceptible to nucleophilic attack. In section 3.1. experiments were cited which imply that the carbonyl oxygen of the product would probably be derived from the solvent medium. Thus it appears feasible that the first step in the consecutive sequence involves the attack upon an electron deficient carbon atom of benzaldoxime by a suitable nucleophilic oxygen species in solution.

In the nickel acetate tetrahydrate catalysed rearrangement in xylene the acetate anion would seem to be an eligible candidate for such a nucleophile, whereas in digol a suitable nucleophile might well be found in the solvent itself.

If this explanation is correct then the relatively stable intermediate, indicated by the kinetic studies, will be a benzimidate of general structure VII, where OR represents a suitable group provided by the reaction medium.

The thermal rearrangement of benzimidates, to yield amides,

is well established[75]. The pyrolysis pattern has been found to depend on the nature of the group R.

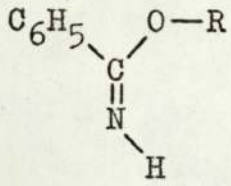

VII

If R is an aryl group then the Chapman rearrangement, involving a 1,3-shift of the aryl group from oxygen to nitrogen, will take place and an N-substituted amide will be produced. However, if R is an alkyl group capable of elimination, the Chapman rearrangement will not be followed. Instead, an elimination reaction will occur to yield a primary amide and an alkene.

The thermal rearrangement of acyl benzimidates is not properly understood. Such materials have not, as yet, been isolated as stable compounds, although they are postulated as intermediates in the production of amides from various reagents[76]

In the cases of the rearrangement in digol, the intermediate postulated would be the alkyl benzimidate VIII, which could therefore eliminate according to the general reaction scheme, producing benzamide and the substituted ethylene IX.

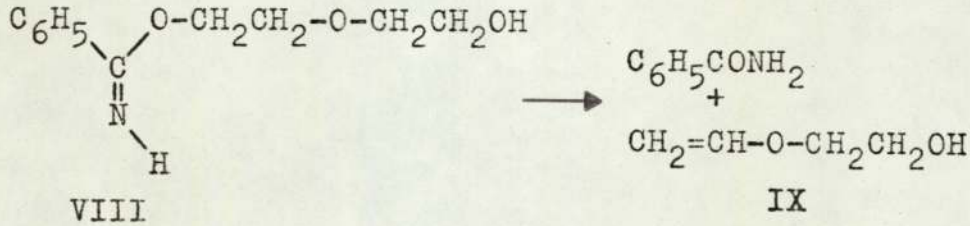

VIII IX 3.21.

In the cases of the rearrangement in xylene, the intermediate is purported to be the acyl benzimidate X, which

undergoes a similar elimination process, to yield benzamide and keten (XI).

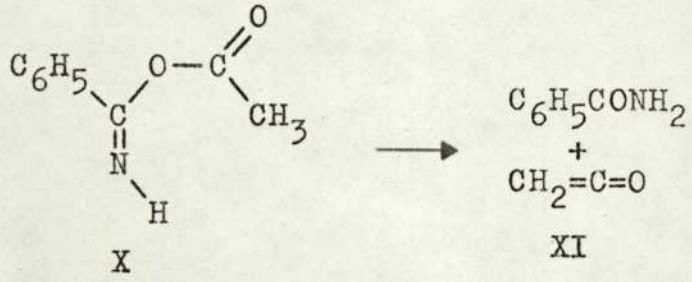

X

$C_6H_5CONH_2$ + $CH_2=C=O$

XI

3.22.

An elimination reaction such as 3.22. would be impossible for the acyl benzimidate XII, in which the acyl group is derived from the formate anion.

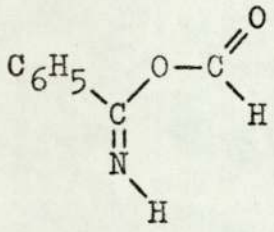

XII

This might well provide an explanation as to why nickel formate dihydrate or nickel chloride hexahydrate plus formic acid are unable to effect rearrangement in xylene.

There are several objections to this theory. Firstly, there is insufficient acetate present to produce benzamide, in the yields observed, according to the stoichiometry of equation 3.22. Secondly, the proposed product of elimination, keten, is a highly reactive species[77]. To circumvent these difficulties it is necessary to postulate that the acetate group is regenerated, either by the combination of keten with the hydroxyl group derived from benzaldoxime, or by the hydrolysis of keten by trace amounts of water.

Although this investigation was primarily concerned with the inorganic aspects of the rearrangement several experiments were undertaken in an attempt to discover the nature of the

stable organic intermediate, indicated by the kinetic studies. These are described in the following section.

3.4.2. The intermediate.

It has been suggested that nitrile intermediates may feature in the rearrangement of aldoximes to amides[70]. In this study such an intermediate would be benzonitrile.

A 0.2M solution of benzonitrile in digol exhibits an absorption at 2230cm^{-1}, with a corrected absorbance of 0.238 at a cell path length of 0.5mm. The kinetics of section 3.3. reveal that the second step in the consecutive sequence is diminishingly slow at 100°C and that ca. 75% of the intermediate should be produced after ca. 50hrs. at a catalyst concentration of 0.012M. An infrared analysis of such a reaction solution revealed no trace of any absorption between 2300cm^{-1}. and 2000cm^{-1}., even when concentrated to one quarter of its original volume. Furthermore, a 0.2M solution of benzonitrile, heated at 189°C in the presence of 0.012M nickel acetate tetrahydrate, showed no evidence of the characteristic benzamide spectrum after several hours.

Thus it seems improbable that benzonitrile is implicated in this rearrangement, or indeed, that it undergoes any hydrolysis whatsoever under the conditions of this study.

Attempts to synthesize the benzimidates from their hydrogen chloride salts (section 2.3.4.), by treatment with sodium carbonate in ethanol, produced only intractable oils which could not be crystalized. However, both 2-methoxyethyl-benzimidatehydrogenchloride (XIII) and 2-(2-hydroxyethyl)ethyl-benzimidatehydrogenchloride (XIV) were found to yield benzamide upon heating in digol with stoichiometric amounts of sodium carbonate, either in presence or absence of catalytic amounts

of nickel acetate tetrahydrate.

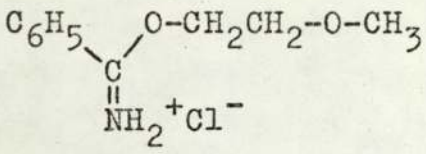

XIII

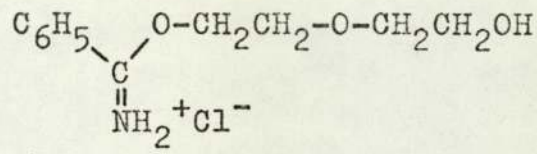

XIV

The yields of benzamide were lower than predicted from the kinetic studies, especially for the pyrolysis of XIII. However, the presence of chloride ion in these experiments may well give rise to alternative routes to benzamide. The Pinner fission[78], involving nucleophilic attack by chloride ion on the protonated imidate, is an established pyrolysis pattern of imidate hydrogen chloride salts. Such a reaction may also explain the anomolous behaviour of those chloride containing catalysts (section 3.4.1.).

The appearance of a significant peak at 1724cm^{-1}., during the thermal decomposition of these benzimidates, supports the belief that the reaction is not exactly representative of the second stage of the rearrangement. Such a peak had, in fact, been observed during the rearrangement of benzaldoxime, but it was of much lower intensity (section 3.4.3.).

In deference to these phenomena the kinetics of benzamide production from the benzimidate hydrogen chloride salts were not investigated further. However, it should perhaps be mentioned that the thermal rearrangement of alkyl benzimidates is not generally quantitative[75], in accord with the implication of the kinetic studies of section 3.3., for the second step of the consecutive reaction.

3.4.3. The thermal decomposition of digol.

During the rearrangement in digol the growth of a small peak at 1724cm^{-1}., entirely absent in the spectra of standard

benzamide solutions in digol, was observed.

The supposition that this arose from the thermal decomposition of the solvent was confirmed by heating digol at 184°C for several hours, both in the presence and absence of nickel acetate tetrahydrate. Inspection of table 3.8. reveals that the breakdown of the solvent is inhibited by the presence of the catalyst. Indeed, during a typical kinetic run the absorption at 1724cm^{-1}. did not usually exceed 0.08.

Table 3.8.

Sample	Absorbance at 1724cm^{-1}.(corr.)	Time of heating (mins.)
Digol	0.022	90
	0.30	180
Digol +0.012M $Ni(OAc)_2 4H_2O$	0.041	90
	0.14	180

This absorption is arguably due to a carbonyl group. It would seem probable that it is the alcoholic group of digol that undergoes modification, presumably to yield an aldehydic group. The pyrolysis of ethylene glycol is known to produce acetaldehyde in small quantities[79].

3.4.4. The thermal decomposition of benzaldoxime.

It has been suggested that benzaldoxime may decompose to produce benzaldehyde, ammonia and nitrogen during its rearrangement with nickel catalysts[61].

$$3C_6H_5CHNOH \longrightarrow 3C_6H_5CHO + NH_3 + N_2 \qquad 3.23.$$

Thus it was of considerable importance to establish whether such a process as 3.23. was likely under the conditions of this study.

The condenser attached to G_2 (figure 2.1.) was fitted with a suitable bubbler, containing either a few drops of hydrochloric acid or a small head of Nessler's reagent[80], during a standard run. No white fumes were observed in the former experiment. In the latter, more sensitive test, a faint colouration was noticed after some time, indicating the release of a small quantity of ammonia.

Standard solutions of benzaldehyde and benzamide were prepared in digol and subjected to infrared analysis. Table 3.9. reveals the carbonyl absorption of benzaldehyde to be readily detectable and clearly distinguishable from that of benzamide, although a slight reinforcement is observed.

Table 3.9.

Solution	Absorbance(corr.)	Wavenumber(cm^{-1}.)
Benzaldehyde(0.1M)	0.379	1700
Benzamide(0.1M)	0.591	1675
Benzaldehyde(0.1M)	0.389	1700
+benzamide(0.1M)	0.617	1675

No absorption at 1700cm^{-1}. had been discernible during any kinetic run.

The classic silver mirror test for aldehydes[81] was found to be unsuitable in this instance, since it proved positive for a standard 0.2M solution of benzaldoxime in digol.

These experiments show that the decomposition of the reagent is negligible under the conditions of this study. Indeed, if ammonia were produced in significant quantity, a blue colouration, due to the hexamminenickel(II) ion[82], might be expected in consequence. This was never observed.

The fact that the nickel catalysed isomerization of

benzaldoxime to benzamide in digol is not quantitative is therefore not due to the decomposition of benzaldoxime.

3.4.5. The isomeric form of benzaldoxime prior to rearrangement

It is generally believed[65,67] that the nickel catalysed rearrangement of aldoximes to amides involves a trans Beckmann rearrangement of the β-isomer coordinated to the metal and consequently that the α-isomer must necessarily undergo transformation to the β-isomer, prior to the production of amide.

In view of this assertion it was of interest to investigate the isomeric form of benzaldoxime, prior to rearrangement, under the conditions of this study.

The n.m.r. spectra of α and β-benzaldoxime in digol are shown in figure 3.10. Principal differences arise in the position of resonance of the C-H proton and the ortho protons of the aromatic ring. Unfortunately the presence of the paramagnetic nickel catalyst will cause line broadening of these spectra and therefore the exact experimental conditions of the kinetic study cannot be reproduced. However, the diamagnetic species, zinc chloride, was also found to effect rearrangement in digol and was therefore chosen as a substitute.

Experiments were undertaken at various catalyst concentrations and temperatures and are summarized in table 3.10.

Since it is the α-isomer of benzaldoxime that is the stable form[40c], it is this isomer that is predominant at elevated temperature and inspection of table 3.10 confirms this. All the spectra showed this to be the case at 100°C and moreover, that the positions of resonance were constant

irrespective of the concentration of zinc chloride. This latter observation implies that the α-isomer is not substantially coordinated to the metal.

Table 3.10.

Solution (conc.)		Temp.(°C)	Observations (mins)
Isomer	$ZnCl_2$		
α (0.3M)		50	α spectrum (90)
		100	α spectrum (90)
β (0.3M)		50	β spectrum (90)
		100	α spectrum (5)
α (0.3M)	(0.05M)	50	α spectrum (90)
		100	α spectrum (90)
β (0.3M)	(0.05M)	50	β spectrum (90)
		100	α spectrum (15)
α (0.3M)	(0.3M)	100	α:β ca.11:1 (80)
β (0.3M)	(0.3M)	100	α:β ca.10:1 (80)

Although the unambiguous detection of small quantities of the β-isomer is difficult in the presence of large amounts of the α-isomer, it seems probable that the introduction of zinc chloride favours the existence of the β-isomer. Work in these laboratories[83] has shown that certain metal ions in solution are able to catalyse the isomerization of the α-isomer to the β-isomer at ambient temperatures. This observation is in accord with the suggestion previously noted (section 3.1.) that the α-isomer must necessarily be converted to the β-isomer to produce a stable metal-aldoxime complex. However, it also demonstrates that such an isomerization is not stoichiometric and that the β-isomer may then be released into solution.

The overall scheme for this system may therefore be envisaged in terms of the following general processes.

$$\alpha \underset{}{\overset{K_I}{\rightleftharpoons}} \beta \qquad 3.24.$$

$$Zn + \alpha \overset{K_\alpha}{\rightleftharpoons} Zn\alpha \qquad 3.25.$$

$$Zn + \beta \overset{K_\beta}{\rightleftharpoons} Zn\beta \qquad 3.26.$$

$$Zn\alpha \xrightarrow{k_I} Zn\beta \qquad 3.27.$$

The observations of table 3.10. require that the equilibrium constants K_I, K_α and K_β be small and furthermore that the establishment of overall equilibrium at 100°C be relatively slow in the presence of zinc chloride.

It is unlikely that this latter requirement arises from the equilibrium 3.26., since such simple complex formation processes are generally rapid. The slow step is therefore suggested to be the process 3.27., namely the isomerization of the α-isomer to the β-isomer within the coordination sphere of the metal.

Figure 3.10.

Comparison of the n.m.r. spectra of α and β-benzaldoxime (in digol).

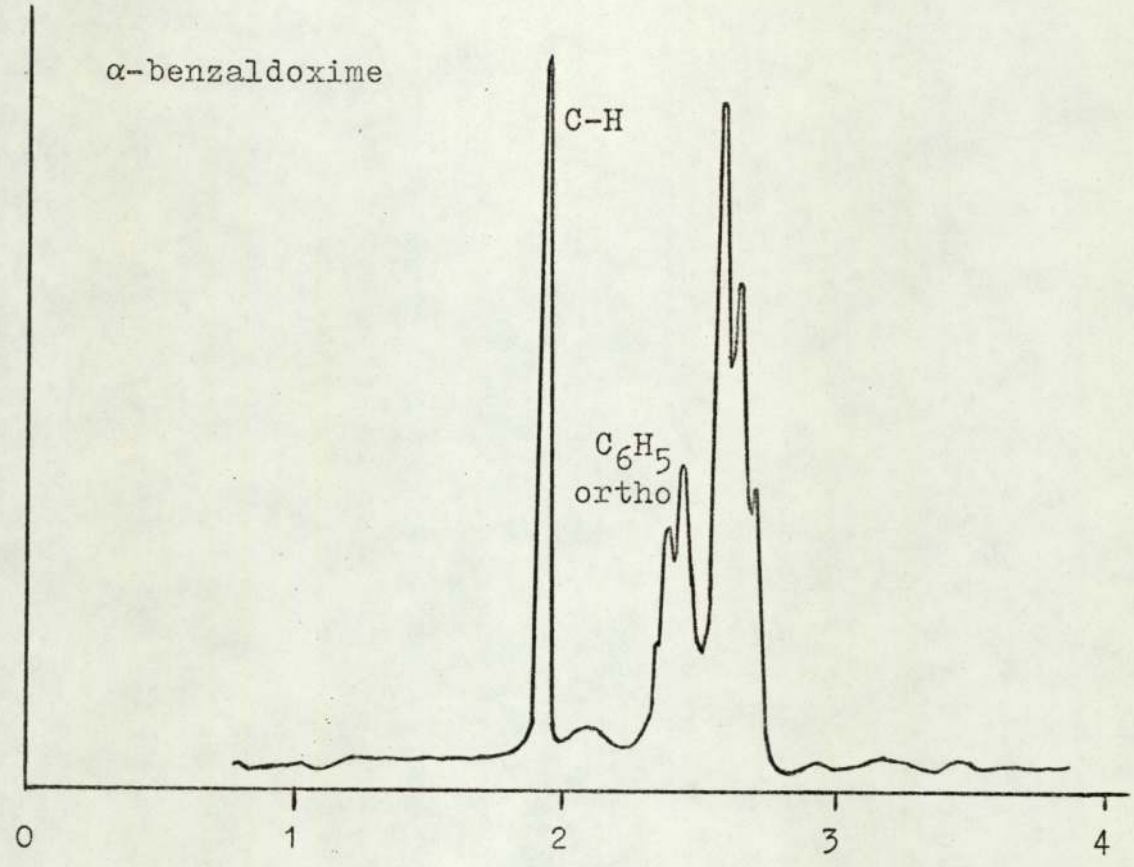

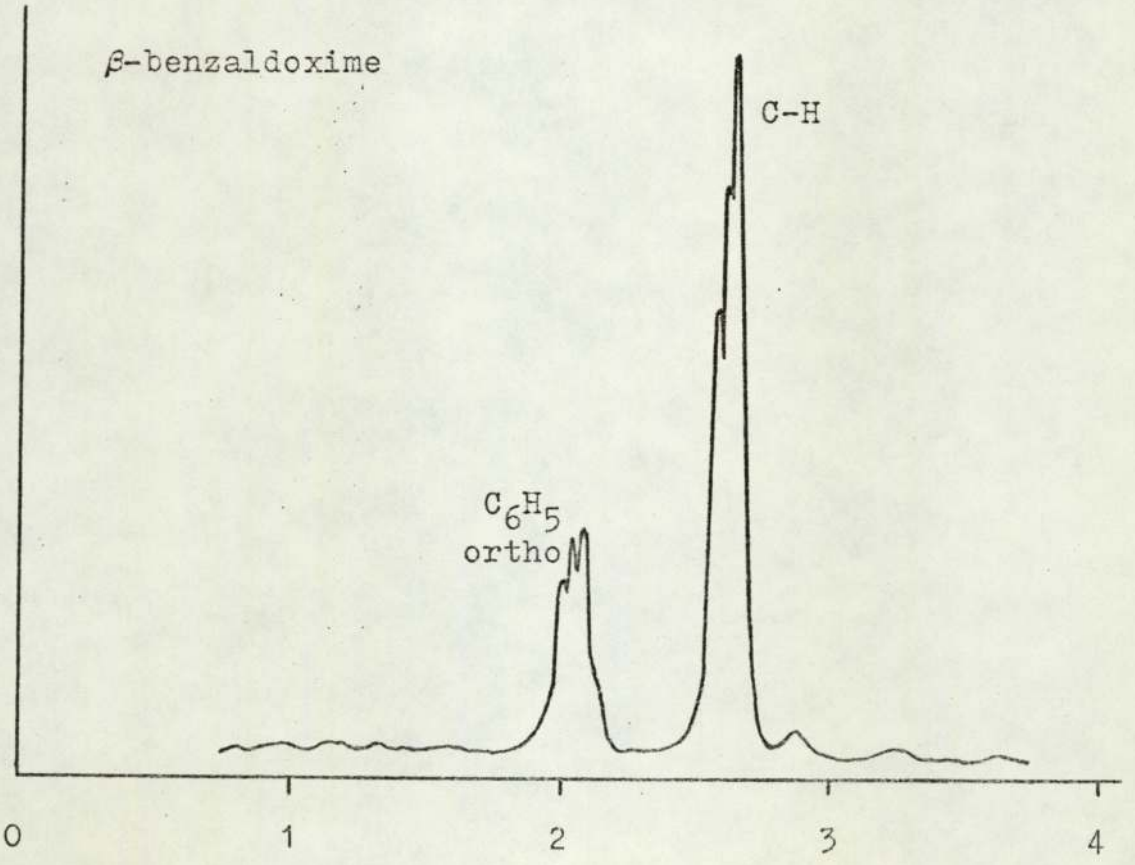

3.5. Discussion.

Complexes of β-benzaldoxime and nickel salts are relatively easy to prepare (section 2.3.5.). Strangely enough, attempts to synthesize corresponding complexes of zinc salts in these laboratories have been unsuccessful[84]. Thus it would appear that the ability of a metal ion to form the usual stable N-coordinated complexes of β-benzaldoxime is not a necessary criterion on which its catalytic potential may be assessed. Therefore, the possibility that the reactive species is a loose O-coordinated complex cannot be ignored. It may be shown with molecular models, in fact, that the only complex of a metal ion and benzaldoxime which enables the C-H group to approach the coordination sphere of the metal ion is one in which the α-isomer achieves O-coordination.

Such O-coordinated complexes are proposed in the case of boron trifluoride (section 3.1.). However, this coordination centre is alleged to effect the dehydration of p-chloro-benzaldoxime to p-chlorobenzonitrile. It is conceivable that the ability of nickel to entertain a greater number of ligands in its coordination sphere than boron might lead to a different modified chemistry of such O-coordinated aldoximes. In this context either an inner sphere process, involving the attack of a coordinated solvent molecule, or an outer sphere process, involving the attack of a free solvent molecule, upon the carbon atom of the C-H group in benzaldoxime, might be considered.

Both these processes could arguably be enhanced by the nickel assisted stabilization of the common transition state XV, through the favourable five-membered ring structure, according to the scheme 3.28.

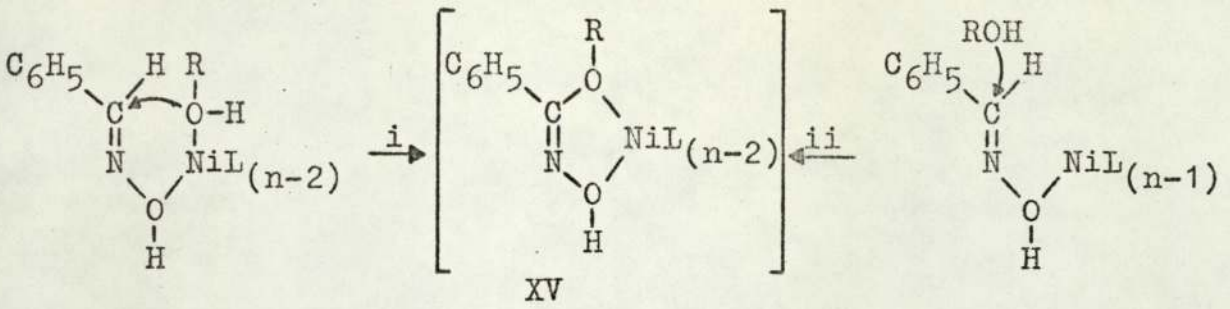

XV

3.2

The remaining ligands on nickel are designated as L and are presumed to be solvent molecules for the reasons discussed later.

An alternative possibility, supported throughout this investigation, is that the function of nickel is to modify the electronic distribution of benzaldoxime such that the carbon atom of the C=N group is rendered susceptible to nucleophilic attack. This is arguably best facilitated by N-coordination of the β-isomer, whence the electron withdrawing effect of the metal ion on the C=N bond is most pronounced.

An inner sphere process, involving the attack of a coordinated solvent molecule upon the electron deficient carbon atom, is unlikely in this case since the C-H group is removed from the coordination sphere of the metal ion. However, an outer sphere attack by a free solvent molecule may be postulated, according to scheme 3.29.

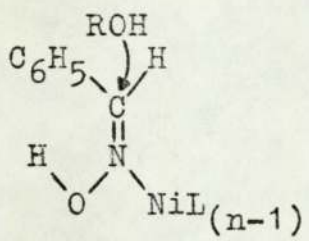

3.29.

It is difficult to envisage how nickel could undertake the stabilization of the transition state in a process of this nature, through the inherent four-membered ring structure.

Thus the respective merits of these mechanistic schemes

are to be found in the stabilization of the transition state, in the case of the O-coordinated α-isomer, and in the modification of the chemistry of the ligand upon coordination, in the case of the N-coordinated β-isomer. A reactive species involving O-coordination of the β-isomer has neither of these advantages. In addition, N-coordination of the α-isomer is sterically improbable. These two latter possibilities are therefore rendered unlikely.

Calculation of the entropy of activation, $\Delta S_a^{\ddagger}$, for the nickel dependent step gives a value of ca. $-34 cal.deg^{-1}.mol^{-1}$. The nickel dependent rate constant, k_a, is equal to the product of the preequilibrium constant, K_1, and the rate constant for the first rate determining step, k_1, (section 3.3.6.). The observed entropy of activation may therefore be expressed as

$$\Delta S_a^{\ddagger} = \Delta S_1^{o} + \Delta S_1^{\ddagger}$$

where ΔS_1^{o} is the entropy change for the preequilibrium and $\Delta S_1^{\ddagger}$ is the entropy of activation for the first step. In order to make a realistic guess for the value of ΔS_1^{o} the nature of the preequilibrium should ideally be known. In the case of the system under investigation here the relevant consideration is whether the preequilibrium involves the replacement of solvent or acetate ion by benzaldoxime, from the coordination sphere of nickel. The former process requires no overall change in charge and ΔS_1^{o} may therefore be expected to be small in magnitude. For instance, for the process

$$Ni(aq)^{2+} + NH_3 \rightleftharpoons Ni(NH_3)(aq)^{2+}$$

the entropy change is ca. $-0.5 cal.deg^{-1}.mol^{-1}$.[85]

However, the replacement of acetate ion by benzaldoxime involves an overall increase in charge and therefore a substantial negative value for ΔS_1^o might be expected. For instance, for the process

$$M(OAc)(aq)^+ \rightleftharpoons M(aq)^{2+} + OAc^-$$

an entropy change of ca. $-11 cal.deg^{-1}.mol^{-1}$. may reasonably be predicted for nickel[86].

It does not seem likely that the acetate ion would remain in the coordination sphere of nickel in the presence of an acceptable donor solvent such as digol at these temperatures. Thus it is suggested that the majority of the catalytic species is merely solvated nickel and therefore that the large negative value of the observed entropy of activation is primarily due to the first step in the reaction, the cleavage of the C-H bond of benzaldoxime.

Although it is injudicious to place too close an interpretation upon entropy arguments it is difficult to see how the unimolecular, inner sphere process 3.28.(i) could account for the observed entropy of activation. The substantial negative value found is certainly consistent with the bimolecular, outer sphere processes 3.28.(ii) and 3.29., in which a solvent molecule is incorporated.

The hydrolysis of 2-cyano-1,10-phenanthroline upon nickel has been reported to involve an outer sphere attack by free hydroxide ion upon the carbon atom of the C≡N group[87]. However, the entropy of activation is found to be $+14 cal.deg^{-1}.mol^{-1}$. and appears to contravene that normally expected for such a bimolecular process. Although the entropy change associated with the preequilibrium for complex formation is

not apparently included in this figure data is available for this process[88] and shows the value to be effectively zero. Thus the positive value quoted for the entropy of activation does, in fact, arise principally from the hydrolysis step. The apparent anomoly is explained in terms of the reduced solvation of the transition state, resulting from the bonding of the developing imino anion to nickel, which is suggested to displace a solvent molecule and to release the solvent shell around the hydroxide nucleophile.

This system is similar to the process 3.28.(ii) inasmuch as the displacement of a coordinated solvent molecule is concerned. Although the nature of the postulated transition state XV cannot be predicted thoroughly it seems unlikely that its charge would be greater than that of the reactive species. The observed large negative value of the entropy of activation would therefore seem inconsistent with the process 3.28.(ii). The more plausible mechanism appears to be that of the scheme 3.29. and consequently it is this process which is proposed for the first step of the reaction.

If the reactive species does, in fact, contain β-benzaldoxime then the process for nickel, analogous to equation 3.27. for zinc (section 3.4.5.), must be relatively rapid compared to the subsequent rate determining steps, since the first step is clearly shown to be C-H bond cleavage. It should be noted, however, that at 100°C the time of half reaction for the first step is predicted to be ca. 25hrs. for nickel.

Finally, it is suggested that the effect of O-coordination of an aldoxime to a Lewis acid or transition metal ion would quite possibly be to confine the modified chemistry of the

ligand to the N-O-H moeity and this could reasonably be expected to lead to dehydration to the nitrile. Such behaviour is observed in the case of boron trifluoride[70].

Calculation of the entropies of activation for the main and side reactions of the intermediate gives values of ca. $-17 cal.deg^{-1}.mol^{-1}$. and $+8 cal.deg^{-1}.mol^{-1}$. respectively. The elimination reaction of the alkyl benzimidate VIII, postulated for the former reaction (section 3.4.1.), might be expected to show a positive entropy of activation. The significant negative value found suggests, possibly, that the solvent may play some role in the main reaction path[89]. The small positive entropy of activation, found for the side reaction, might be taken to imply a molecular fragmentation of the intermediate to produce side products.

The nature of the side products in this reaction are unknown. It has been reported[65] that the compound N,N'-benzylidenebis(benzamide) is produced during the nickel acetate tetrahydrate catalysed rearrangement of benzaldoxime to benzamide, in xylene. This product was suggested to result from the condensation of benzamide with either benzaldoxime or benzaldehyde. The kinetic studies and related experiments of this chapter preclude such reactions in digol.

3.6. Proposed reaction mechanism.

The following overall reaction mechanism is postulated for the nickel(II) catalysed rearrangement of benzaldoxime to benzamide in digol.

The catalytic species is designated as NiL_n, where L_n refers to suitable ligands derived from the reaction medium, most probably solvent molecules.

Initially, the relatively rapid establishment of the equilibrium 3.30., heavily in favour of free α-benzaldoxime, is suggested.

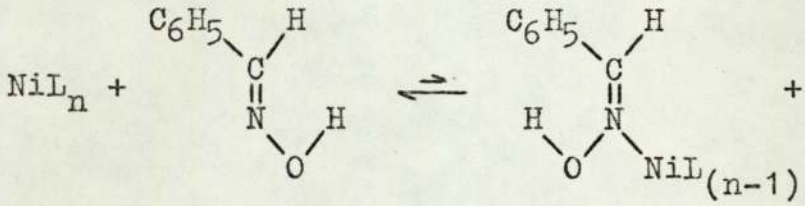

XVI

The complex XVI contains one β-benzaldoxime ligand, coordinated through the nitrogen atom to nickel(II), which is presumed to cause modification of the electronic distribution of the ligand, such that the carbon atom of the C=N group is electron deficient. The first rate determining step in the consecutive sequence is suggested to be nucleophilic attack, at this carbon atom, by a suitable oxygen containing nucleophile in solution, in this case digol. Although nothing is known about the cleavage of the N-O bond it seems reasonable to propose that the loss of hydroxide occurs simultaneously, according to equation 3.31.

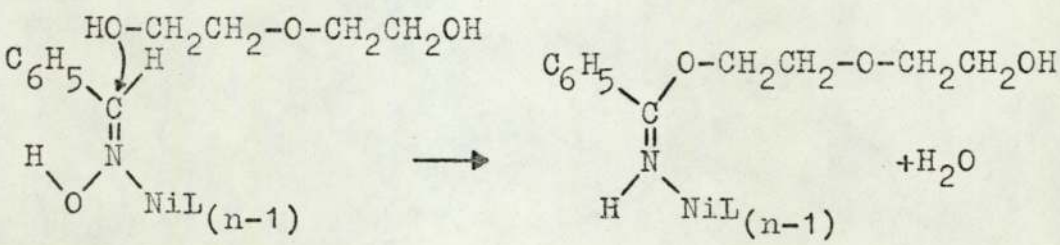

XVII

The complex XVII, of the alkyl benzimidate VIII (section 3.4.1.), is probably almost completely dissociated in digol

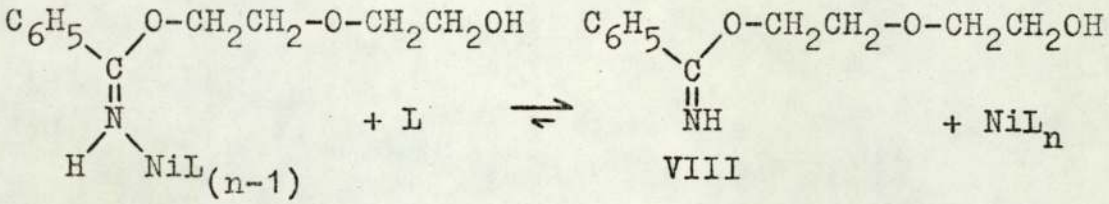

Subsequently the alkyl benzimidate VIII is believed to undergo an elimination reaction to produce benzamide and the alkene IX, and also at least one side reaction leading to side products.

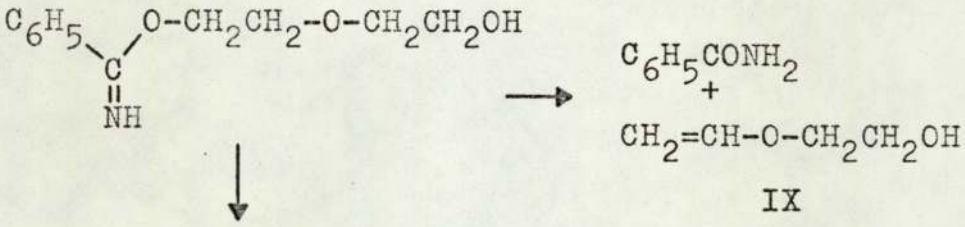

Side products

4. An investigation of the ligand substitution reactions of the tetrachloroplatinite(II) ion in aqueous systems of acetonitrile.

4.1. Introduction.

The stable complex dichlorobis(acetonitrile)platinum(II) was first prepared by Hoffmann and Bugge[90] and assigned the cis configuration, on the basis of its reactions, by Lebedinski and Golovnaya[91]. The infrared spectrum of this complex shows the increase in the nitrile group stretching frequency, relative to that of the free nitrile, typically observed for dihalobis(nitrile)platinum(II) complexes[92]. This is suggested to exclude the possibility of direct pi interaction between the C≡N bond and the metal ion and to imply coordination to occur through the nitrogen atom of the nitrile group.

Although the kinetics of the ligand substitution reactions of square planar complexes of platinum(II) have been extensively investigated[93], the simple systems of the tetrachloroplatinite(II) ion and organic nitriles appear to have been overlooked.

It has been previously mentioned (section 2.2.2.) that the formation of a deep blue solution (blau) is observed, under certain conditions, in aqueous systems of potassium tetrachloroplatinite and acetonitrile. A kinetic study of this phenomenon is reported in chapter 5. Inasmuch as the production of the blau proved to be dependent upon a complex series of processes, any additional, independent kinetic information upon the system was important. Accordingly an investigation of the ligand substitution reactions of the tetrachloroplatinite(II) ion in aqueous solutions containing acetonitrile was undertaken.

The simple aqueous system of the tetrachloroplatinite(II)

ion, in the absence of additional ligands, has been comprehensively studied at ambient temperatures[94,95,96,97,98]. Grantham, Elleman and Martin[94] reported the first hydrolysis step to be first order in the tetrachloroplatinite(II) ion and the replacement of coordinated water by chloride ion to be first order in the trichloroaquoplatinite(II) ion and first order in chloride ion (equation 4.1.).

$$PtCl_4^{2-} + H_2O \underset{k_{-s}}{\overset{k_s}{\rightleftharpoons}} PtCl_3(H_2O)^- + Cl^- \qquad 4.1.$$

In addition, they were able to show the ionization constant for the weak acid, the trichloroaquoplatinite(II) ion, to be ca. 10^{-7}mol.litre^{-1}, from the potentiometric titration of aged solutions of the tetrachloroplatinite(II) ion (equation 4.2.).

$$PtCl_3(H_2O)^- \overset{K_i}{\rightleftharpoons} PtCl_3(OH)^{2-} + H^+ \qquad 4.2.$$

They suggested the second hydrolysis step to be relatively slow compared to the first (equation 4.3.).

$$PtCl_3(H_2O)^- + H_2O \rightleftharpoons PtCl_2(H_2O)_2 + Cl^- \qquad 4.3.$$

Elding and Leden[97] reported the equilibrium constant for the first hydrolysis step to be greater, by a factor of ca. 10, than that for the second, at 25°C.

In the system under investigation here it was necessary to establish accurate kinetic information upon the hydrolysis of the tetrachloroplatinite(II) ion. The literature data[94,98] refers to studies over an ambient temperature range and it was felt that extrapolation to the higher temperatures involved in this study could lead to significant inaccuracies.

Initially, therefore, the hydrolysis of the tetrachloroplatinite(II) ion was investigated over an elevated temperature range. The results obtained were subsequently used to enable a kinetic evaluation of the ligand substitution reactions of the tetrachloroplatinite(II) ion in aqueous systems of acetonitrile, over a similar temperature range.

This work is reported in the remaining sections of chapter 4.

4.2. Kinetics of the ligand substitution reactions of the tetrachloroplatinite(II) ion.

The ultraviolet-visible spectrum of a fresh solution of potassium tetrachloroplatinite exhibits principle absorptions at 196nm. and 218nm. in the ultraviolet, with extinction coefficients of ca. 9000 and at 334nm. and 395nm. in the visible, with extinction coefficients of ca. 900. As the solution ages the absorptions at 218nm. and 395nm. gradually disappear. The ultraviolet-visible spectra of a fresh and a fully aged solution of potassium tetrachloroplatinite are shown in figure 4.1.

Thus the concentration of the tetrachloroplatinite(II) ion may be monitered as a function of the optical density at a suitable wavelength near 218nm. or 395nm., providing Beer's law is obeyed. The former wavelength was chosen since more dilute solutions could be studied. Since lithium perchlorate was used to maintain the ionic strength and has an appreciable absorption below 210nm., the wavelength chosen for study was 228nm. The perchlorate ion was found to have no significant absorption at this wavelength, at concentrations of up to 0.1M.

A plot of the concentration of fresh potassium tetrachloroplatinite against the optical density at 228nm. is shown in figure 4.2. and exhibits a good straight line dependence, revealing Beer's law to be obeyed at this wavelength.

All kinetic studies were undertaken at a potassium tetrachloroplatinite concentration of 10^{-4}M, unless otherwise stated.

4.2.1. Hydrolysis of the tetrachloroplatinite(II) ion.

The experimental technique was based on that described in section 2.2.2.2. with the exception that acetonitrile was replaced by known concentrations of potassium chloride.

The behaviour of the tetrachloroplatinite(II) ion in aqueous solution may be considered in terms of the following reactions.

$$PtCl_4^{2-} + H_2O \underset{k_{-s}}{\overset{k_s}{\rightleftharpoons}} PtCl_3(H_2O)^- + Cl^- \qquad 4.1.$$

$$PtCl_3(H_2O)^- \overset{K_i}{\rightleftharpoons} PtCl_3(OH)^{2-} + H^+ \qquad 4.2.$$

Support for the assertion that the second hydrolysis step is slow, in comparison with the first, was found in this study and is reported in section 4.2.2. Thus higher aquation steps may be neglected. Direct substitution by hydroxide ion may be ignored since the hydroxide ion exhibits a low nucleophilicity for platinum(II)[95,96]. Furthermore, over the pH range of this study, the concentration of hydroxide ion is infinitesimally small.

Considering, therefore, 4.1. and 4.2.

Let

$r_o = \left[PtCl_4^{2-}\right]$ at zero time

$r = \left[PtCl_4^{2-}\right]$ at time t

$a_2 = \left[PtCl_3(H_2O)^-\right]$ at time t

$a_3 = \left[PtCl_3(OH)^{2-}\right]$ at time t

$H = \left[H^+\right]$ and $Cl = \left[Cl^-\right]$

Therefore, we may define

$$r_o = r + a_2 + a_3 \qquad 4.4.$$

and $$K_i = (a_3/a_2)H \qquad 4.5.$$

We have that

$$-\frac{dr}{dt} = k_s r - k_{-s} a_2 Cl$$

From 4.4. and 4.5.

$$-\frac{dr}{dt} = k_s r - \frac{k_{-s} Cl(r_o - r)}{(1+K_i/H)}$$

This may be rearranged to the exact equation

$$\frac{dr}{dt} = -(k_s + \frac{k_{-s} Cl}{(1+K_i/H)})(r - \frac{k_{-s} Cl r_o}{((1+K_i/H)k_s + k_{-s} Cl)})$$

Integration of this gives the general equation

$$\frac{(r-r_\infty)}{(r_o-r_\infty)} = e^{-k_{obs}t} \qquad 4.6.$$

where $r_\infty = \left[PtCl_4^{2-}\right]$ at infinite time

Equation 4.6. is the form of a first order equation governing the disappearance of the tetrachloroplatinite(II) ion. The observed rate constant, k_{obs}, is related to the rate constant for the forward reaction, k_s, that for the back reaction, k_{-s}, and the ionization constant, K_i, by the relation

$$k_{obs} = k_s + \frac{k_{-s} Cl}{(1+K_i/H)} \qquad 4.7.$$

The concentration of the tetrachloroplatinite(II) ion, r, is measured as a function of the optical density, D, at 228nm. Thus equation 4.6. may be rewritten as

$$\frac{(D-D_\infty)}{(D_o-D_\infty)} = e^{-k_{obs}t} \qquad 4.8.$$

It may be shown that if all three platinum(II) species, depicted in the equilibria 4.1. and 4.2., absorb at 228nm. equation 4.8. is still valid.

At low pH, such that the hydrogen ion concentration, H, is very much greater than the ionization constant, K_i, equation 4.7. will reduce to

$$k_{obs} = k_s + k_{-s}Cl \qquad 4.9.$$

and no acid should be produced.

Using the apparatus described in section 2.2.2.2. the pH of the solution may be monitered during the establishment of the equilibrium 4.1. If there is no change in the pH the equilibrium 4.2. may be considered not to operate and equation 4.9. to hold. This is experimentally observed below pH 5.

Accordingly a series of kinetic runs were undertaken at pH 4 and varying chloride ion concentration. The required pH was attained by suitable addition of perchloric acid and the ionic strength maintained at 0.1 with lithium perchlorate. Each series was repeated at four different temperatures.

The experimentally observed curves are described by equation 4.8. The accuracy of k_{obs} depends upon the experimentally unreliable value of D_o. In order to avoid this problem the data was treated in the manner described in appendix 6. The observed rate constant was calculated using the least squares computer program HYDR, for $D = D_\infty(1 - e^{-kt})$, shown in appendix 2. The results are tabulated in figure 4.3.

Consistent with the prediction of equation 4.9. plots of k_{obs} against chloride ion concentration at each temperature give good straight lines. These plots are exhibited in figures 4.5. and 4.6. Evaluation of the slope in each case gives a

value for k_{-s}. Equation 4.9. then enables a calculation of k_s, which may be checked against the intercept. The values thus obtained are shown in table 4.1. and include the standard deviation of k_{-s}, calculated from figures 4.5. and 4.6. and the approximate formula given in appendix 5.

Table 4.1.

Temp.(°C)	$k_s(min^{-1})$	$k_{-s}(l.mol^{-1}min^{-1})$
50.0	0.0335	1.30 ±4%
57.0	0.0685	2.37 ±4%
64.0	0.141	4.11 ±3%
70.0	0.244	6.36 ±4%

Arrhenius plots for k_s and k_{-s} are shown in figures 4.7. and 4.8. In both cases a good straight line dependence is shown. Evaluation of the slopes gives activation energies of 22.5 $Kcal.mol^{-1}$ for the aquation of the tetrachloroplatinite(II) ion and 17.6 $Kcal.mol^{-1}$ for the replacement of coordinated water by chloride ion, from the trichloroaquoplatinite(II) ion. The standard deviations of these activation energies are calculated to be within ±2% (appendix 5).

Equation 4.7. predicts that k_{obs} will show a dependence upon the hydrogen ion concentration. However, a significant variation in k_{obs} will occur only over a narrow pH range. At high pH, such that the hydrogen ion concentration is very much less than the ionization constant, equation 4.7. will reduce to $k_{obs} = k_s$. At low pH equation 4.7. will reduce to equation 4.9., as previously discussed. Thus k_{obs} will vary with pH between the limits k_s and $k_s + k_{-s}Cl$. The amount by which k_{obs} will vary with pH is therefore governed by the $k_{-s}Cl$ term. Clearly it is desirable to make this a maximum, however, an

increase in the concentration of chloride ion serves to displace the equilibrium 4.1. in favour of the tetrachloroplatinite(II) ion. Hence, the curve describing its disappearance becomes difficult to measure accurately. Chloride ion concentrations of 0.01M were used.

The actual pH range over which k_{obs} varies measurably was found experimentally to be between 5 and 7. k_{obs} is tabulated as a function of pH at 64°C in figure 4.4.

Equation 4.7. may be rearranged

$$1/(k_{obs}-k_s) = 1/k_{-s}Cl + K_i/k_{-s}ClH \qquad 4.10.$$

Thus, a plot of $1/(k_{obs}-k_s)$ against 1/H should give a straight line, of slope $K_i/k_{-s}Cl$ and intercept $1/k_{-s}Cl$. Unfortunately, k_{obs} is never much greater than k_s at this chloride ion concentration. Hence, the reciprocal $1/(k_{obs}-k_s)$ is prone to considerable error. Furthermore, holding the pH constant at a particular value is experimentally difficult. Thus the plot obtained and shown in figure 4.9. is as expected rather poor. However, evaluation of the slope of the best straight line through the points enables a value of 3.5×10^{-7} mol litre^{-1} to be estimated for the ionization constant, K_i. Calculation of the standard deviation of K_i suggests an accuracy of $\pm 0.6 \times 10^{-7}$ mol litre^{-1}.

Finally, the effect of the ionic strength, μ, upon k_{obs} was investigated at 64°C. The concentration of chloride ion was chosen at 0.01M. Table 4.2. reveals k_{obs} to be independent of the ionic strength over the range 0.01 to 0.1. Presumably this is due to the minor contribution from the back reaction at this chloride ion concentration.

Table 4.2.

μ	$k_{obs}(min^{-1})$
0.01	0.184
0.05	0.184
0.10	0.185

4.2.2. Hydrolysis of the trichloroaquoplatinite(II) ion.

Above pH 5 the hydrolysis of the tetrachloroplatinite(II) ion is accompanied by the release of acid. In the absence of added chloride ion the equilibrium 4.1. will not operate and the first aquation step will be essentially complete. The amount of acid produced per platinum atom will therefore depend on the pH, since the constancy of the ionization constant, K_i, must be maintained. At pH 7 equation 4.5. predicts that there should be ca. 0.78mol of hydrogen ion released per mol of platinum(II) at 64°C.

Figure 4.10. shows a typical acid release profile under these conditions. Here 4mls. of added base corresponds to one proton released per platinum atom. It is seen that the curve is not asymptotic to a value of ca. 3mls., as would be expected for only one hydrolysis step. In fact, a slow production of acid is observed after the completion of the first hydrolysis step is established spectrophotometrically, indicating the presence of a second slow aquation step. Furthermore, the slow generation of acid is continued beyond a value of two protons per platinum atom. Thus the existence of a third and even a fourth aquation step is suggested. Ultimately a greyish precipitate develops, probably platinum metal.

These experiments confirm the supposition[94] that the first step, in the stepwise aquation of the tetrachloroplatinite(II)

ion, is relatively rapid in comparison with the subsequent steps.

4.2.3. Substitution of chloride ion by acetonitrile in the tetrachloroplatinite(II) ion.

The ligand substitution reactions of square planar complexes of platinum(II) have been shown to proceed through two parallel routes[93,99]. The first involves an initial slow substitution by the solvent, followed by a rapid replacement of the solvent by the ligand. The second involves a slow direct substitution by the ligand itself.

The behaviour of the tetrachloroplatinite(II) ion in aqueous solution containing acetonitrile may therefore be considered in terms of the following reactions.

$$PtCl_4^{2-} + H_2O \underset{k_{-s}}{\overset{k_s}{\rightleftharpoons}} PtCl_3(H_2O)^- + Cl^- \qquad 4.1.$$

$$PtCl_3(H_2O)^- + CH_3CN \overset{K_R}{\rightleftharpoons} PtCl_3(CH_3CN)^- + H_2O \qquad 4.11.$$

$$PtCl_4^{2-} + CH_3CN \underset{k_{-L}}{\overset{k_L}{\rightleftharpoons}} PtCl_3(CH_3CN)^- + Cl^- \qquad 4.12.$$

As in section 4.2.1. the deprotonation of the trichloroaquoplatinite(II) ion may be ignored below pH 5.

It may be shown that the disappearance of the tetrachloroplatinite(II) ion, for this reaction scheme, is governed by an equation of identical form to equation 4.6. (section 4.2.1.). In this case the observed rate constant, k_{obs}, is related to the kinetic parameters of the system by the expression

$$k_{obs} = k_s + k_L L + \frac{(k_{-s}+k_{-L}L)}{(1+K_R L)} \qquad 4.13.$$

where L = $[CH_3CN]$.

In the absence of added acetonitrile equation 4.13. reduces to equation 4.9., consistent with the scheme discussed in section 4.2.1. In the absence of added chloride ion equation 4.13. becomes

$$k_{obs} = k_s + k_L L \qquad 4.14.$$

which is in fact the two-term rate law governing the ligand substitution reactions of square planar platinum(II)[99].

The disappearance of the tetrachloroplatinite(II) ion was monitored spectrophotometrically as before at pH 4 and a constant ionic strength of 0.1. However, chloride ion was replaced by known concentrations of acetonitrile, which was found to absorb at 195nm., with an extinction coefficient of 1.6 and therefore to have a negligible interference at the concentrations used. Again studies were undertaken at four different temperatures.

In contrast to the work with added chloride ion the experimentally observed curves are not fully described by equation 4.8. The latter portion includes a contribution from an absorbing species not directly related to the tetrachloroplatinite(II) ion. Under these conditions equation 4.6. may no longer be expressed in the form of equation 4.8. Fortunately, the production of this absorbing species occurs slowly and its contribution to the experimental curves is not substantial. Consequently, the first ca. 75% of the curves were treated satisfactorily with the least squares computer program HYDR, for $D = D_\infty (1 - e^{-kt})$, as before and the values of k_{obs} thus obtained are shown in figure 4.11.

Consistent with the prediction of equation 4.14. plots of

k_{obs} against acetonitrile concentration at each temperature give good straight lines. These plots are shown in figures 4.12. and 4.13. The intercept, k_s, is included as a valid point since its value is known from the previous work (section 4.2.1.). The rate constant for the direct substitution path, k_L, may be evaluated from the slope in each case. The values thus obtained are shown in table 4.3. and include the standard deviation, calculated from figures 4.12. and 4.13. and the approximate formula given in appendix 5.

Table 4.3.

Temp.(°C)	k_L(l.mol^{-1}min^{-1})
50.5	1.09 ±3%
57.0	1.64 ±2%
64.0	2.90 ±3%
70.0	4.38 ±3%

An Arrhenius plot for k_L is shown in figure 4.14., from which an activation energy of 16.2 Kcal.mol^{-1} is calculated. The standard deviation is calculated to be within ±5% (appendix 5).

Figure 4.1.

Ultraviolet-visible spectra of fresh and fully aged aqueous solutions of potassium tetrachloroplatinite.

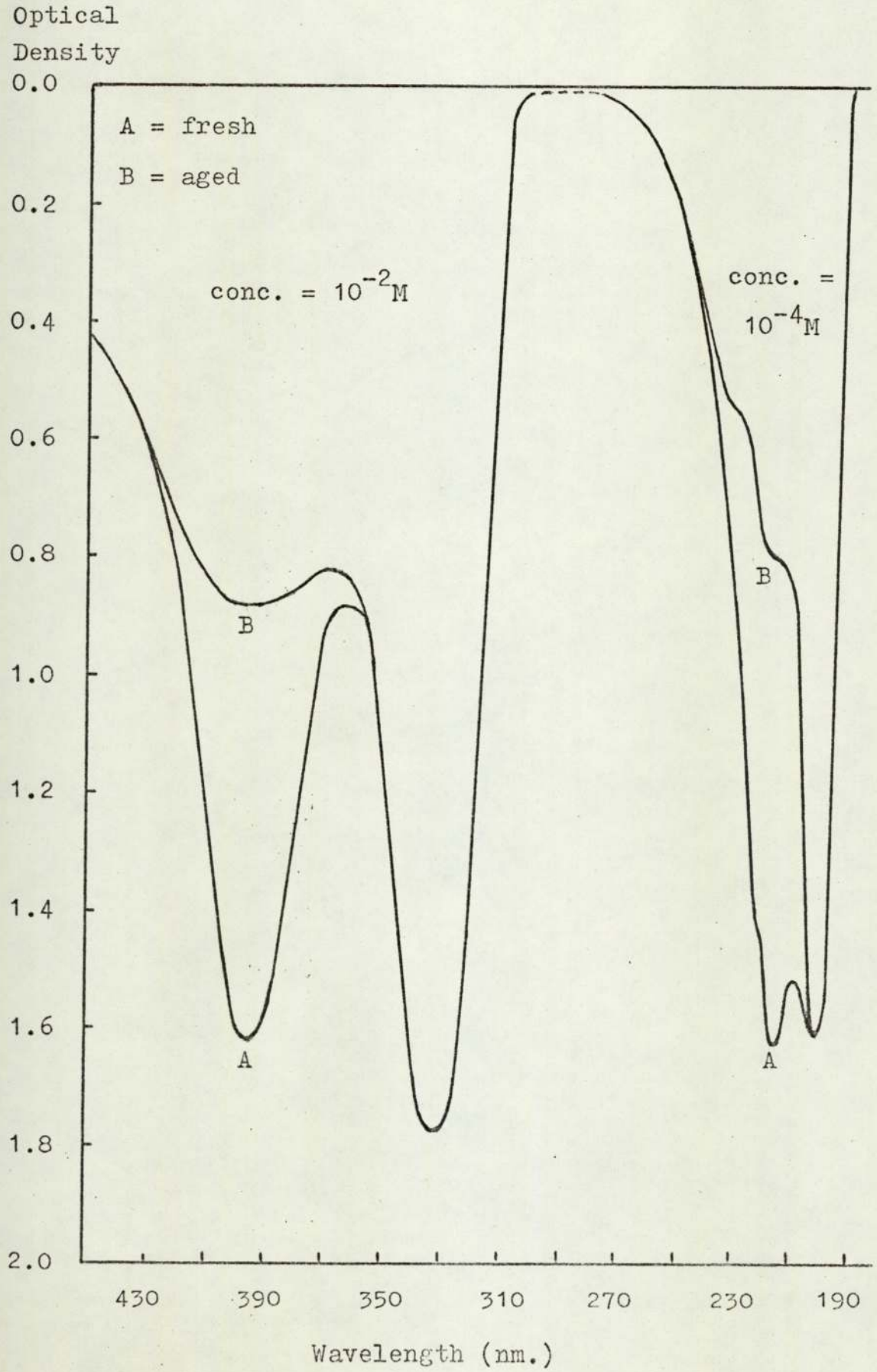

Figure 4.2.

Plot of optical density at 228nm. against concentration of potassium tetrachloroplatinite.

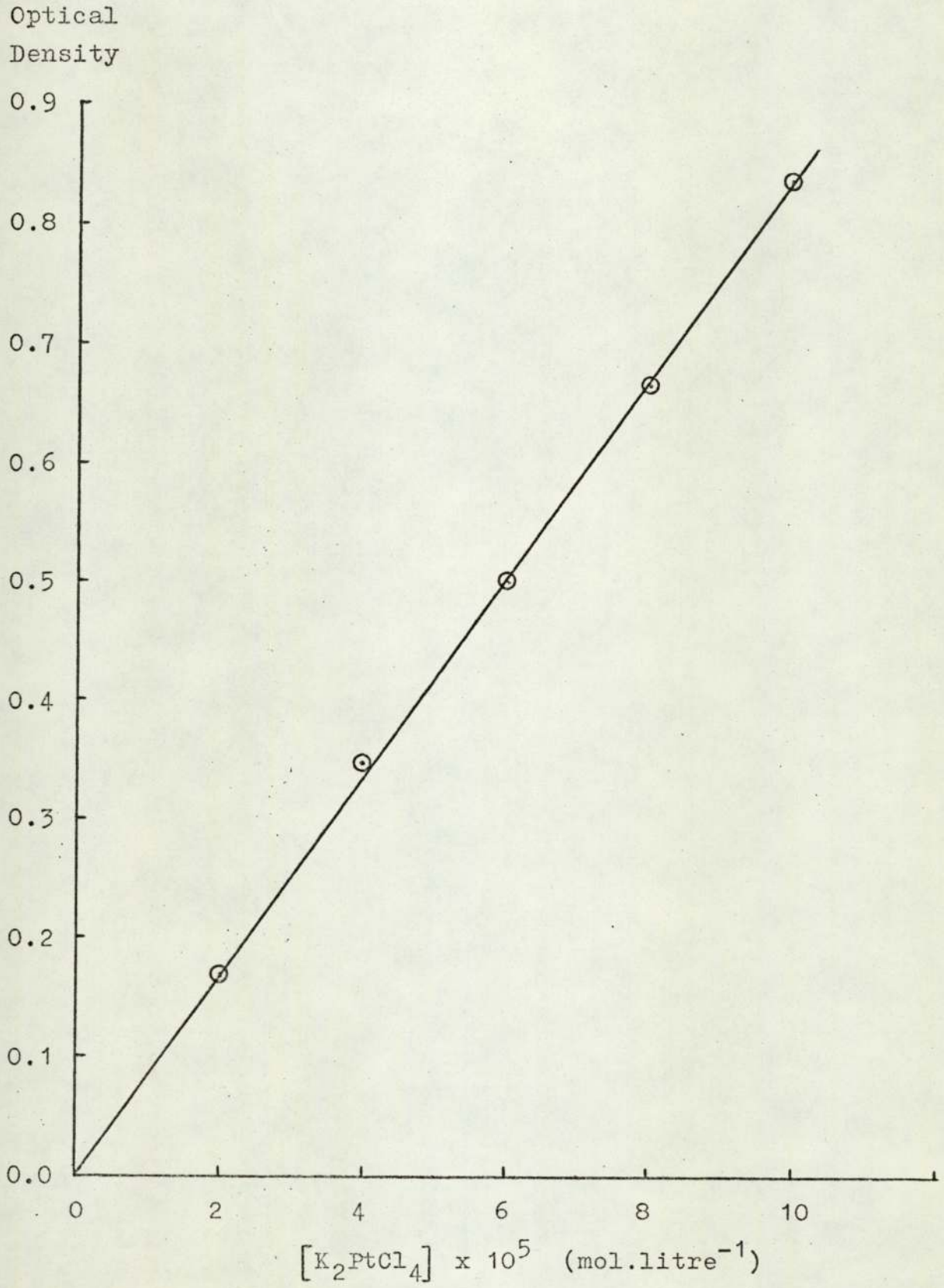

Figure 4.3.

Variation of k_{obs} with $[Cl^-]$ at pH 4 and an ionic strength of 0.1.

Temp. (^oC)	$[Cl^-]$ (mol.litre^{-1})	k_{obs} (min^{-1})
50.0	0.005	0.0402
	0.010	0.0463
	0.015	0.0528
	0.020	0.0598
57.0	0.005	0.0813
	0.010	0.0917
	0.015	0.104
	0.020	0.117
64.0	0.005	0.163
	0.010	0.184
	0.015	0.204
	0.020	0.223
	0.030	0.269
	0.040	0.313
70.0	0.005	0.277
	0.010	0.309
	0.015	0.338
	0.020	0.374

Figure 4.4.

Variation of k_{obs} with pH at a chloride ion concentration of 0.010M and an ionic strength of 0.1.

Temp. (^oC)	pH	k_{obs} (min^{-1})
64.0	5.0	0.181
	6.0	0.176
	6.3	0.164
	6.6	0.158
	6.85	0.153

Figure 4.5.

Plots of k_{obs} against $[Cl^-]$ at a concentration of 10^{-4}M potassium tetrachloroplatinite, pH 4 and an ionic strength of 0.1.

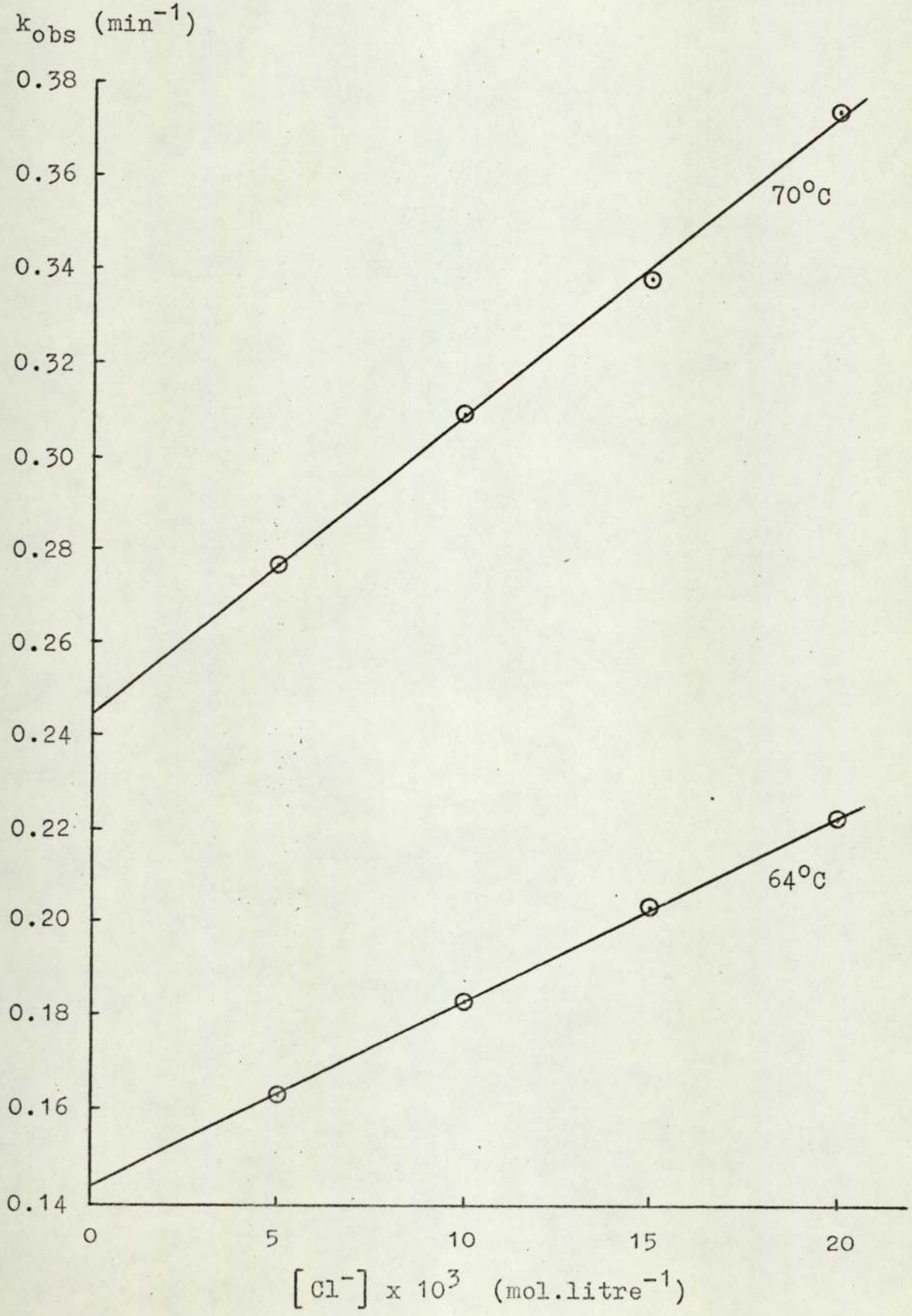

Figure 4.6.

Plots of k_{obs} against $[Cl^-]$ at a concentration of 10^{-4}M potassium tetrachloroplatinite, pH 4 and an ionic strength of 0.1.

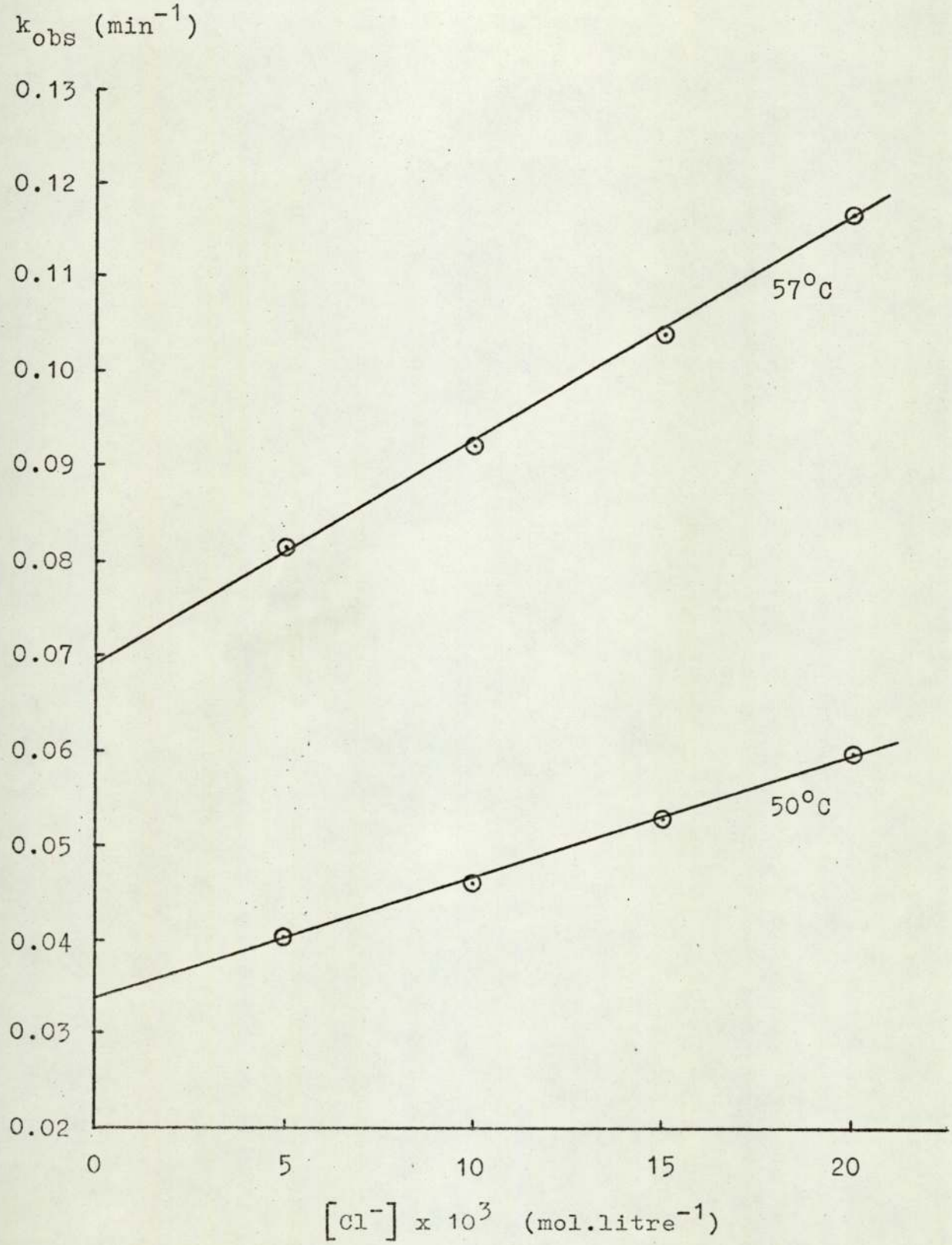

Figure 4.7.

Plot of $\log_{10} k_s$ against 1/T

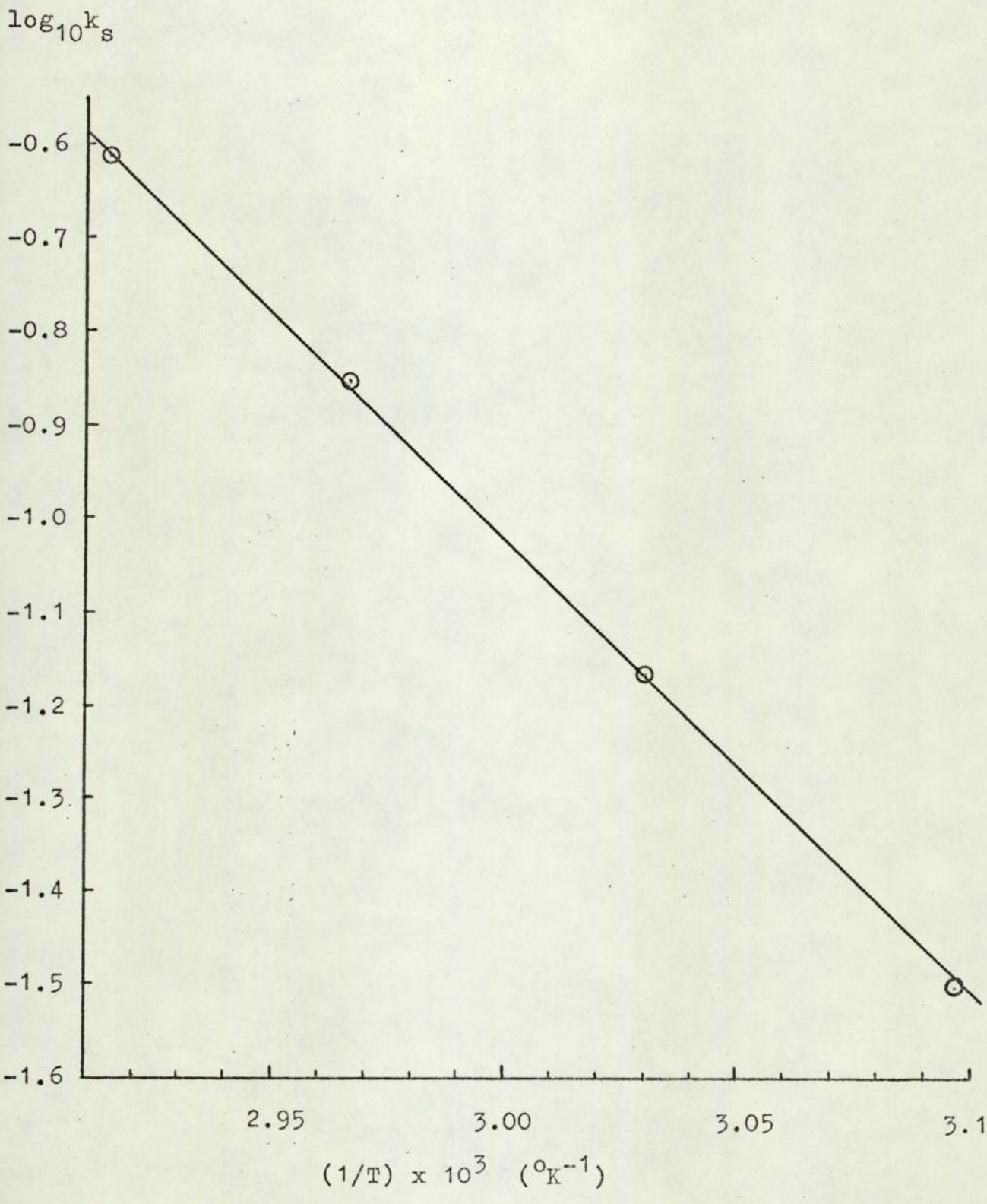

Figure 4.8.

Plot of $\log_{10} k_{-s}$ against 1/T

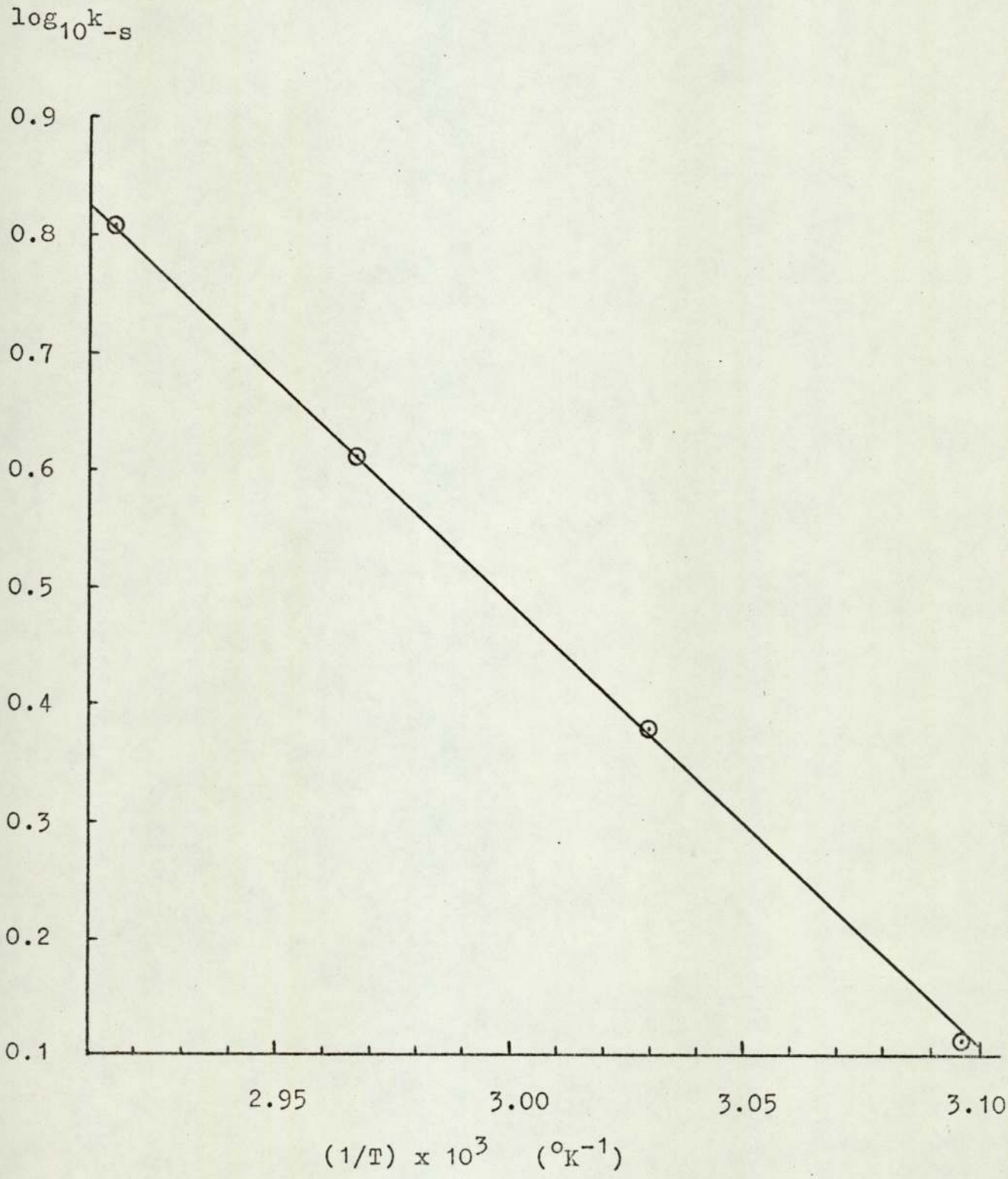

Figure 4.9.

Plot of $1/(k_{obs}-k_s)$ against $1/[H^+]$

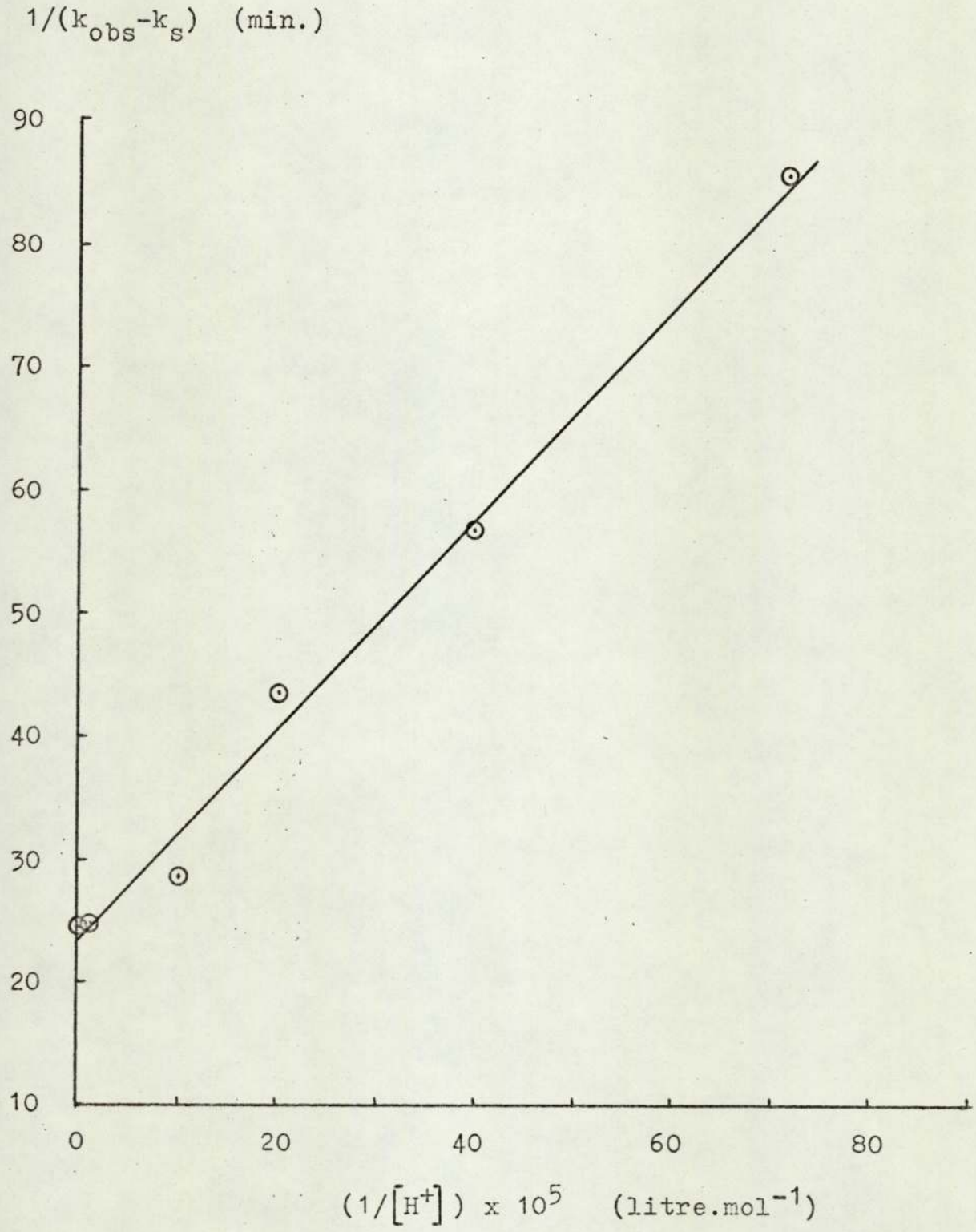

Figure 4.10.

Plot of the volume of base added against time at a concentration of 10^{-4}M potassium tetrachloroplatinite, pH 7 and 64°C.

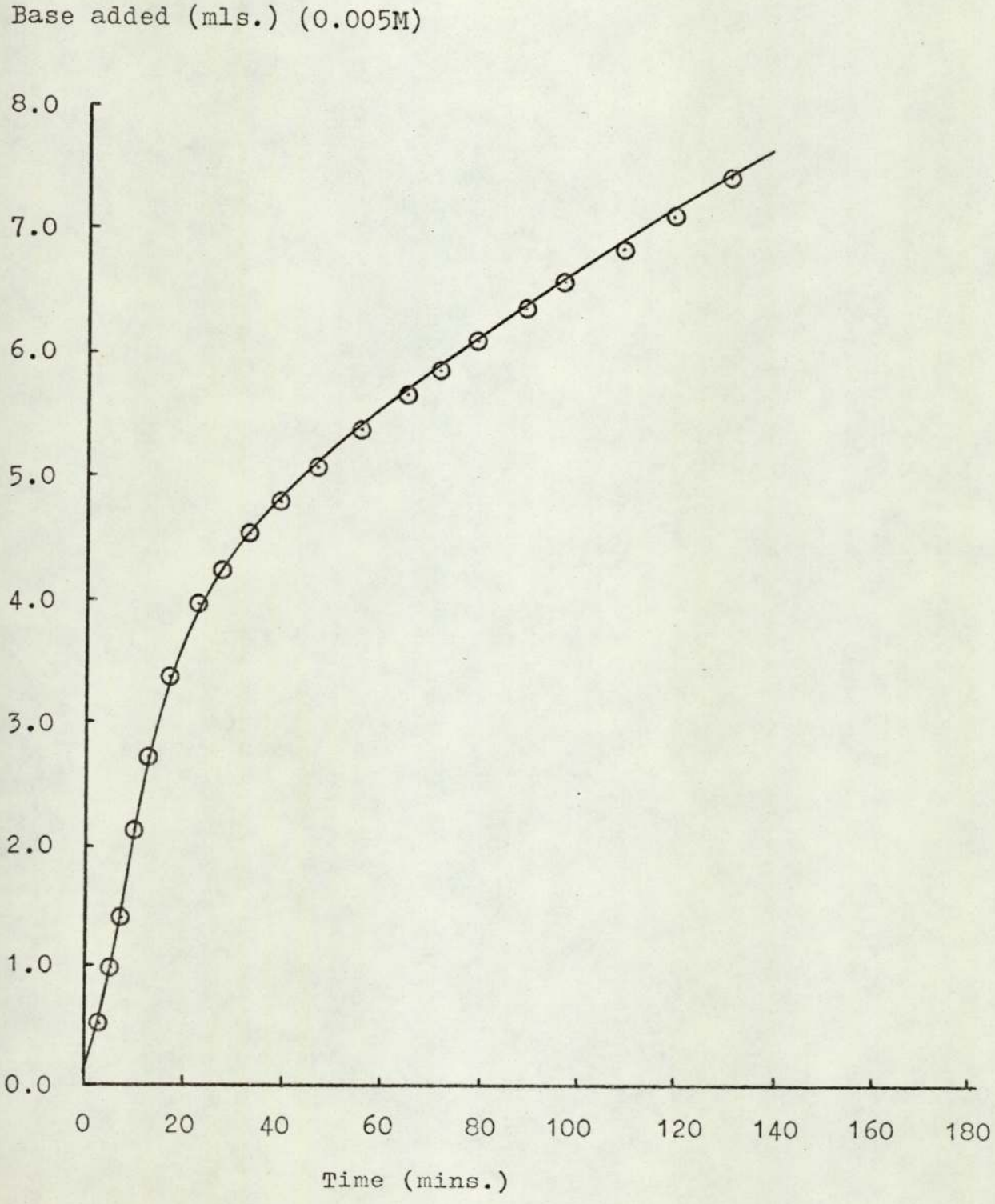

Figure 4.11.

Variation of k_{obs} with $[CH_3CN]$ at pH 4 and an ionic strength of 0.1.

Temp. (^{o}C)	$[CH_3CN]$ (mol.litre^{-1})	k_{obs} (min^{-1})
50.5	0.01	0.0447
	0.02	0.0549
	0.03	0.0663
	0.04	0.0767
57.0	0.01	0.0848
	0.02	0.101
	0.03	0.118
	0.04	0.134
64.0	0.01	0.176
	0.02	0.202
	0.03	0.230
	0.04	0.261
	0.05	0.292
	0.06	0.321
70.0	0.01	0.286
	0.02	0.328
	0.03	0.373
	0.04	0.420

Figure 4.12.

Plots of k_{obs} against $[CH_3CN]$ at a concentration of 10^{-4}M potassium tetrachloroplatinite, pH 4 and an ionic strength of 0.1.

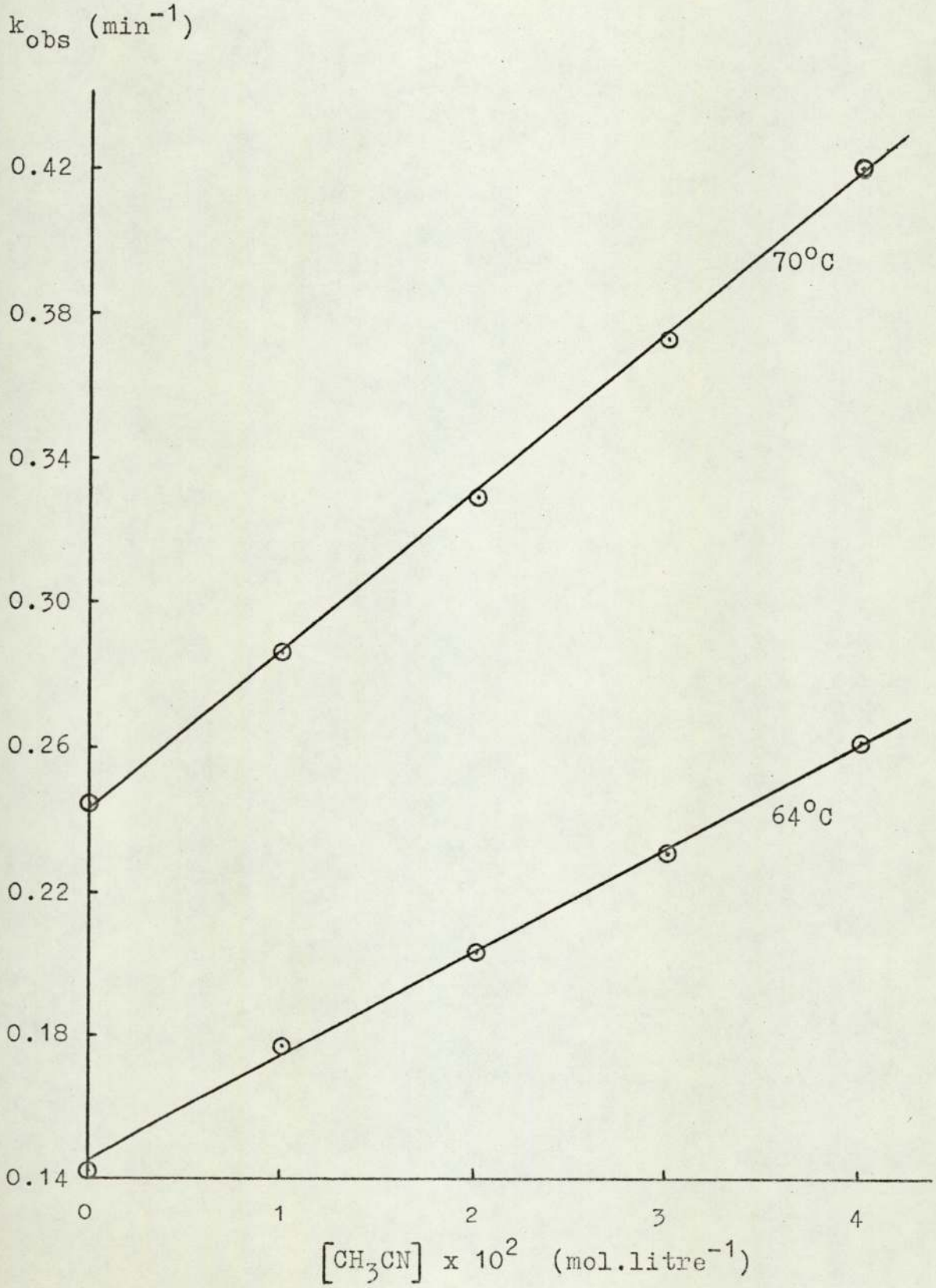

Figure 4.13.

Plots of k_{obs} against $[CH_3CN]$ at a concentration of 10^{-4}M potassium tetrachloroplatinite, pH 4 and an ionic strength of 0.1.

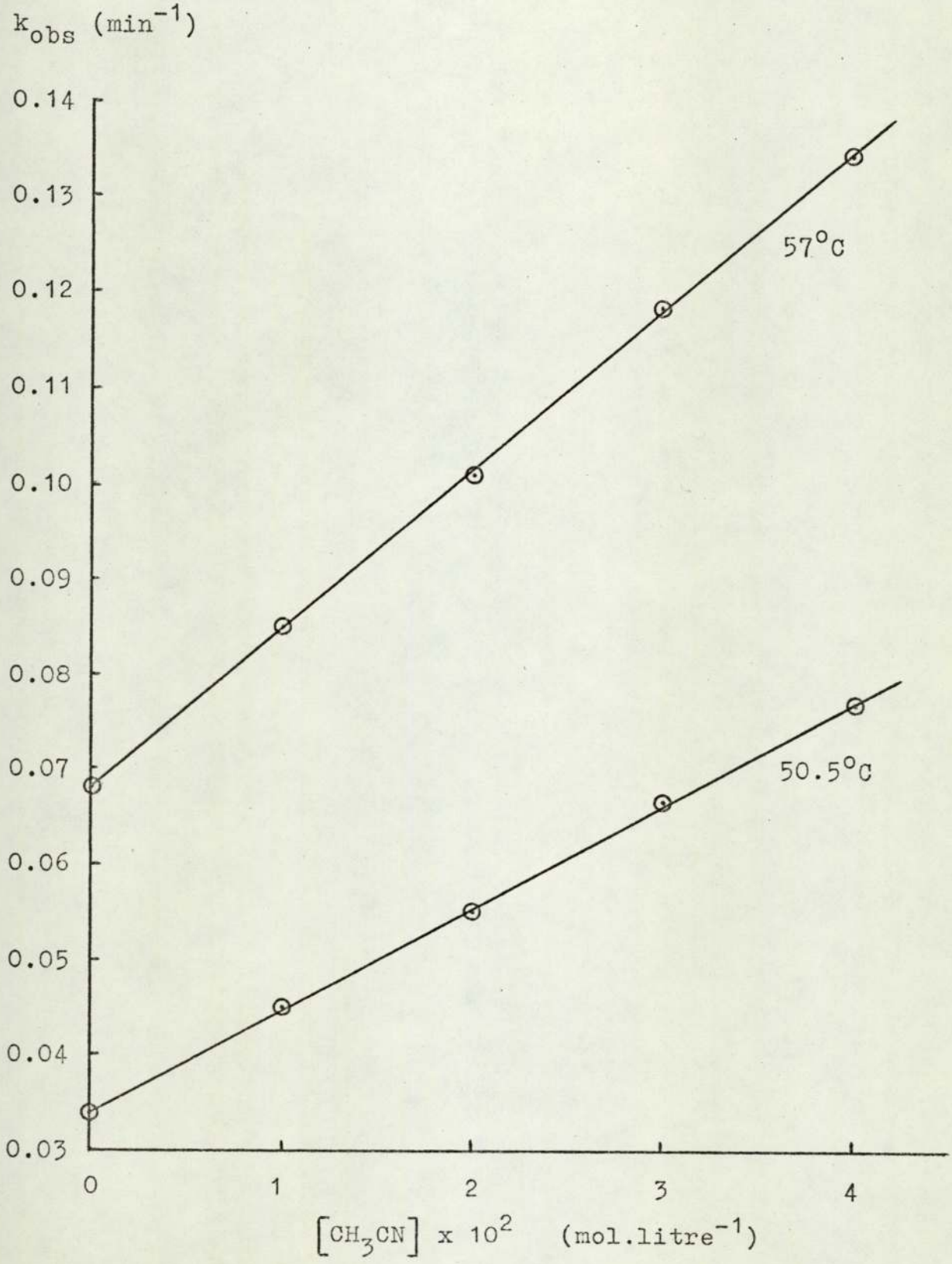

Figure 4.14.

Plot of $\log_{10} k_L$ against 1/T

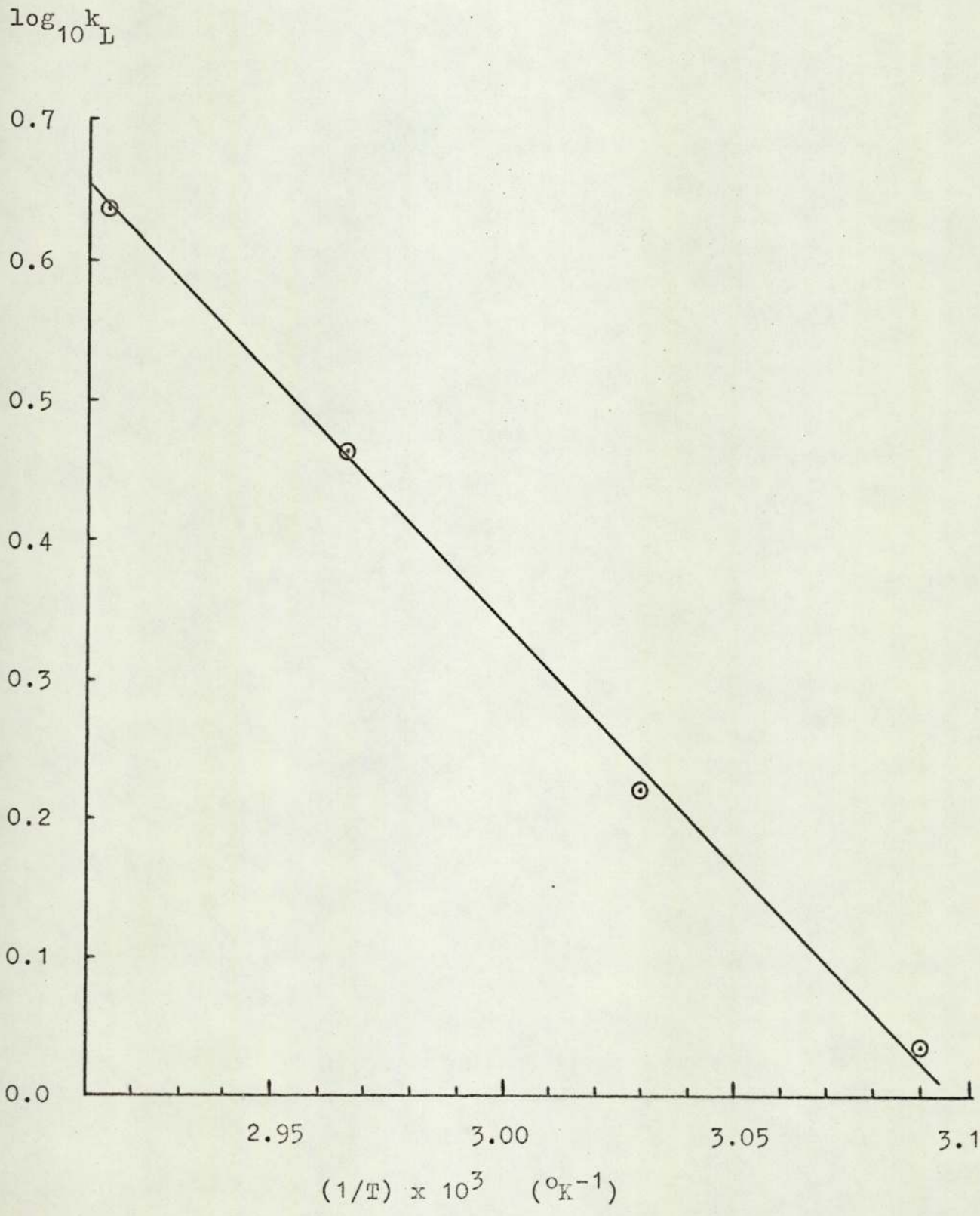

4.3. Discussion.

The parameters of activation, calculated at 64°C for the three reactions investigated in this chapter, are shown in table 4.4. and are based on the assumption of a transmission coefficient of unity. Table 4.4. includes the available literature data for the purpose of comparison.

Table 4.4.

Reaction	$\Delta H^{\ddagger}$(Kcal.mol^{-1})	$\Delta S^{\ddagger}$(cal.deg^{-1}.mol^{-1})	Ref.
$PtCl_4^{2-} + H_2O$	21.8	-14.7	Within
	21.6	-6.4	98
	21	-8	94
$PtCl_3(H_2O)^- + Cl^-$	16.9	-14.5	Within
	17.2	-12.4	98
	15	-18	94
$PtCl_4^{2-} + CH_3CN$	15.5	-19.4	Within

In each case the entropy of activation, $\Delta S^{\ddagger}$, is negative, consistent with the associative mechanism expected for the ligand substitution reactions of square planar platinum(II), in which bond development plays an important role in the formation of the transition state[100]. The value obtained here, for the aquation of the tetrachloroplatinite(II) ion, is almost twice that reported by Grantham et al[94], whilst that for the reverse reaction is in fair agreement. The discrepancy of ca. -7cal.deg^{-1}.mol^{-1}, in the former case, is undoubtedly due to the different expression of the forward rate constant, k_s. The data of table 4.4., obtained here, refers to rate constants expressed in second order units, in which k_s includes the water concentration. Evaluation of $\Delta S^{\ddagger}$, in which k_s is expressed in first order units, gives a value comparable to that of Grantham

et al.

The entropy change, ΔS^{o}, for the aquation reaction may readily be calculated from the data of table 4.4., obtained here, and is seen to be effectively zero. The value of +9cal. $deg^{-1}.mol^{-1}$ reported by Grantham et al, due to the first order expression of k_s, is claimed to be in good agreement with that expected from the treatment of Latimer and Jolly[101]. Quite why this is suggested is difficult to appreciate. The results of these authors refer to the stepwise replacement of coordinated water by fluoride ion upon the aluminium(III) ion in aqueous solution. For the process

$$AlF_4^-(aq) + F^-(aq) \rightleftharpoons AlF_5^{2-}(aq) \qquad 4.15.$$

ΔS^{o} was found to be +5cal.$deg^{-1}.mol^{-1}$. The predicted value of +15.6cal.$deg^{-1}.mol^{-1}$, obtained by calculating ΔS^{o} for the process 4.16., was based on the assumption that the principle factor concerned in the process 4.15 was the effect of the substitution of a coordinated water molecule by the fluoride ion.

$$H_2O(coord) + F^-(aq) \rightleftharpoons H_2O(aq) + F^-(coord) \qquad 4.16.$$

The difference in these values of ca. -11cal.$deg^{-1}.mol^{-1}$ was suggested to arise from the effect of the increase in charge on the complex ion upon the surrounding water molecules.

The aquation of the tetrachloroplatinite(II) ion may be compared to the reverse of the process 4.15., for which ΔS^{o} is -5cal.$deg^{-1}.mol^{-1}$. Although this value cannot be used to make a quantitative prediction for ΔS^{o} for the aquation reaction, it seems that the value of Grantham et al of +9cal.$deg^{-1}.mol^{-1}$ is somewhat unrealistic. Moreover, Latimer and Jolly suggest that the entropy changes in processes of this kind are more

dependent upon solvent replacement considerations than charge alteration effects. This again militates against the value of Grantham et al, since a calculation of ΔS^{o} for the reverse of the process 4.16., analogously involving chloride ion, would not be likely to produce a significant positive value.

Drougge, Elding and Gustafson[98] have remarked that in order to compare the entropies of activation for the forward and reverse reactions of the equilibrium 4.1., all relevant species in the system should be referred to the same standard state. However, incongruously enough, they cited a value for ΔS^{o} for the aquation reaction of $+6 cal.deg^{-1}.mol^{-1}$, also based upon a first order expression of k_s.

Finally, it should be mentioned that calculation of $\Delta S^{\ddagger}$, for the majority of ligand substitution reactions of square planar platinum(II), has revealed the values to be remarkably similar, irrespective of the nature or charge of the entering or leaving group[100]. This fact is apparent in table 4.4. for those values of $\Delta S^{\ddagger}$ in which k_s is expressed in second order units.

It appears, therefore, that the value of ΔS^{o} for the aquation reaction quoted here as approximately zero is the more realistic one and thus that the expression of k_s in second order units is justified.

Table 4.4. reveals the enthalpy of activation, $\Delta H^{\ddagger}$, for each of the three reactions to be fairly small. This is usually found to be the case for the ligand substitution reactions of square planar platinum(II) and is taken as further evidence for the associative mechanism[100]. The values obtained for both the forward and reverse reactions of the equilibrium 4.1. are in excellent agreement with those reported by Drougge

et al. Grantham et al's values are somewhat different, especially for the reverse reaction, however, as Drougge et al have pointed out, the discrepancy is probably due to the method employed in the determination of k_{-s}, which was calculated from the equation

$$K_s = k_s/k_{-s}$$

where K_s refers to the equilibrium constant for the equilibrium 4.1.

Drougge et al reported the enthalpy change, ΔH^o, for the aquation reaction to be 4.4 Kcal.mol^{-1}, over the temperature range 15-35^{o}C, and suggested it to exhibit a small temperature dependence. Although the value of 4.9 Kcal.mol^{-1}, calculated here at 64^{o}C from table 4.4., is slightly larger and might therefore be considered to support this claim, the difference is within the standard deviations of the activation energies for the forward and reverse reactions (section 4.2.1.), from which the value of ΔH^o is derived.

Table 4.4. reveals $\Delta H^{\ddagger}$ for the substitution of coordinated chloride ion by water, in the tetrachloroplatinite(II) ion, to be significantly greater than that for the substitution by acetonitrile. Moreover, $\Delta S^{\ddagger}$ for the solvent substitution path is seen to be somewhat less negative than that for the direct substitution path. These observations imply that the developing bond to the nitrile is stronger than that to water and that the resultant transition state is altogether more rigid for the direct substitution path.

Experiments reported in section 5.3.7. support this in the sense that the reverse reaction for the direct substitution path (equation 4.12.) appears to be none existent at chloride

ion concentrations in which the reverse reaction for the solvent substitution path (equation 4.1.) is predominant.

5. Further investigations of the reactions in aqueous systems of the tetrachloroplatinite(II) ion and acetonitrile.

5.1. Introduction.

It was mentioned in section 4.1. that the production of a deep blue solution occurs, under certain conditions, in aqueous systems of the tetrachloroplatinite(II) ion and acetonitrile.

In view of the reported hydrolysis of acetonitrile in the complex dichlorobis(acetonitrile)platinum(II), in the presence of aqueous solutions of some silver salts[54,102], this phenomenon was of considerable interest.

This reaction was first discovered by Hoffmann and Bugge[102], who observed that the treatment of the nitrile complex with an aqueous solution of silver sulphate produced a blue solution, which they named platinblau. Although it was generally agreed that the product contained the hydrolysed nitrile ligand and no coordinated chloride ion, the structure remained the subject of much speculation and several different suggestions were advanced[53,54]. It was not until Brown, Burbank and Robin[53] undertook an extensive investigation of a related complex, derived from the original nitrile complex and trimethylacetamide, that the structure was finally resolved. Using a variety of physical techniques, they were able to show that their complex existed in three tautomeric forms (figure 5.1.).

Figure 5.1.

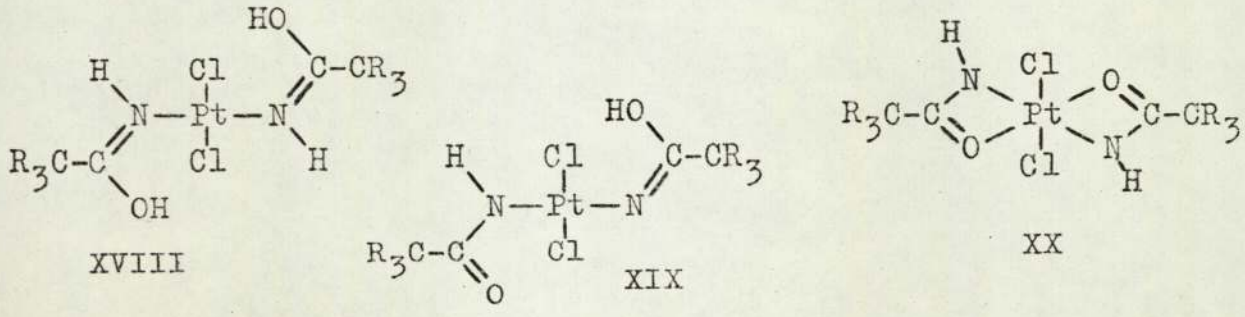

XVIII XIX XX

Here R refers to the methyl group. Since the isomers XIX and XX contain deprotonated forms of the amide ligand, they were assigned as complexes of platinum(IV). The yellow, crystaline complex XIX exhibits the previously unknown iminol anion of the amide as a ligand. The blue, amorphous complex XX was suggested to correspond to the original platinblau[102], which was accordingly assigned as dihydroxybis(acetamido)-platinum(IV) (XXI).

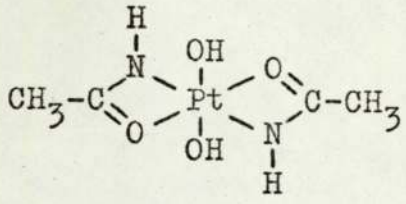

XXI

The metal ion promoted hydrolysis of organic nitriles has been the subject of recent interest. Although, as yet, only a few studies have been undertaken, it is already apparent that these hydrolysis reactions may be accomplished through a diversity of mechanistic routes. However, all the systems investigated to date share the common involvement of the hydroxide ion.

Breslow, Fairweather and Keana[87] reported the hydrolysis of 2-cyano-1,10-phenanthroline upon nickel(II) to involve an external attack of free hydroxide ion upon the carbon atom of the nitrile group. In this particular reaction the nitrile group is not coordinated to the metal and the enhancement in hydrolysis rate, of the order of 10^7, relative to that of the free nitrile, is found to be due primarily to the difference in the entropy of activation for the two processes. This is interpreted in terms of the ability of nickel to stabilize the transition state, XXII, through the favourable five-membered

ring structure, according to the scheme 5.1.

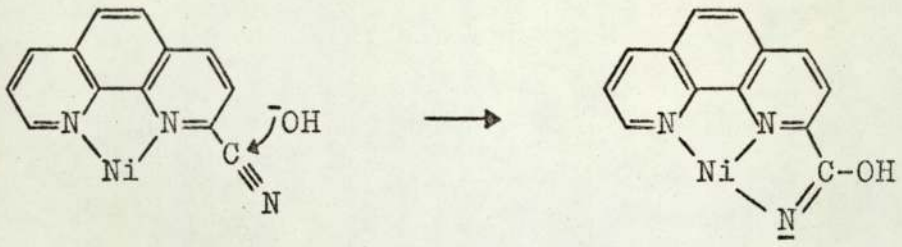

5.1.

XXII

The hydrolysis was also found to be effected by copper(II) and zinc(II). In the former case the reaction was extremely rapid.

Komiya, Suzuki and Watanabe[103] investigated the hydrolysis of the related nitrile, 2-cyanopyridine, in the presence of several metal complexes. They observed that labile complexes, containing loosely bound ligands, facilitated hydrolysis, whereas inert complexes were less effective.

The hydrolysis of several nitriles, initially coordinated to the pentamminecobalt(III) ion, have been recently studied. In these systems attack by coordinated hydroxide ion is improbable and external attack is postulated. In the case of benzonitrile a rate enhancement of ca. 2×10^6 has been reported by Pinnel, Wright and Jordan[104]. In contrast to the hydrolysis of 2-cyano-1,10-phenanthroline upon nickel(II)[87] this was found to be due not only to an increase in the entropy of activation, but also to a significant lowering of the enthalpy of activation. Presumably this reflects the ability of cobalt(III) to polarize the nitrile bond, thus facilitating nucleophilic attack by the hydroxide ion at the electron deficient carbon atom. An identical mechanism has been proposed for the analogous acetonitrile system, by Buckingham, Keene and Sargeson[105], however, no parameters of activation were quoted. In addition,

the methyl protons of the nitrile ligand were observed to exchange, although this was suggested to occur independently. The products of hydrolysis in these reactions were found to be N-bonded carboxamido complexes, which underwent protonation in acid solution. In the case of the acetamido complex protonation was claimed to occur at the carbonyl oxygen atom.

Buckingham, Sargeson and Zanella[106] proposed internal attack of coordinated hydroxide ion upon the nitrile group to occur in the complex $Co(en)_2Br(NH_2CH_2CH_2CN)^{2+}$, in the presence of the mercury(II) ion. Since the nitrile is coordinated through the amine group, this reaction again represents an example of a nitrile group situated in a position of influence near the coordination sphere of the metal, but not directly bonded to it. The reaction is somewhat specialized since the mercury(II) ion apparently plays an important role in the mechanism. Initially, the mercury(II) ion is believed to remove the coordinated bromide ion, thus permitting the rapid entry of water, within the coordination sphere of cobalt(III). Subsequently, it is suggested that the water ligand is deprotonated and that the mercury(II) ion assists the nucleophilic attack of the coordinated hydroxide ion upon the nitrile group.

Examples of the true metal catalysed hydrolysis of nitriles to amides have been reported by Bennet and Yoshida[107]. Several non-ionic, planar, tertiary phosphine complexes of rhodium, iridium and platinum were found to catalyse the conversion of acetonitrile to acetamide in high yield. The presence of coordinated hydroxide was observed to be essential to the successful function of the catalyst. This led to the unusual proposal that the mechanism involved the external attack of

acetonitrile upon the coordinated hydroxide ion.

The metal ion enhanced reactivity of organic nitriles is not confined to hydrolysis. Barnard[108] has demonstrated the generality of the alcoholysis of 2-cyanopyridine, in the presence of iron(II), cobalt(II), nickel(II) and copper(II). The products of reaction were found to be complexes of the appropriate carboximidate ligand (XXIII).

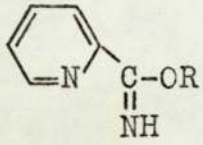

XXIII

Breslow[87] has reported that internal attack by coordinated alcohols upon the nitrile group is improbable, in the case of 2-cyano-1,10-phenanthroline and nickel(II). Presumably, therefore, the mechanism of alcoholysis involves external attack.

Ironically, the amminolysis of acetonitrile in the complex dichlorobis(acetonitrile)platinum(II), somewhat related to the hydrolysis reaction of Hoffmann and Bugge[102], has proved to be similarly enigmatic. Initially, the product was thought to contain four ammonia and two acetonitrile ligands and therefore to constitute an example of six-coordinate platinum(II)[109,110]. However, Golovnaya and Chia-Chiang[111] were able to show, on the basis of several chemical experiments, that this was not likely. They proposed that the product contained the acetamidine ligand in a four-coordinate platinum(II) complex. Subsequently, Stephenson[112] confirmed this by a detailed X-ray structural investigation. The complex was assigned as diammine-bis(acetamidine)platinum(II) (XXIV). Genuine six-coordinate complexes of platinum(II) are quite rare[113], although some square planar complexes show evidence of weak axial interactions.

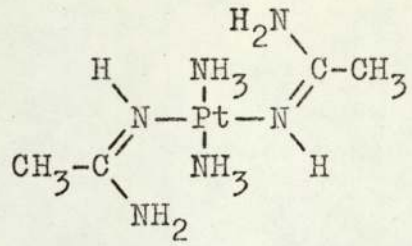

XXIV

Komiya, Suzuki and Watanabe[114] attempted the aminolysis of the nitrile group in the complex dichlorobis(2-cyanopyridine) copper(II), with a selection of amines, in methanol. However, the products of reaction were found to arise from the methanolysis of the nitrile group, analogous to the reactions of Barnard[108].

Initial attempts to undertake a kinetic study of the original reaction of Hoffmann and Bugge[102] were abandoned due to the continual precipitation of silver chloride, observed during the formation of dihydroxybis(acetamido)platinum(IV), which would have invalidated any direct spectrophotometric measurements upon the reaction.

The formation of the deep blue solution, under certain conditions, in aqueous systems of the tetrachloroplatinite(II) ion and acetonitrile, seemed to constitute a very similar reaction, without the complication of silver chloride precipitation. Accordingly this system was chosen for a kinetic study, the results of which are reported in the remaining sections of chapter 5.

5.2. Initial studies.

Essentially the reaction is very simple. An aqueous solution of potassium tetrachloroplatinite is heated at ca. 65°C in the presence of excess acetonitrile, whereupon a blue colour gradually develops, hereinafter referred to as "the blau", with a visible, broad peak maximum centred at 604nm. Consistent with previous observations[54], the pH of the solution was found to drop significantly during the reaction.

In the early experiments the concentration of acetonitrile was high (5M) and the blau was produced very slowly, over a period of days. Identical experiments done in 0.1M solutions of acetonitrile produced dark-blue colourations within the hour. However, prolonged reaction resulted in the precipitation of a dark-blue material. Further reactions done at lower platinum concentrations produced the blau under homogeneous conditions. Satisfactory experimental conditions were found at concentrations of 0.002M potassium tetrachloroplatinite and 0.1M acetonitrile.

5.2.1. Qualitative experiments.

In the presence of a large excess of potassium chloride (0.1M) the reaction is effectively inhibited. The reaction sequence from the tetrachloroplatinite(II) ion to the blau must necessarily involve the loss of several, if not all, chloride ion ligands from platinum. Since these steps are probably reversible, the suppression of the reaction is not surprising. This explanation is supported by the kinetic study (section 5.3.7.).

Reactions performed in either 0.05M nitric acid or 0.05M sodium hydroxide also produced no blau. In the latter case

a grey precipitate develops, probably platinum metal[94]. Blau solutions left to stand in strong acid (1M) are slowly destroyed. Ultimately purple-red solutions are produced.

The presence of platinum(IV) in the blau solutions is suggested by their behaviour with reducing agents. Treatment with sodium dithionite rapidly yields light-yellow solutions presumably containing platinum(II)[53]. Thus the oxidation of platinum(II) to platinum(IV) is indicated in the reaction sequence. Such a process might arise due to either a disproportionation (equation 5.2.) or an oxidation by molecular oxygen (equation 5.3.).

$$2Pt(II) \longrightarrow Pt(0) + Pt(IV) \qquad 5.2.$$

$$Pt(II) + \tfrac{1}{2}O_2 \longrightarrow Pt(IV) + O(-II) \qquad 5.3.$$

No platinum metal is observed in a successful reaction and so disproportionation appears unlikely. However, the reaction is suppressed under an atmosphere of argon suggesting the involvement of molecular oxygen. This was confirmed in a more rigorous experiment, in which air was first removed from the solution by the freeze-thaw technique. The pH of the solution was found to drop in the usual manner, however, no blau was produced.

The implication of these experiments, that the production of the blau is dependent upon the presence of molecular oxygen, whereas the release of acid occurs in its absence, is supported by the kinetic studies of sections 5.3. and 5.4.

5.2.2. Ion-exchange experiments.

The isolation of a solid product from the reaction medium proved surprisingly difficult. Rotary evaporation of the

solvent served to progressively increase the pH until the material was clearly affected. Solid residues obtained from such treatment were obviously complex mixtures, containing yellow, green and blue components. Thin-layer chromatography of such residues, using a variety of solvents on silica and cellulose supports, confirmed the presence of more than one species. Treatment of the plates with silver nitrate solution suggested potassium chloride to be one of these. However, attempts to remove it by column chromatography were not successful.

In an effort to avoid this problem work was undertaken with ion-exchange resins. The reaction solution was run down a cation-exchange column, in the H^+ form, and subsequently down an anion-exchange column, in the OH^- form. It was hoped to produce a neutral solution of the blau by removal of both potassium ion and chloride ion. Unfortunately, the treatment produced a final pale-blue solution, which exhibited a peak maximum at 613nm., and had an optical density considerably less than that of the original solution. This behaviour was found to be typical, irrespective of the acid and base strengths of the resins employed. The majority of the blau was observed to be held at the top of the cationic column, whilst signs were also apparent along the remainder of the column length.

The most probable explanation for the retention of the blau on the cationic resin is that it is converted into a cation by protonation, under the acidic conditions of the final solution (equation 5.4.). Simple protonation equilibria are rapid and might account for a uniform retention along the column length. However, the majority of the blau is held at the top of the column, suggesting a further slow equilibrium

to operate (equation 5.5.).

$$A + nH^+ \overset{K_n}{\rightleftharpoons} AH_n^{n+} \qquad 5.4.$$

$$AH_n^{n+} \rightleftharpoons B^{n+} \qquad 5.5.$$

It seems probable that the equilibrium 5.5. represents a molecular rearrangement, arising as a result of protonation[115].

Several observations support this scheme. Firstly, less blau is retained, along the column length, on a cationic resin in the K^+ form. Considering the equilibrium 5.4., we have that

$$K_n = \frac{\left[AH_n^{n+}\right]}{\left[A\right]\left[H^+\right]^n}$$

If the reaction solution is run down a cationic column, in the H^+ form, AH_n^{n+} will be removed and replaced by H^+. In order to maintain the constancy of K_n, A must be removed. Thus the equilibrium 5.4. is displaced in favour of AH_n^{n+}. However, if the resin is employed in the K^+ form, both AH_n^{n+} and H^+ will be removed. Hence, qualitatively, the equilibrium 5.4. might be expected to be relatively unaffected.

Secondly, the peak maximum of the final solution, after ion exchange, is about 613nm., whilst that of the reaction solution is about 604nm. Thus spectrophotometric evidence suggests two distinct species, consistent with a molecular rearrangement. Furthermore, this is corroborated by the experiments cited in section 5.4.5., which show that the blau produced at pH 7 has a peak maximum at 612nm., and that if the pH is subsequently adjusted to 4 a gradual drop in the peak maximum to 599nm. is observed, over a period of days.

The blau can be recovered only slowly by elution with 10% potassium chloride solution, suggesting it to have a high selectivity coefficient. The resins employed in this study have pore sizes of ca. 400nm.[116], thus the possibility that the blau is, in fact, physically trapped in the resin matrix is unlikely.

In view of the extreme sensitivity of the blau to an acidic environment the use of ion-exchange resins in its isolation was abandoned.

5.2.3. Experiments with buffers.

Since the reaction involves the release of acid, the formation of the blau must necessarily occur under conditions of variable pH. If meaningful kinetic measurements are to be made upon the reaction the pH throughout its duration must be held constant. This may be accomplished by the use of standard buffer solutions[117].

An initial investigation of the feasibility of the reaction in buffered media is summarized in tables 5.1. and 5.2. The studies were undertaken in potassium hydrogen phthalate (table 5.1.) and potassium dihydrogen phosphate (table 5.2.) buffers, at concentrations of 0.002M potassium tetrachloroplatinite and 0.1M acetonitrile and at 65°C.

Table 5.1.

Buffer solution (mls.)		pH		Observations (mins.)
$KHC_8O_4H_4$(0.1M)	NaOH(0.1M)	Initial	Final	
50.0	0.30	3.98	3.82	Yellow(2), green(15), brown(120), no pptn.
50.0	22.6	5.02	4.85	Yellow(1), green(10), opaque(90), pptn.

Table 5.2.

Buffer solution (mls.)		pH		Observations (mins.)
KH_2PO_4(0.1M)	NaOH(0.1M)	Initial	Final	
50.0	5.6	5.98	5.63	Yellow(1), green(10), blue(60), no pptn.
50.0	29.1	7.05	6.81	Yellow(10), green(30), opaque(60), pptn.
50.0	46.1	8.05	7.62	Yellow(15), green(50), opaque(90), pptn.

An inspection of tables 5.1. and 5.2. reveals firstly, that the normal reaction path is not generally followed and secondly, that the pH of the solution varies significantly.

However, the presence of platinum(IV) is indicated in these experiments since treatment with sodium dithionite produces lighter coloured solutions in all cases. The failure of the buffers to keep the pH constant was found to be due to the relatively high platinum concentration.

Since the reaction at pH 6 appeared the most promising it was investigated spectrophotometrically at 626nm., using the technique described in section 2.2.2.1. The study was undertaken at concentrations of 0.0005M potassium tetrachloroplatinite and 0.1M acetonitrile and at 65°C.

Figure 5.2. establishes that Beer's law is obeyed under these conditions. Some of the early runs are shown in figure 5.3. and are seen to be somewhat irreproducible. However, if the profiles are treated with suitable arbitrary factors they may be reduced to a reasonably consistent curve. This implies firstly, that the starting platinum concentration is not constant and secondly, that the platinum concentration is not featured in the rate equation governing the production of the blau.

The method of addition of the potassium tetrachloroplatinite solution was clearly unacceptable. Substantial inaccuracies arose due to the small volumes involved. However, the introduction of larger volumes inevitably resulted in a significant initial temperature drop. Thus, a modified procedure, based on that described in section 2.2.2.1., was developed. This involved the preheating of buffered solutions of potassium tetrachloroplatinite to the required temperature, which were then mixed with thermostatted solutions of acetonitrile, buffered at the same pH.

During the course of these experiments it was noticed that the buffered stock solutions of potassium tetrachloroplatinite deteriorated with age. After several days a faint-grey suspension developed, suggesting platinum to be involved in some reaction with phosphate buffer. In view of this and also the anomolous behaviour in phthalate buffer (table 5.1.), the reaction was investigated, using the modified procedure, in a range of buffered solutions at pH 6. These results are summarized in table 5.3.

Table 5.3.

Buffer solution[117]	mls.	pH	Observations (peak max.)
$KHC_8O_4H_4$(0.1M)	50.0	6.04	Rapid reaction (654nm. sh)
NaOH(0.1M)	45.0		
CH_3CO_2H(0.2M)	5.0	5.96	Slow reaction (534nm.)
CH_3CO_2Na(0.2M)	95.0		
$HOC(CH_2CO_2H)CO_2H$(0.07M)	100.0	6.03	No reaction after 70mins.
NaOH(0.2M)	81.0		
$(CH_2CO_2H)_2$(0.01M)	50.0	6.01	Fairly rapid reaction (616
NaOH(0.01M)	90.0		

The reaction profiles at 626nm., for each buffer, are shown in figure 5.4. Table 5.3. and figure 5.4. clearly demonstrate that the reaction is dependent upon the nature of the buffering medium. This is perhaps not surprising since the organic acids, employed as buffers, are potential ligands containing oxygen donor atoms quite acceptable to platinum(IV). Figure 5.4. shows no two buffers to be comparable and therefore all must be regarded as potentially interfering. For this reason their use in maintaining a constant pH was abandoned.

During this study the phenomenon of bubble development on the optical faces of the cell walls was encountered. Figure 5.5. illustrates the drastic effect this may have upon the observed optical density in some cases. Gradual bubble development is potentially more dangerous, since it can remain undetected whilst progressively affecting the measured optical density. The problem can be effectively eliminated by taking the following precautions. Firstly, the cells must be cleansed scrupulously with chromic acid prior to use, to remove the small particles upon which the bubbles form. Secondly, the cell must be tapped sharply once the contents are at thermal equilibrium, since it is as the temperature of the solution rises that the gases are expelled.

In this section work is described which, although not directly concerned with the kinetic studies, provided a basis from which the problem was subsequently tackled. The technique employed had to combine several important features. It had to be able to moniter the reaction spectrophotometrically, sustain a constant pH and temperature, minimize the evaporation of both solvent and acetonitrile and provide adequate contact between the reaction solution and atmospheric oxygen.

The system finally developed to meet these requirements is described in section 2.2.2.2.

Figure 5.2.

Plot of optical density at 626nm. against initial platinum concentration, for a blau produced in phosphate buffer at pH 6.

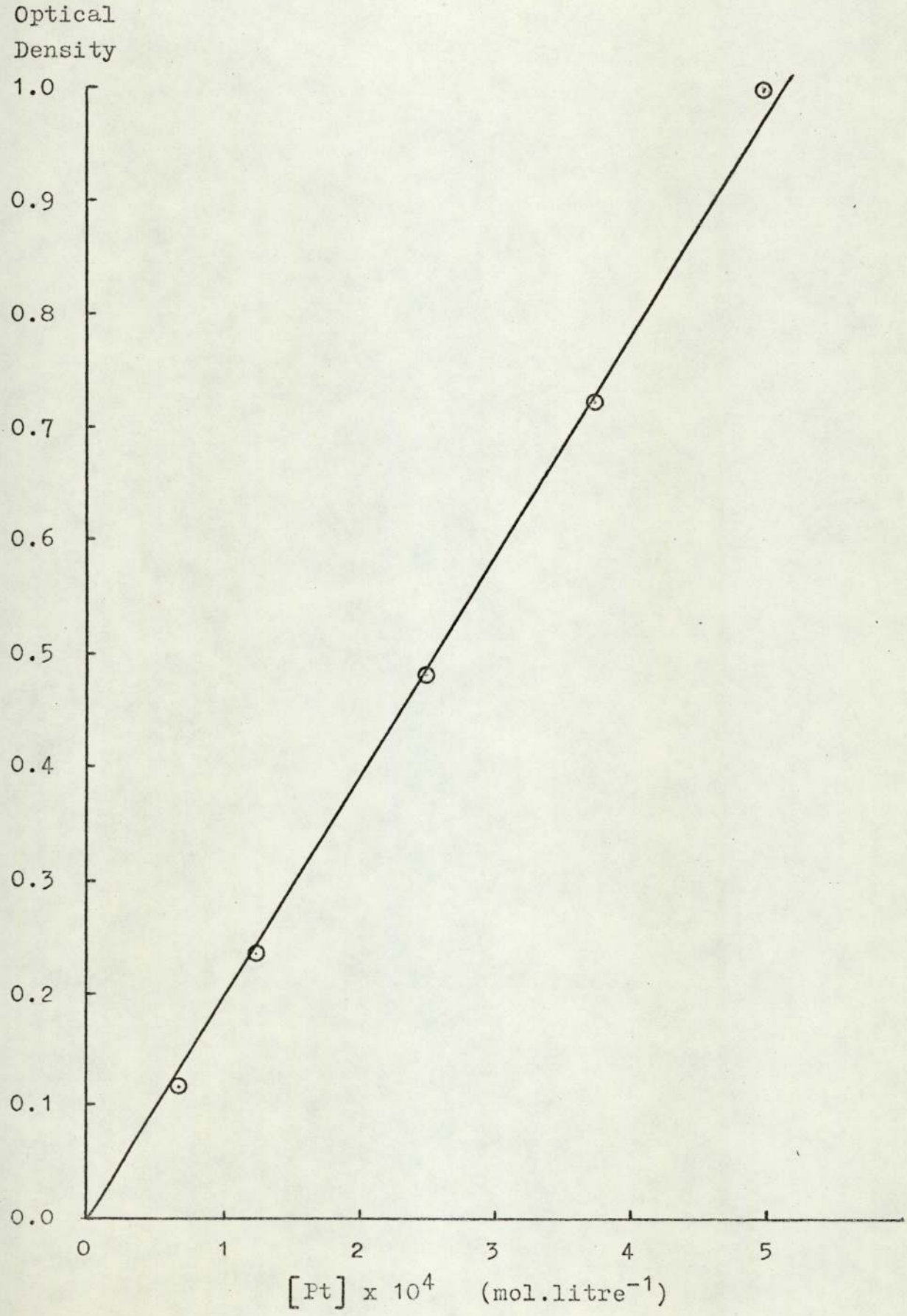

Figure 5.3.

Some reaction profiles at 626nm. for the production of the blau in phosphate buffer at pH 6.

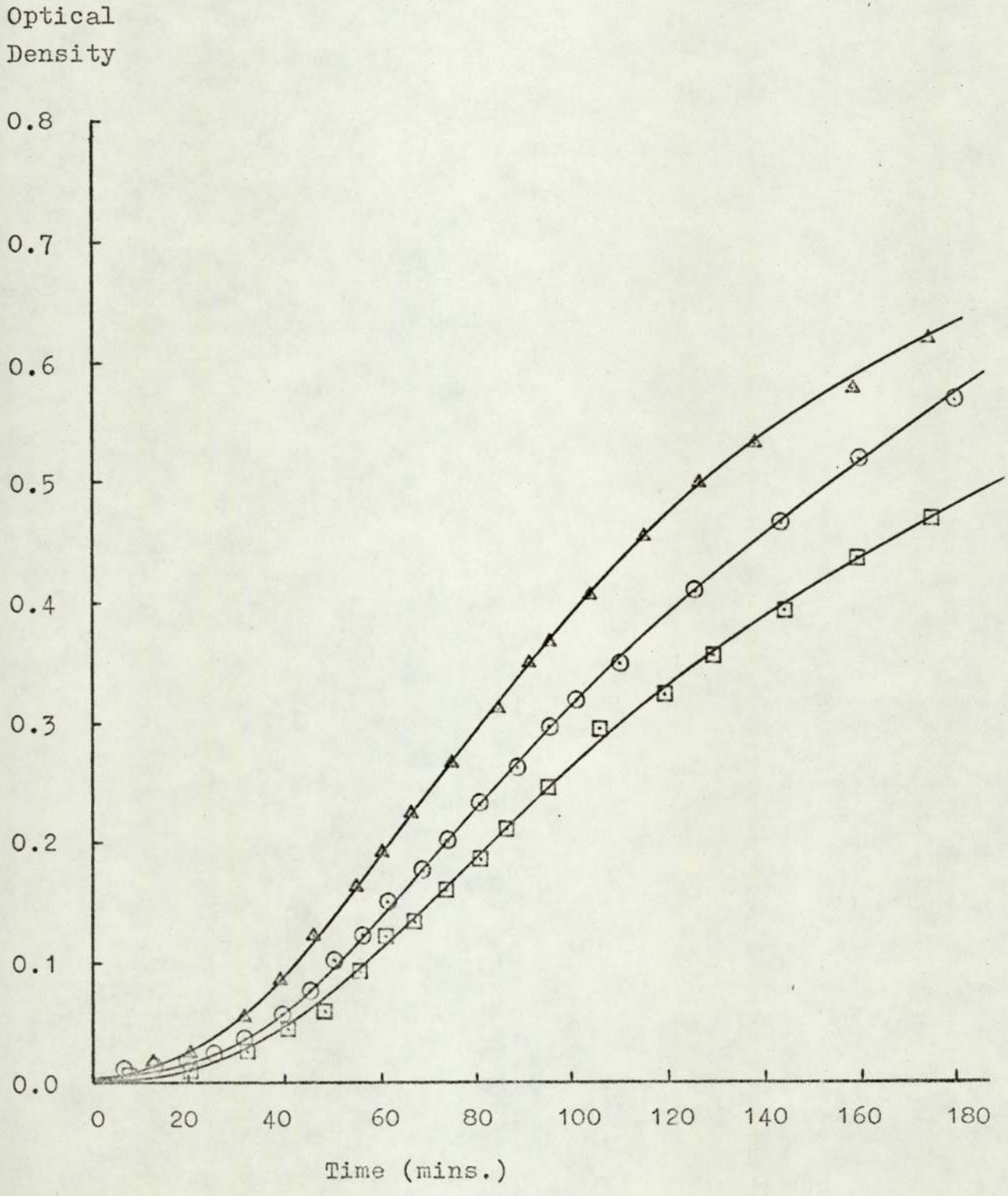

Figure 5.4.

Reaction profiles at 626nm. for the production of the blau in a series of buffers at pH 6.

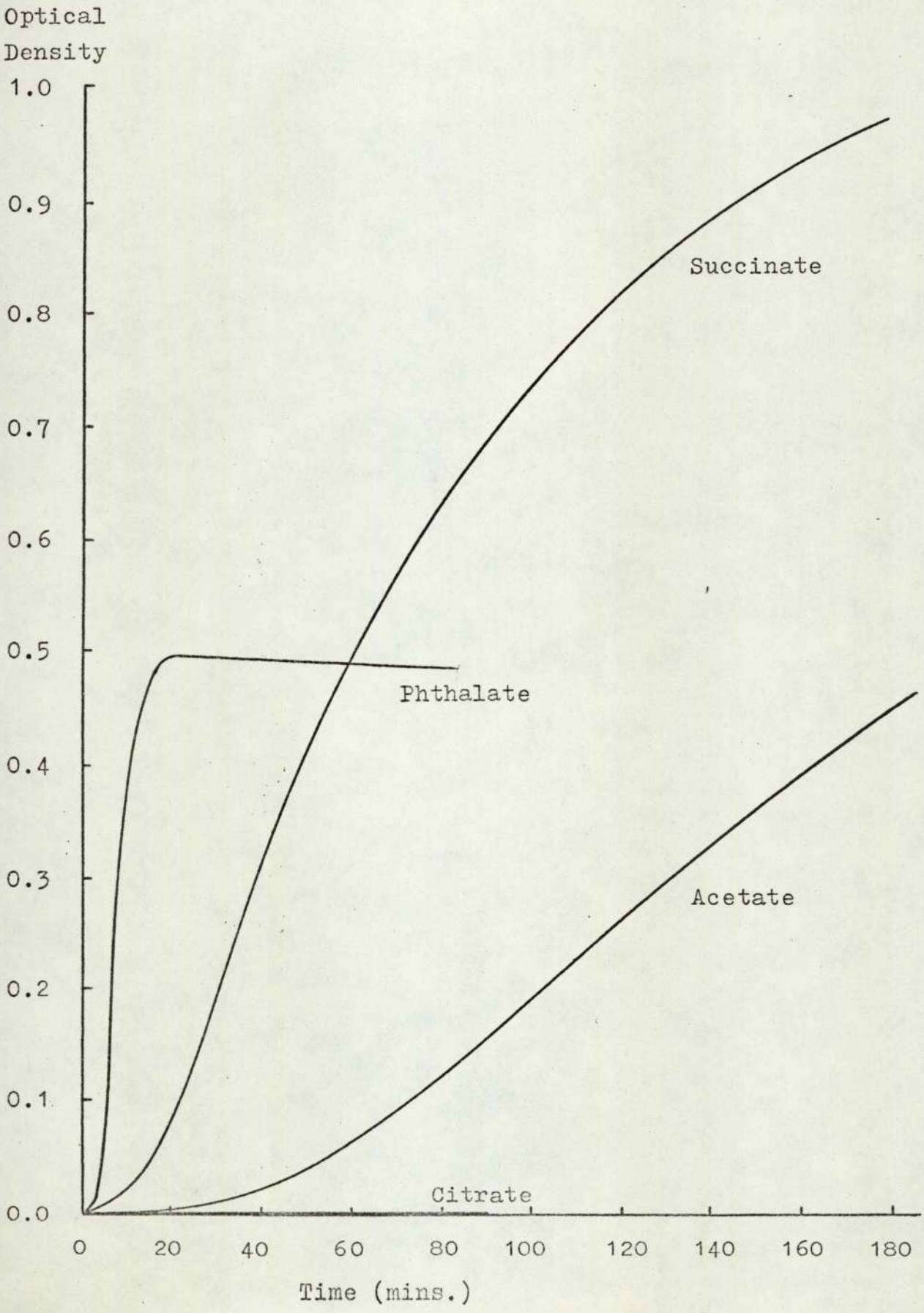

Figure 5.5.

Reaction profile at 626nm. for the production of the blau in phosphate buffer at pH 6, illustrating the effect of bubble development on the optical faces of the cell walls.

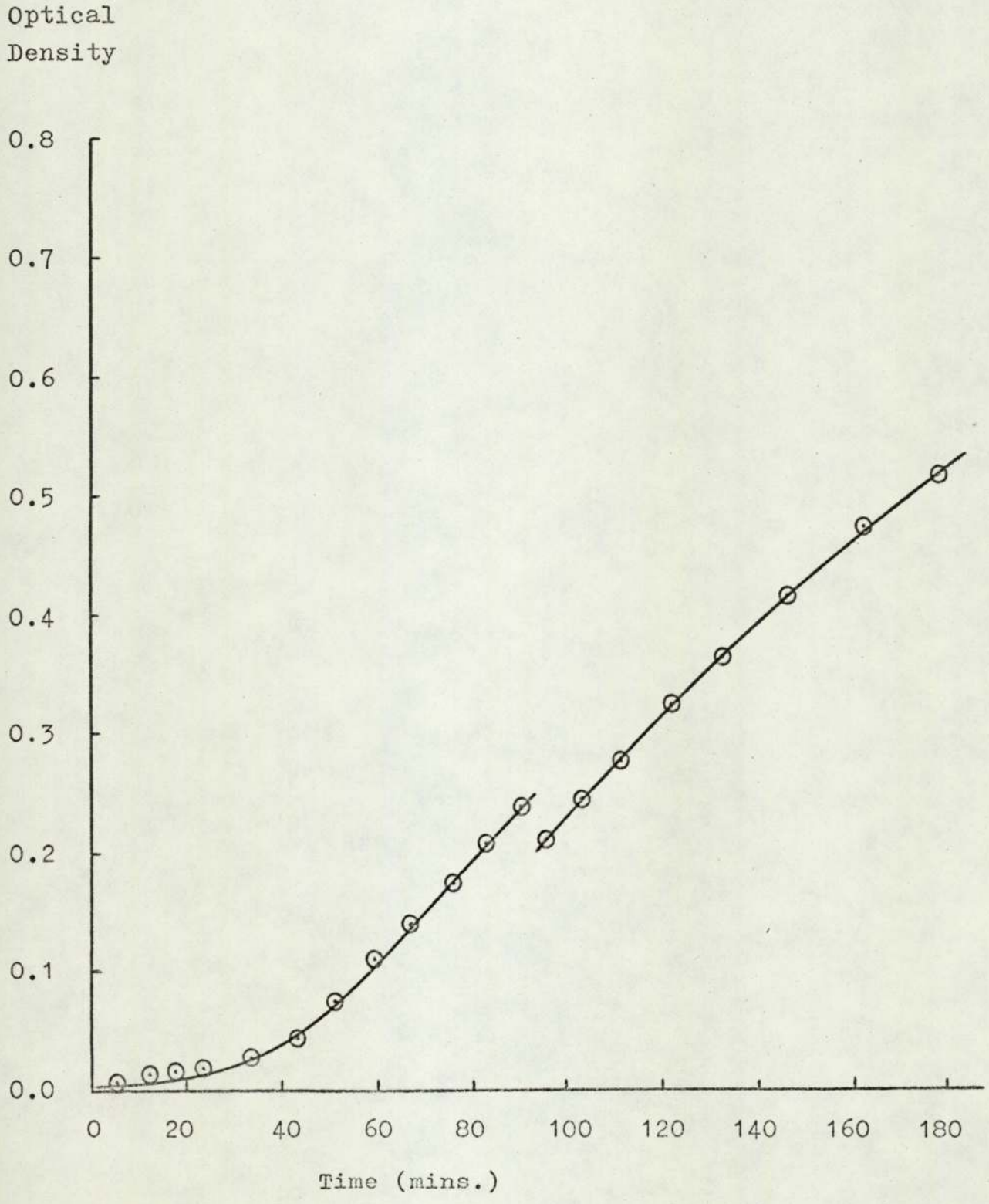

5.3. Kinetics of acid release.

The release of acid, during the production of the blau, may be followed kinetically by monitering the amount of a standard solution of potassium hydroxide, necessarily added to maintain a constant pH, as a function of time.

The apparatus designed to accomplish this and the concentration of added base (0.02M) were mentioned in section 2.2.2.2. The theoretical change in pH, when one drop (0.04ml.) of 0.02M potassium hydroxide is added to 200mls. of water at pH 7, is given by

$$\Delta pH = (pK_w + \log_{10}[OH^-]) - 7 \qquad 5.6.$$

Evaluation of equation 5.6. at 64°C predicts a pH change of ca. 0.5. In all experiments performed, the addition of one drop of base did not alter the pH of a run solution by more than 0.05, implying the species in solution to have a buffering effect.

Firstly, it was established that reproducible results could be obtained. Figure 5.6. shows two plots of the volume of base added against time under identical conditions. The profiles reveal a slight 'S' shaped character, suggesting acid production in a consecutive reaction. However, the curves could not be fitted satisfactorily to equation 3.4. (chapter 3), using the least squares computer program SEQUEXP (appendix 1). Neither could they be fitted to a first order equation, using the least squares computer program HYDR (appendix 2).

In section 4.2.2. it was proposed that the stepwise hydrolysis of the tetrachloroplatinite(II) ion at pH 7 is responsible for the observed release of more than two protons

per platinum atom. The final burette reading in these experiments always corresponded to more than two and less than three protons released per platinum atom, over the pH range 6 to 8. Therefore, the possibility of a stepwise release of acid was considered and led to the development of the following general scheme.

$$A \xrightarrow{k_a} B$$

$$B \underset{}{\overset{K_b}{\rightleftharpoons}} B' + xH^+$$

$$B \xrightarrow{k_b} C$$

$$C \underset{}{\overset{K_c}{\rightleftharpoons}} C' + yH^+$$

Let

$a_o = [A]$ at zero time

$a = [A]$, $b = [B]$, $c = [C]$ at time t

$b' = [B']$, $c' = [C']$ at time t

and $H = [H^+]$.

We have that

$$K_b = (b'/b)H^x \qquad 5.7.$$

and

$$K_c = (c'/c)H^y \qquad 5.8.$$

From 5.7. and 5.8.

$$(b + b') = b(1+K_b/H^x) \qquad 5.9.$$

$$(c + c') = c(1+K_c/H^y) \qquad 5.10.$$

We have that

$$\frac{da}{dt} = -k_a a$$

Integration of this gives

$$a = a_o e^{-k_a t} \qquad 5.11.$$

Also we have that

$$\frac{d(b + b')}{dt} = k_a a - k_b b$$

From 5.9. and 5.11. and collecting the constant terms

$$\frac{d(b + b')}{dt} = k_a a_o e^{-k_a t} - \alpha_b (b + b')$$

This equation is of the same mathematical form as that for two consecutive reactions[74]. Integration produces the equation

$$(b + b') = \frac{k_a a_o}{(\alpha_b - k_a)} (e^{-k_a t} - e^{-\alpha_b t}) \qquad 5.12.$$

We have that

$$a_o = a + b + b' + c + c'$$

Therefore from 5.11. and 5.12.

$$(c + c') = a_o (1 + \frac{k_a}{(\alpha_b - k_a)} e^{-\alpha_b t} - \frac{\alpha_b}{(\alpha_b - k_a)} e^{-k_a t}) \qquad 5.13.$$

The burette reading may be related to the acid produced, at time t, by the relation

$$[OH^-] = xb' + yc' \qquad 5.14.$$

From 5.7., 5.8., 5.9., 5.10. and 5.14. and collecting the constant terms

$$\left[OH^-\right] = \frac{yK_c}{(K_c+H^y)}(z(b + b') + (c + c')) \qquad 5.15.$$

$$\text{where } z = \frac{xK_b(K_c+H^y)}{yK_c(K_b+H^x)} \qquad 5.16.$$

Finally, from 5.12., 5.13. and 5.15. it may be shown that

$$\left[OH^-\right] = \left[OH^-\right]_\infty\left(1+\frac{(zk_a-\alpha_b)e^{-k_at}+(1-z)k_ae^{-\alpha_bt}}{(\alpha_b-k_a)}\right) \qquad 5.17.$$

$$\text{where } \left[OH^-\right]_\infty = \frac{yK_ca_o}{(K_c+H^y)} \qquad 5.18.$$

and $\left[OH^-\right]_\infty$ is the burette reading at infinite time.

It was found that the experimental data could be fitted satisfactorily to equation 5.17., using the least squares computer program HREL shown in appendix 3. Values of the psuedo first order rate constant, k_a, the composite rate constant, α_b, and the factor, z, were obtained. Since equation 5.17. is not symmetrical, k_a and α_b are unambiguously defined as relating to the first and second steps of the consecutive sequence respectively. The final burette reading, $\left[OH^-\right]_\infty$, being an experimentally determinable quantity, was not refined by the program HREL. However, a tolerance of two drops (0.08mL) was considered permissible and the value of $\left[OH^-\right]_\infty$ allowed to vary between such limits. The fits were improved slightly if an initial correction, defined as $\left[OH^-\right]_o$, was introduced to allow for the small quantity of acid produced during the rapid establishment of the initial equilibrium 4.2. (chapter 4). This is explained in more detail in appendix 7.

From 5.18. we define

$$\phi = \frac{[OH^-]_\infty}{a_o} = \frac{yK_c}{(K_c+H^y)}$$

and from 5.16.

$$\Phi = z\phi = \frac{xK_b}{(K_b+H^x)}$$

It is easily shown that these quantities may be expressed as

$$\phi = \frac{yc'}{(c + c')}$$

and $$\Phi = \frac{xb'}{(b + b')}$$

Thus, the quantity ϕ represents the fraction of acid released by the product species, expressed in terms of the total concentration of product species. The quantity Φ is similarly defined for the intermediate species. Elucidation of the dependence of the quantities ϕ and Φ upon the hydrogen ion and acetonitrile concentrations should provide an insight into the intimate structures of the equilibria governing the product and intermediate species respectively. For this reason it is these quantities that are reported in the subsequent sections.

All kinetic runs were undertaken at a potassium tetrachloroplatinite concentration of 0.0004M, unless otherwise stated. The release of acid was found to be independent of the ionic strength of the reaction medium. Table 5.4. reveals this to be the case in the presence of added chloride ion,

under which conditions reactions involving charged species would be expected. This feature was also reported in section 4.2.1. (chapter 4). Runs were performed at concentrations of 0.01M potassium chloride and 0.1M acetonitrile and at pH 7 and 64°C.

Table 5.4.

μ	$k_a(min^{-1})$	$\alpha_b(min^{-1})$	ϕ	Φ
0.01	0.0560	0.0285	2.15	0.971
0.05	0.0561	0.0286	2.11	0.942

5.3.1. Variation of the pH.

Runs were performed at a concentration of 0.1M acetonitrile and at 64°C.

Table 5.5. reveals k_a to be invariant, α_b to be directly dependent and ϕ and Φ to be inversely dependent upon the hydrogen ion concentration.

Table 5.5.

pH	$k_a(min^{-1})$	$\alpha_b(min^{-1})$	ϕ	Φ
6.0	0.0600	0.0634	2.03	0.223
6.3	0.0600	0.0575	2.06	0.388
6.7	0.0600	0.0510	2.14	0.665
7.0	0.0605	0.0432	2.25	0.978
7.2	0.0601	0.0393	2.28	1.16
7.7	0.0602	0.0312	2.50	1.58
8.0	0.0591	0.0166	2.68	1.80

5.3.2. Variation of the acetonitrile concentration at pH 7.

Runs were performed at pH 7 and 64°C.

Table 5.6. reveals k_a and ϕ to be invariant, α_b to be

directly dependent and Φ to be inversely dependent upon the acetonitrile concentration.

Table 5.6.

$[CH_3CN]$	$k_a(min^{-1})$	$\alpha_b(min^{-1})$	ϕ	Φ
0.02M	0.0603	0.0258	2.28	1.15
0.04M	0.0595	0.0374	2.29	1.07
0.07M	0.0600	0.0414	2.18	1.01
0.10M	0.0605	0.0432	2.25	0.978
0.24M	0.0601	0.0533	2.25	0.929
0.38M	0.0604	0.0579	2.23	0.819
0.50M	0.0600	0.0633	2.26	0.688
0.65M	0.0601	0.0647	2.25	0.572

5.3.3. Variation of the acetonitrile concentration at pH 7.7.

Runs were performed at pH 7.7 and 64°C.

Table 5.7. reveals k_a, α_b, ϕ, and Φ to be essentially independent of the acetonitrile concentration.

Table 5.7.

$[CH_3CN]$	$k_a(min^{-1})$	$\alpha_b(min^{-1})$	ϕ	Φ
0.10M	0.0602	0.0312	2.50	1.58
0.24M	0.0598	0.0289	2.47	1.43
0.38M	0.0597	0.0288	2.52	1.51
0.50M	0.0596	0.0291	2.50	1.47
0.65M	0.0598	0.0325	2.57	1.43

5.3.4. Variation of the temperature.

Runs were undertaken at a concentration of 0.1M acetonitrile and at pH 7.

Table 5.8. shows k_a and α_b to be similarly dependent

upon the temperature and ϕ and Φ to remain essentially unaffected.

Table 5.8.

Temp.(^{o}C)	k_a(min^{-1})	α_b(min^{-1})	ϕ	Φ
50.0	0.0143	0.0122	2.09	1.15
57.0	0.0288	0.0232	2.05	1.14
64.0	0.0605	0.0432	2.25	0.978
71.0	0.110	0.0771	1.98	1.13
78.0	0.210	0.143	2.06	0.980

Arrhenius plots of the data of table 5.8. are shown in figure 5.7. Calculation of the activation energies gives values of 21.6 Kcal.mol^{-1} for the first step and 19.8 Kcal.mol^{-1} for the second step.

5.3.5. Dependence upon the presence of argon and oxygen.

Runs were performed at a concentration of 0.1M acetonitrile and at pH 7 and 64^{o}C.

Table 5.9. shows that the presence of excess argon or excess oxygen has essentially no effect upon k_a, α_b, ϕ or Φ. The slight variation in these parameters may be attributed to the volatilization of acetonitrile during the bubbling of the gases through the reaction solution.

Table 5.9.

Atmosphere	k_a(min^{-1})	α_b(min^{-1})	ϕ	Φ
Argon	0.0601	0.0422	2.00	0.971
Air	0.0605	0.0432	2.25	0.978
Oxygen	0.0602	0.0431	1.98	0.931

The data of table 5.9. supports the experiments of section

5.2.1. and implies that the oxidation of platinum(II) to platinum(IV) does not occur during the stepwise release of acid in the initial stages of the reaction producing the blau.

The systematic errors in the determination of k_a, α_b, $[OH^-]_\infty$, and z are suggested to be respectively within ±1%, ±2%, ±1%, and ±5%, from the reproducibility runs undertaken, including that depicted in figure 5.6. Thus, it is the quantity $\bar{\Phi}$ that is the least reliable of those parameters of acid release quoted in tables 5.4. to 5.9.

The standard deviations of the activation energies for the first and second steps of acid release are calculated to be within ±3%, from figure 5.7. and the approximate formula given in appendix 5.

5.3.6. Interpretation of the results.

The experimentally determined quantities α_b, $\emptyset$ and $\bar{\Phi}$ were fitted to suitable functions of the hydrogen ion and acetonitrile concentrations, using a variety of least squares computer programs and a small Micro 16 computer. Values of the appropriate equilibrium and rate constants, involved in these functions, were refined for the best overall fit.

The replacement of the first chloride ion from the tetrachloroplatinite(II) ion was shown in section 4.2.3. to be both rapid and dependent upon the acetonitrile concentration. The reaction may be envisaged in terms of the parallel process

$$PtCl_4^{2-} + H_2O + CH_3CN \begin{array}{l} \xrightarrow{k_s} PtCl_3(H_2O)^- + Cl^- + CH_3CN \\ \qquad\qquad K_R \big\downarrow\big\uparrow \\ \xrightarrow{k_L} PtCl_3(CH_3CN)^- + Cl^- + H_2O \end{array} \qquad 5.19.$$

Tables 5.5., 5.6. and 5.7. reveal that the first rate

determining step, in the release of acid, is relatively slow and independent of the pH and acetonitrile concentration. It is suggested, therefore, that this step, designated A → B in the general scheme, involves the replacement of a second chloride ion by water, from the species trichloroacetonitrile platinum(II), to produce intermediate species derived from the $PtCl_2$ moeity. This is illustrated by the scheme 5.20.

$$PtCl_3(CH_3CN)^- + H_2O \xrightarrow{k_a} PtCl_2(H_2O)(CH_3CN) + Cl^- \qquad 5.20.$$

The intermediate species may be considered in terms of the following equilibrium processes, in which water is assumed.

$$PtCl_2(CH_3CN)_2 \overset{K_1}{\rightleftharpoons} PtCl_2(H_2O)(CH_3CN) + CH_3CN \qquad 5.21.$$

$$\overset{K_2}{\rightleftharpoons} PtCl_2(OH)(CH_3CN)^- + H^+ + CH_3CN \qquad 5.22.$$

$$\overset{K_3}{\rightleftharpoons} PtCl_2(H_2O)_2 + 2CH_3CN \qquad 5.23.$$

$$\overset{K_4}{\rightleftharpoons} PtCl_2(H_2O)(OH)^- + H^+ + 2CH_3CN \qquad 5.24.$$

$$\overset{K_5}{\rightleftharpoons} PtCl_2(OH)_2^{2-} + 2H^+ + 2CH_3CN \qquad 5.25.$$

Obviously, the processes 5.22. to 5.25. proceed in several stages mechanistically. Furthermore, none of these stages would be expected to involve the direct substitution by the hydroxide ion[95,96]. Thus, for instance, the equilibrium 5.22. is a two-stage process, involving the replacement of coordinated acetonitrile by water and the subsequent deprotonation of coordinated water.

The intimate structure of the equilibrium, designated $B \rightleftharpoons B' + xH^+$ in the general scheme, may be deduced from the dependence of the quantity Φ upon the hydrogen ion and

acetonitrile concentrations.

It may be shown that if all the equilibria 5.21. to 5.25. operate then the complete function which describes the dependence of Φ, over all experimental conditions, is

$$\Phi = \frac{(K_2LH + K_4H + 2K_5)}{(L^2H^2 + K_1LH^2 + K_2LH + K_3H^2 + K_4H + K_5)} \qquad 5.26.$$

where $H = [H^+]$ and $L = [CH_3CN]$.

At constant acetonitrile concentration this function may be reduced to the general expression

$$\Phi = \frac{(\alpha H + 2\beta)}{(H^2 + \alpha H + \beta)} \qquad 5.27.$$

where α and β are appropriate functions of the equilibrium constants of equation 5.26. and the acetonitrile concentration.

The data of table 5.5. ~~is~~ are well described by equation 5.27.

At constant pH the overall function may be reduced to the general expression

$$\Phi = \frac{(\gamma L + \partial)}{(L^2 + \epsilon L + \theta)} \qquad 5.28.$$

where γ, ∂, ϵ, and θ are appropriate functions of the equilibrium constants of equation 5.26. and the hydrogen ion concentration.

The data of table 5.6. ~~is~~ are not satisfactorily described by equation 5.28. However, an acceptable fit is obtained if the assumption that γ and ϵ are effectively zero is made. Under these conditions equation 5.28. reduces to

$$\Phi = \frac{\partial}{(L^2 + \theta)} \qquad 5.29.$$

Thus the complete function 5.26. may be reduced to

$$\Phi = \frac{(K_4H + 2K_5)}{(L^2H^2 + K_3H^2 + K_4H + K_5)} \qquad 5.30.$$

Table 5.10. shows the values of the three equilibrium constants which provide the best calculated fit for Φ, from equation 5.30., over all experimental conditions.

Table 5.10.

Equil.constant	Value
K_3	1.14×10^{-1} mol^2.litre^{-2}
K_4	3.29×10^{-8} mol^3.litre^{-3}
K_5	1.14×10^{-16} mol^4.litre^{-4}

The values of table 5.10. and equation 5.30. produce the fit shown in table 5.11. for Φ.

Table 5.11.

L = 0.1M			pH = 7		
pH	Φ (obs.)	Φ (calc.)	L	Φ (obs.)	Φ (calc.)
6.0	0.223	0.223	0.02M	1.15	1.00
6.3	0.388	0.386	0.04M	1.07	0.998
6.7	0.665	0.697	0.07M	1.01	0.991
7.0	0.978	0.983	0.24M	0.929	0.908
7.2	1.16	1.17	0.38M	0.819	0.783
7.7	1.58	1.59	0.50M	0.688	0.690
8.0	1.80	1.76	0.65M	0.572	0.567

The form of equation 5.30. implies that the equilibria 5.21. and 5.22. are inconsequential. At high pH and low acetonitrile concentration these equilibria might arguably

become important. Under these conditions the progressive breakdown of equation 5.30. might be expected. This idea is supported by inspection of table 5.11.

The difficulty experienced in establishing the dependence of Φ upon the acetonitrile concentration may be attributed firstly, to its low sensitivity to this reagent (table 5.6.) and secondly, to its high sensitivity to pH (table 5.5.). Thus small inconsistencies in the pH will produce relatively large errors in the determination of Φ.

The second rate determining step, in the release of acid, is suggested to involve the replacement of a third chloride ion, from the intermediate species derived from the $PtCl_2$ moeity, by the composite attack of water and acetonitrile. The intimate reactions of the intermediate species, designated $B+B' \rightarrow C+C'$ in the general scheme, may be deduced from the dependence of the composite rate constant, α_b, upon the hydrogen ion and acetonitrile concentrations.

Table 5.7. reveals that α_b is independent of the acetonitrile concentration at pH 7.7. The major species at this pH are dichlorohydroxyaquoplatinum(II) and dichlorodihydroxyplatinum(II). Therefore, it seems probable that these species are not attacked by acetonitrile. Table 5.6. shows that α_b is substantially dependent upon the acetonitrile concentration at pH 7. The species dichlorobis(acetonitrile) platinum(II) is not predominant at this pH, over the range of acetonitrile concentration of this study. This suggests that the marked dependence arises principally from the attack of acetonitrile upon the species dichlorodiaquoplatinum(II). This supposition is supported by the absence of an L^3 term in the function found to most adequately define the variance of α_b,

over all experimental conditions.

Thus the following intimate set of reactions are proposed for the intermediate species

$$PtCl_2(CH_3CN)_2 + H_2O \xrightarrow{k_1} PtCl(H_2O)(CH_3CN)_2^+ + Cl^- \quad 5.31.$$

$$PtCl_2(H_2O)_2 + CH_3CN \xrightarrow{k_2} PtCl(H_2O)_2(CH_3CN)^+ + Cl^- \quad 5.32.$$

$$PtCl_2(H_2O)_2 + H_2O \xrightarrow{k_3} PtCl(H_2O)_3^+ + Cl^- \quad 5.33.$$

$$PtCl_2(H_2O)(OH)^- + H_2O \xrightarrow{k_4} PtCl(H_2O)_2(OH) + Cl^- \quad 5.34.$$

$$PtCl_2(OH)_2^{2-} + H_2O \xrightarrow{k_5} PtCl(H_2O)(OH)_2^- + Cl^- \quad 5.35.$$

It may be shown that this scheme predicts the dependence of α_b upon the hydrogen ion and acetonitrile concentrations to be governed by the function

$$\alpha_b = \frac{(k_1L^2H^2 + k_2K_3LH^2 + k_3K_3H^2 + k_4K_4H + k_5K_5)}{(L^2H^2 + K_3H^2 + K_4H + K_5)} \quad 5.36.$$

where $H = [H^+]$ and $L = [CH_3CN]$.

At constant acetonitrile concentration this function may be reduced to the general expression

$$\alpha_b = \frac{(MH^2 + PH + Q)}{(H^2 + \alpha H + \beta)} \quad 5.37.$$

where α and β are defined as before and M, P and Q are appropriate functions of the equilibrium and rate constants of equation 5.36. and the acetonitrile concentration.

The data of table 5.5. is well described by equation 5.37.

At constant pH the overall function may be reduced to the general expression

$$\alpha_b = \frac{(RL^2 + SL + T)}{(L^2 + \theta)} \qquad 5.38.$$

where θ is defined as before and R, S and T are appropriate functions of the equilibrium and rate constants of equation 5.36. and the hydrogen ion concentration.

The data of table 5.6. is satisfactorily described by equation 5.38.

Table 5.12. shows the values of the five rate constants which provide the best calculated fit for α_b, from equation 5.36., over all experimental conditions.

Table 5.12.

Rate constant	Value (min^{-1})
k_1	0.0263
k_2	0.428 litre.mol^{-1}
k_3	0.0301
k_4	0.0401
k_5	0.0240

The values of table 5.12. and equation 5.36. produce the fit shown in table 5.13. for α_b.

Table 5.13.

L = 0.1M			pH = 7		
pH	α_b(obs.)	α_b(calc.)	L	α_b(obs.)	α_b(calc.)
6.0	0.0634	0.0627	0.02M	0.0258	0.0356
6.3	0.0575	0.0582	0.04M	0.0374	0.0372
6.7	0.0510	0.0502	0.07M	0.0414	0.0408
7.0	0.0432	0.0433	0.24M	0.0533	0.0530
7.2	0.0393	0.0391	0.38M	0.0579	0.0589
7.7	0.0312	0.0310	0.50M	0.0633	0.0628
8.0	0.0166	0.0279	0.65M	0.0647	0.0636

The intimate structure of the equilibria governing the product species, designated $C \rightleftharpoons C' + yH^+$ in the general scheme, may be deduced from the dependence of the quantity $\emptyset$ upon the hydrogen ion and acetonitrile concentrations.

A great many equilibrium processes may be considered for the product species. However, those involving acetonitrile may be excluded for the following reasons. Firstly, inspection of table 5.5. reveals that between two and three protons are released per platinum atom, over the pH range of this study. Secondly, tables 5.6. and 5.7. clearly demonstrate that $\emptyset$ is independent of the acetonitrile concentration. The only scheme consistent with these observations is one in which the major product species arise from the equilibrium

$$PtCl(H_2O)(OH)_2^- + 2H^+ \overset{K_6}{\rightleftharpoons} PtCl(OH)_3^{2-} + 3H^+ \qquad 5.39.$$

It may be shown that this equilibrium requires the dependence of $\emptyset$ upon the hydrogen ion concentration to obey the relationship

$$\frac{(3 - \emptyset)}{(\emptyset - 2)} = \frac{H}{K_6} \qquad 5.40.$$

A plot of $(3 - \emptyset)/(\emptyset - 2)$ against H is shown in figure 5.8. and exhibits a good straight line. The value of the ionization constant, K_6, calculated from the slope, is found to be 3.49×10^{-8} mol.litre^{-1}. Calculation of the standard deviation of K_6 suggests an accuracy of $\pm 0.5 \times 10^{-8}$ mol.litre^{-1}.

5.3.7. Variation of the chloride ion concentration.

Runs were performed at an acetonitrile concentration of 0.1M and at pH 7 and 64°C.

The general scheme proposed for the release of acid assumes that the consecutive steps of the reaction are irreversible. In the absence of added chloride ion this assumption would appear justified, since the experimental data are well described by equation 5.17.

In the presence of added chloride ion a gradual breakdown of equation 5.17. is observed as the concentration of chloride ion is increased. However, the final burette reading remains unaffected, over the concentration range of study. These observations suggest that the first step in the consecutive sequence contains a progressive contribution from the back reaction, whilst the second step remains essentially irreversible, as the concentration of chloride ion is increased.

It may be shown that if all steps, prior to the irreversible step, may be considered as equilibria, the latter portion of an acid release curve may be described by a first order equation, taking some mid-point as an arbitrary zero. The position of this mid-point depends upon how rapidly the initial equilibria are established, which, in turn, is subject to the concentration of chloride ion. Thus, in practice, it is found that the portion of a curve which can be satisfactorily fitted to a first order equation depends directly upon the concentration of chloride ion. In fact, at low concentration of chloride ion, such a treatment was found to be unacceptable, since only the latter ca. 30% of the curves could be properly described. Under these conditions the curves were fitted adequately to equation 5.17., in the usual manner.

Table 5.14. shows the values of the observed rate constants. Those obtained from the first order treatment, using a modified

version of the least squares computer program HYDR (appendix 2), are marked with a double-dagger.

Table 5.14.

$[Cl^-]$	$k_{obs}(min^{-1})$	ø
0.002M	0.0365	2.11
0.010M	0.0285	2.15
0.024M‡	0.0225	2.14
0.038M‡	0.0167	2.18
0.050M‡	0.0143	2.16

Under conditions of added chloride ion we may consider the following processes

$$PtCl_4^{2-} + H_2O \overset{K_s}{\rightleftharpoons} PtCl_3(H_2O)^- + Cl^- \qquad 5.41.$$

$$PtCl_4^{2-} + CH_3CN \overset{K_L}{\rightleftharpoons} PtCl_3(CH_3CN)^- + Cl^- \qquad 5.42.$$

$$PtCl_3(CH_3CN)^- + H_2O \overset{K_a}{\rightleftharpoons} PtCl_2X_2 + Cl^- \qquad 5.43.$$

$$PtCl_2X_2 + Y \xrightarrow{\alpha_b} PtClX_2Y + Cl^- \qquad 5.44.$$

where X refers to the non-chloride ligands of the intermediate species and XY refers to the non-chloride ligands of the product species. Since $PtCl_2X_2$ represents the intermediate species, there is justification in the use of the composite rate constant, α_b, as shown.

It may be shown that, provided that all the equilibria 5.41. to 5.43. operate, the observed rate constant, k_{obs}, is governed by the expression

$$\frac{(\alpha_b - k_{obs})}{(k_{obs}.Cl)} = Cl/(K_1K_aL) + K_s/(K_LK_aL) + 1/K_a \qquad 5.45.$$

where Cl = $[Cl^-]$.

No satisfactory plot of $(\alpha_b - k_{obs})/(k_{obs}.Cl)$ against Cl, for equation 5.45. could be found. If the equilibrium constant K_L is large, then, since K_s may readily be shown to be less than unity (table 4.1., chapter 4), equation 5.45. will approximate to

$$\alpha_b/k_{obs} = Cl/K_a + 1 \qquad 5.46.$$

A plot of α_b/k_{obs} against Cl is shown, for equation 5.46, in figure 5.9. and exhibits a good straight line. Evaluation of the slope gives a value of 2.59×10^{-2} mol.litre^{-1} for K_a. Calculation of the standard deviation of K_a suggests an accuracy of $\pm 0.2 \times 10^{-2}$ mol.litre^{-1}.

5.3.8. Discussion.

The most striking feature of the results reported here in section 5.3. is the curious lack of reactivity shown by acetonitrile towards the various species of platinum(II). Inspection of tables 4.1. and 4.3. (chapter 4) reveals that the tetrachloroplatinite(II) ion is attacked mainly by acetonitrile at concentrations greater than 0.05M in this reagent. However, tables 5.6. and 5.7. demonstrate that the product of this reaction, the trichloroacetonitrileplatinum(II) ion, is exclusively attacked by water, even at relatively high acetonitrile concentrations. Indeed, it is apparent that the direct substitution path is unimportant for the majority of the platinum(II) species. The stepwise replacement of chloride ion appears to arise principally from the solvent substitution path.

Presumably the selectivity shown by acetonitrile reflects a relatively low energy transition state for the direct path,

in the case of the tetrachloroplatinite(II) ion, not attainable for the majority of the platinum(II) species. A possible explanation of the discrimination of acetonitrile may be advanced on the basis of the reaction profile of figure 5.10., in which this ligand is considered to behave initially as a pi acid towards platinum(II).

Figure 5.10.

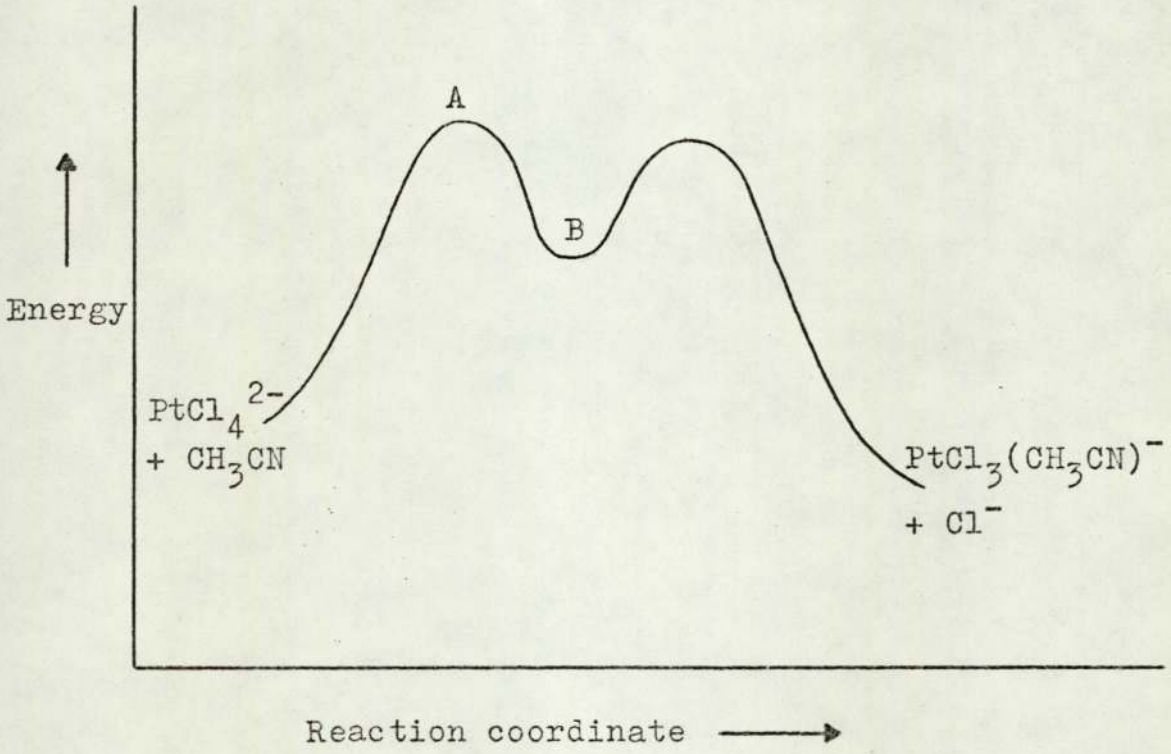

The observed chloride ion dependence of section 5.3.7. implies the replacement of acetonitrile by chloride ion to be difficult. Consequently the trichloroacetonitrileplatinum(II) ion is considered to be of low energy in figure 5.10. Pi interaction between acetonitrile and platinum(II) is proposed in the formation of the five-coordinate transition state, A, and subsequently in the unstable, four-coordinate intermediate, B.

Thus the initial energy barrier for pi complex formation must be overcome, prior to the production of the normal N-

coordinated product. This idea might explain why the direct substitution path is possible for the tetrachloroplatinite(II) ion, since the reactivity of biphilic reagents towards this species is established[99]. However, it is difficult to see how such a scheme could account for the apparent reactivity of acetonitrile towards the species dichlorodiaquoplatinum(II), although it should be noted that there is no 'a priori' guarantee that this species is, in fact, attacked significantly by acetonitrile. The function 5.38. (section 5.3.6.), which includes a term for this process, was merely that which was found to most adequately describe the dependence of the composite rate constant, α_b, upon the acetonitrile concentration

A further feature of this study is the apparent reluctance of platinum(II) to entertain both acetonitrile and water derivatives in its coordination sphere. Thus the non-chloride ligands of the major platinum(II) species are seen to be either all acetonitrile, or all water and hydroxide.

The rate data for the aquation reactions of these species at 64°C is summarized in table 5.15. The rate constant, k_{corr}, is included as a qualitative statistical correction and is merely the ratio of the calculated rate constant for aquation, k_{aq}, to the number of chloride ions on the substrate.

Table 5.15.

Substrate	$k_{aq}(min^{-1})$	$k_{corr}(min^{-1})$
$PtCl_4^{2-}$	0.141	0.0353
$PtCl_3(CH_3CN)^-$	0.0600	0.0200
$PtCl_2(CH_3CN)_2$	0.0263	0.0132
$PtCl_2(H_2O)_2$	0.0301	0.0151
$PtCl_2(H_2O)(OH)^-$	0.0401	0.0201
$PtCl_2(OH)_2^{2-}$	0.0240	0.0120

It is a general feature of square planar platinum(II) substitution reactions that the overall charge on the complex has little influence upon the rate of ligand substitution of that complex[93,99,100]. This fact is apparent in table 5.15. and may be taken as further evidence for the associative mechanism of aquation, in which bond cleavage is not of major importance.

Table 5.8. reveals that Φ is essentially constant with temperature, implying that the intimate equilibria of the intermediate species remain relatively unaffected over the temperature range of study. This is supported by the linear Arrhenius plot observed for α_b (figure 5.7.). However, the composite nature of the replacement of the third chloride ion precludes a realistic interpretation of the apparent activation energy.

Calculation of the parameters of activation at 64°C for the aquation of the trichloroacetonitrileplatinum(II) ion shows that the entropy of activation is $-18.6 cal.deg^{-1}.mol^{-1}$ and that the enthalpy of activation is 20.8 $Kcal.mol^{-1}$. These values may be compared to those of table 4.4. (chapter 4) and, as expected, are quite similar.

The approximate values of the ionization constants for the acid-base equilibria, operating under the conditions of this study, are summarized in table 5.16. The ionization constant, K_{corr}, is included as a qualitative statistical correction. This is derived from the product of the calculated ionization constant, K_{ion}, and a suitable factor. The factor is obtained from the ratio of the number of hydrogen ions, available for deprotonation, on the substrate, to the number of sites, available for protonation, on the product.

Table 5.16.

Substrate	K_{ion}(mol.litre^{-1})	K_{corr}(mol.litre^{-1})
$PtCl_3(H_2O)^-$	3.5×10^{-7}	1.8×10^{-7}
$PtCl_2(H_2O)_2$	2.9×10^{-7}	0.73×10^{-7}
$PtCl_2(H_2O)(OH)^-$	0.35×10^{-7}	0.35×10^{-7}
$PtCl(H_2O)(OH)_2^-$	0.35×10^{-7}	0.52×10^{-7}

Figure 5.6.

Two plots of the volume of base added against time at a concentration of 0.1M acetonitrile, pH 7 and 64°C.

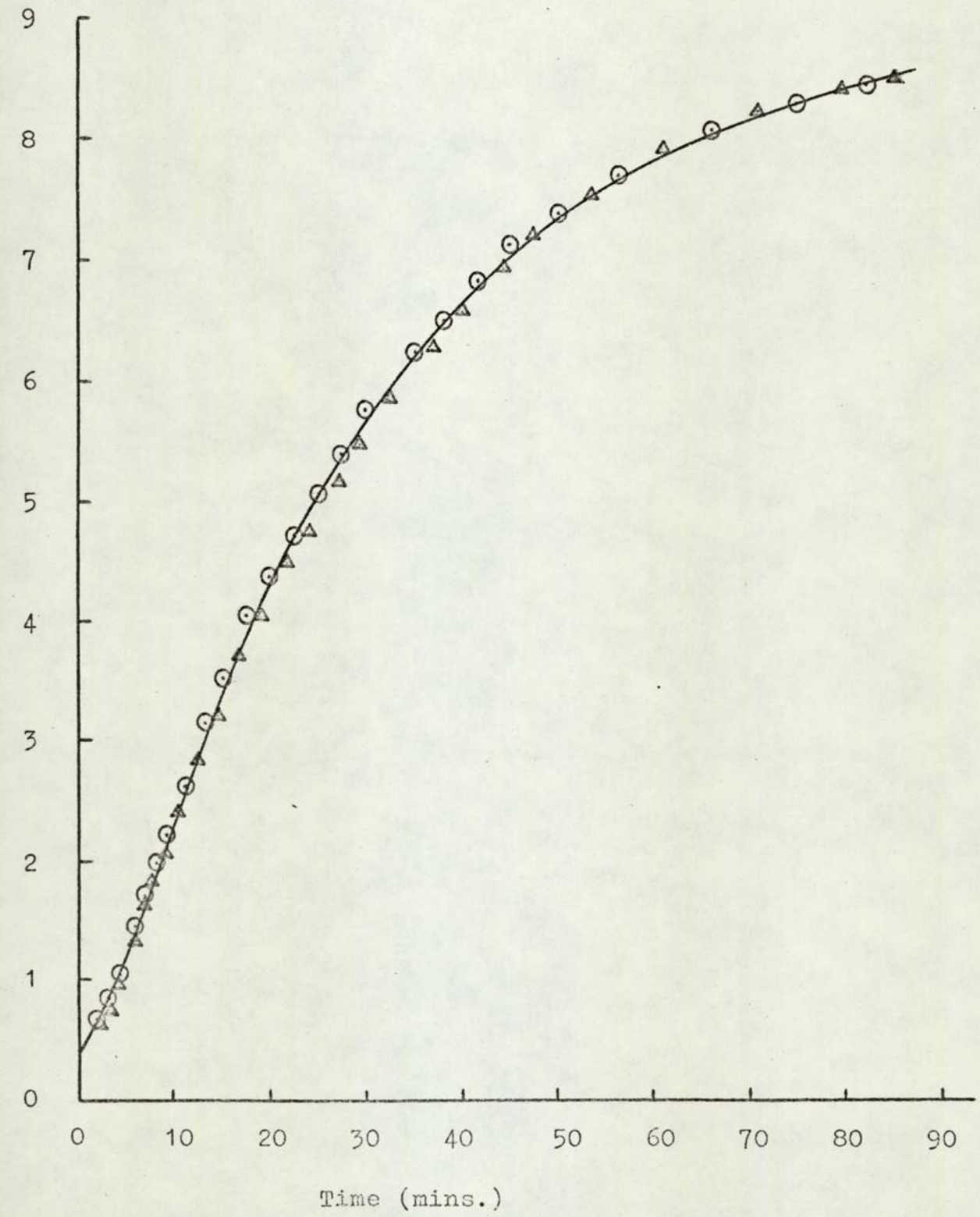

Figure 5.7.

Plots of $\log_{10} k_a$ and $\log_{10} \alpha_b$ against 1/T at a concentration of 0.1M acetonitrile and pH 7.

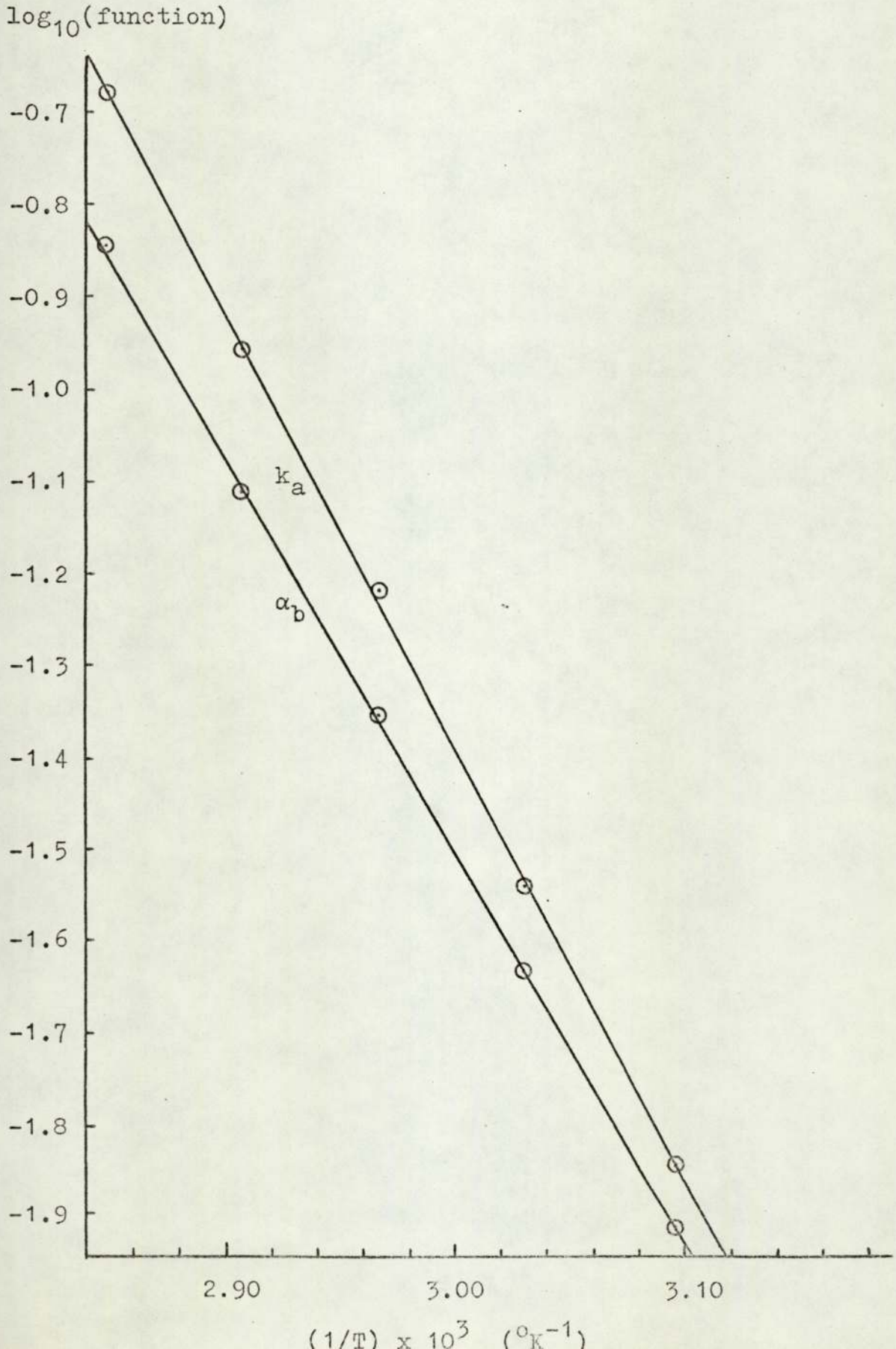

Figure 5.8.

Plot of $(3 - \bar{\nu})/(\bar{\nu} - 2)$ against $[H^+]$ at an acetonitrile concentration of 0.1M and at 64°C.

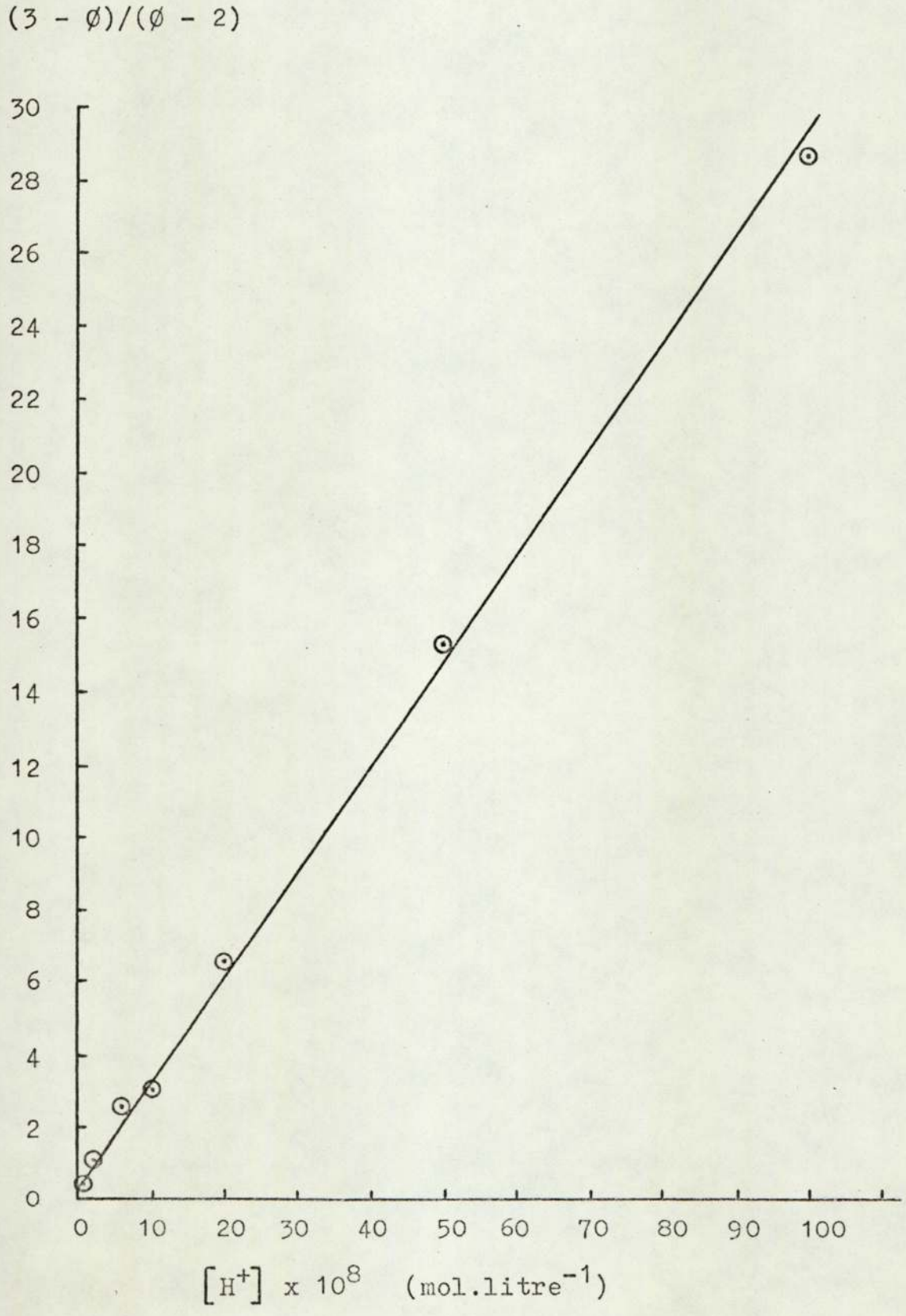

Figure 5.9.

Plot of α_b/k_{obs} against $[Cl^-]$ at an acetonitrile concentration of 0.1M, pH 7 and at 64°C.

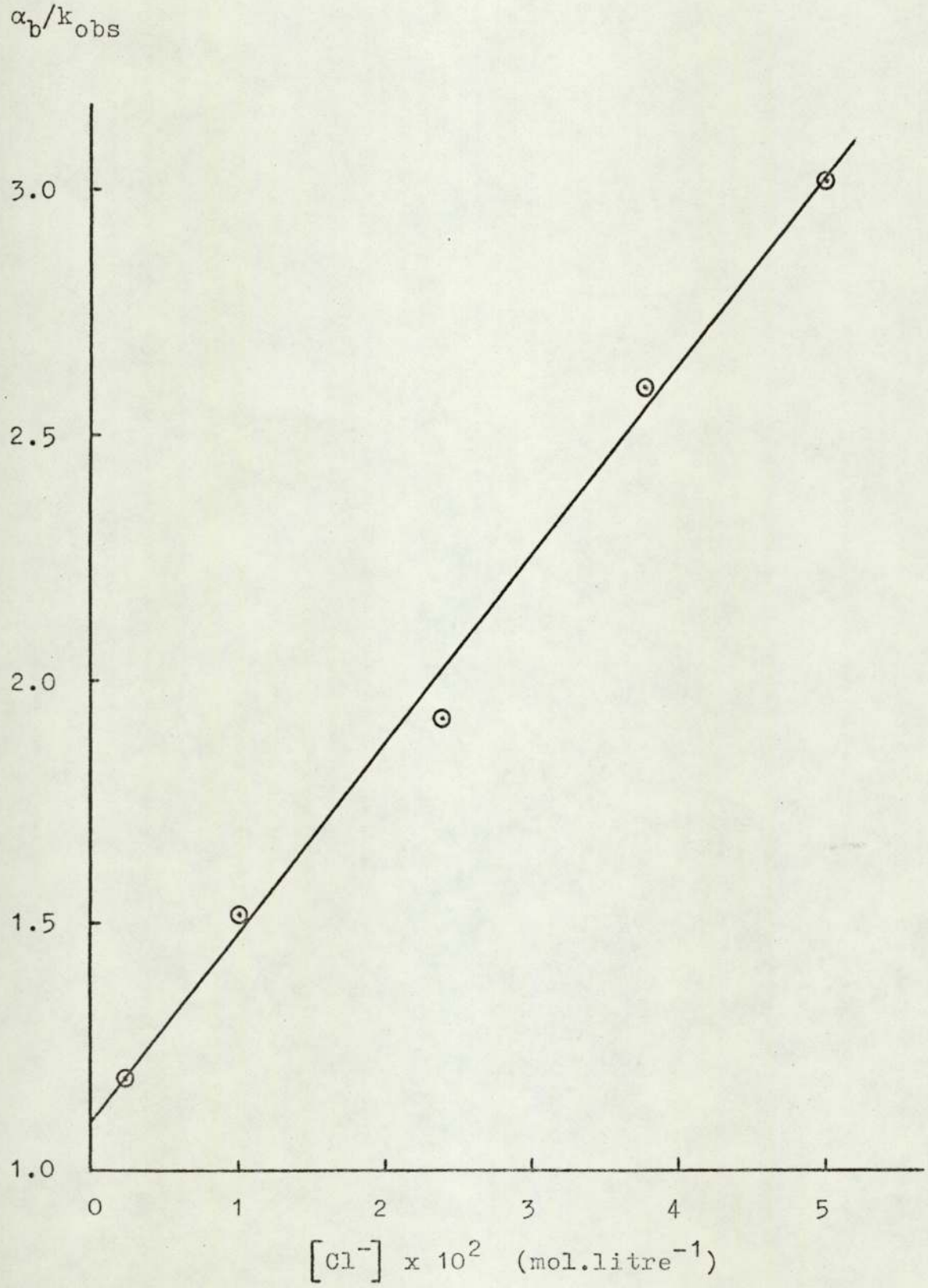

5.4. Kinetics of the production of the blau.

The formation of the blau was followed simultaneously to the release of acid, during a kinetic run, by using the apparatus described in section 2.2.2.2. The visible spectrum of a typical run solution, produced at an acetonitrile concentration of 0.1M and pH 7, is shown in figure 5.11. and exhibits an absorption maximum at ca. 612nm. A plot of the initial platinum concentration against the optical density at this wavelength, for such solutions, is shown in figure 5.12. and reveals Beer's law to be obeyed. The visible spectrum was found to remain essentially unaltered over the pH range 6 to 8.

Firstly, it was established that reproducible results could be obtained. Figure 5.13. shows two plots of the observed optical density against time under identical conditions. The profiles are seen to exhibit a general 'S' shaped character, but feature a pronounced induction period, suggesting the production of the blau to involve several rate determining steps.

The least squares computer program SEQUEXP (appendix 1) was developed specifically to enable an experimental curve to be fitted to a variable number of consecutive psuedo first order reactions. Furthermore, the program allows a predetermined number of consecutive steps to be defined, in the sense that their associated rate constants may be held constant at some suitable value. The remainder, and also the optical density at infinite time, may then be varied according to the least squares procedure, to give the optimum calculated fit. This treatment will be referred to as the constrained approach and is possible only if those rate constants that

are held may be determined independently. In this study such a criterion is fulfilled by the rate constants k_a and α_b, obtained from the kinetics of acid release (section 5.3.).

The treatment was found necessary since in some cases the blau profiles were best described by four consecutive reactions. If none were defined a number of equally good mathematical fits could be obtained, each comprising a different set of calculated rate constants. The chemical significance of these solutions was therefore questionable.

The constrained approach afforded good calculated fits for four consecutive reactions at high hydrogen ion and acetonitrile concentrations, however, the fits became rather worse as the concentration of these species decreased. A first order treatment of the latter portion of the profiles, taking a suitable mid-point as an arbitrary zero, produced good fits over all experimental conditions. The observed rate constant, α_c, was found to be in good agreement with that for the slowest step obtained from the acceptable fits using the constrained approach. It should be mentioned, however, that the production of the blau was accompanied by a gradual precipitation, which clearly affected the observed optical density during the very last stages of reaction. Accordingly the curves were fitted to ca. 90% completion.

These results demonstrate the presence of a third rate determining step, in addition to the two observed from the release of acid, governing the production of the blau. They also suggest the existence of a fourth rate determining step, less clearly defined. The rate constant, α_d, associated with this step, shows a marked dependence upon the experimental conditions. At high hydrogen ion and acetonitrile concentration

the relation

$$k_a \sim \alpha_b > \alpha_d \qquad 5.47.$$

is observed. Under these conditions the fourth step has a significant influence upon the reaction kinetics. Therefore, α_d may be determined accurately. However, at low hydrogen ion and acetonitrile concentrations the relation 5.47. is reversed and the influence of α_d upon the reaction is slight. Consequently, α_d may no longer be obtained properly and moreover, errors in the determination of k_a and α_b will give poor calculated fits

The observed rate constants cited in the following sections were either obtained from the constrained approach or from the first order treatment, with a modified version of the least squares computer program HYDR (appendix 2). Those runs treated in the latter fashion are marked with a double-dagger. The overall yield of the blau is expressed in terms of the optical density at infinite time, D_{inf}, calculated from the computed fits.

All kinetic runs were undertaken at a concentration of potassium tetrachloroplatinite of 0.0004M. Table 5.17. shows that the production of the blau is independent of the ionic strength of the reaction medium, at an acetonitrile concentration of 0.1M, pH 7 and 64°C.

Table 5.17.

μ	$\alpha_c(min^{-1})$	D_{inf}
0.01‡	0.00531	1.24
0.05‡	0.00540	1.19

Table 5.18. reveals that the production of the blau is essentially independent of the presence of added chloride ion, under these conditions, although a slight inverse dependence of D_{inf} upon the concentration of chloride ion is perhaps implied.

Table 5.18.

$[Cl^-]$	$\alpha_c(min^{-1})$	D_{inf}
0.002M‡	0.00525	1.17
0.010M‡	0.00530	1.24
0.024M‡	0.00471	1.13
0.038M‡	0.00533	0.963
0.050M‡	0.00456	0.853

5.4.1. Variation of the pH.

Runs were performed at a concentration of 0.1M acetonitrile and at 64°C.

Table 5.19. shows α_c and D_{inf} to be essentially independent and α_d to be inversely dependent upon the hydrogen ion concentration.

Table 5.19.

pH	$\alpha_c(min^{-1})$	$\alpha_d(min^{-1})$	D_{inf}
6.0	0.00613	0.0291	1.12
6.3	0.00604	0.0509	1.26
6.7	0.00586	0.0825	1.22
7.0‡	0.00557		1.34
7.2‡	0.00571		1.24
7.7‡	0.00595		1.39

Above pH 6.7 α_d is too large to have any real influence

upon the reaction.

5.4.2. Variation of the acetonitrile concentration.

Runs were performed at pH 7 and 64°C.

Table 5.20. reveals α_c to decrease rapidly to an approximately constant value, with increasing acetonitrile concentration, and suggests a similar dependence for α_d, although for the latter two runs* α_c and α_d are probably quite similar and consequently neither can be determined accurately (appendix 4). The dependence of D_{inf} is rather curious and is seen to rise to a maximum and then to decrease rapidly, with increasing acetonitrile concentration.

Table 5.20.

$[CH_3CN]$	$\alpha_c(min^{-1})$	$\alpha_d(min^{-1})$	D_{inf}
0.04M‡	0.0109		1.03
0.07M‡	0.00674		1.21
0.10M‡	0.00557		1.34
0.24M	0.00570	0.0391	0.788
0.38M	0.00554	0.0295	0.601
0.50M*	0.00517	0.0185	0.555
0.65M*	0.00507	0.0240	0.311

At acetonitrile concentrations of less than 0.24M α_d is too large to have any influence upon the reaction.

5.4.3. Variation of the temperature.

Runs were performed at a concentration of 0.1M acetonitrile and at pH 7.

Under these conditions α_d cannot be determined properly. Table 5.21. reveals D_{inf} to be effectively constant over the temperature range of study.

Table 5.21.

Temp.(^{o}C)	α_c(min^{-1})	D_{inf}
50.0‡	0.00177	1.33
57.0‡	0.00292	1.38
64.0‡	0.00557	1.34
71.0‡	0.00938	1.29
78.0‡	0.0163	1.08

An Arrhenius plot of the data of table 5.21. is shown in figure 5.14. and exhibits a good straight line. Calculation of the activation energy gives a value of 17.6 Kcal.mol^{-1}.

5.4.4. Dependence upon the presence of argon and oxygen.

Runs were performed at a concentration of 0.1M acetonitrile and at pH 7 and 64^{o}C.

Unfortunately, the passage of these gases through the reaction solution was found to cause 'spiking' on the optical density trace, undoubtedly due to the rapid flow of small bubbles across the spectrophotometer beam. This was rather pronounced in the argon run and produced an abnormally thick experimental curve. Thus the data for this run is probably in error. Moreover, in both runs D_{inf} was found to be less than expected, although the similar values imply the common responsibility of evaporation of acetonitrile, due to the gaseous flow. Consequently, these runs cannot be compared with that under atmospheric conditions at an acetonitrile concentration of 0.1M. Inspection of the values of D_{inf} from table 5.20. suggests that the acetonitrile concentration in these gaseous experiments is ca. 0.07M. Both runs are included in table 5.22., for the purpose of comparison with those runs under argon and oxygen.

Table 5.22.

Atmosphere	$\alpha_c(min^{-1})$	D_{inf}
Argon‡	0.00485	1.18
Air(0.07M)	0.00674	1.21
Air(0.10M)	0.00557	1.34
Oxygen	0.0101	1.15

The limitations of these experiments preclude any serious interpretation of the data of table 5.22. Nevertheless, it seems highly probable that α_c does, in fact, have a substantial dependence upon molecular oxygen.

5.4.5. Nature of the blau.

The microcrystalline, blue powder, isolated from the run solutions by the method described in section 2.3.6. (chapter 2), was investigated by a number of physical techniques. The results are summarized in table 5.23.

Table 5.23.

Technique	Peak	Assignment
Infrared	(cm^{-1}.)	
spectroscopy	3430 (medium)	O-H (stretch)
	3335 (medium)	N-H (stretch)
	2990 (weak)	C-H (stretch)
	2930 (weak)	C-H (stretch)
	1570 (strong)	C=O (stretch)
Mass	(mass units)	
spectroscopy	58	CH_3CONH
	43	CH_3CO
	42	CH_3CNH
n.m.r.	(Tau)	
spectroscopy	6.6	CH_3

Elemental analysis could not be reproduced. Samples showed a variable potassium and chloride content, however, the potassium to chloride ration was effectively 1:1 in each case suggesting potassium chloride to be a contaminant. The carbon to nitrogen ratio differed in each sample, indicating the retention of solvent, although desiccation was thorough. The analytical figures reported in section 2.3.6. reveal a platinum to nitrogen ratio of 1:2, consistent with two ligands per metal atom.

Support for the ionic nature of the chloride in the samples was found in their infrared spectra. The platinum-chlorine symmetric stretch at 344cm^{-1}. is completely absent[118]. The complex XVIII (figure 5.1., section 5.1.) has a reported[53] absorption at 342cm^{-1}. and the prepared complex dichlorobis-(acetonitrile)platinum(II) (section 2.3.6.) shows a strong absorption in this region at 343cm^{-1}. Thus the absence of coordinated chloride in the blau seems confirmed. A tentative assignment of the principle absorptions in the infrared spectra is shown in table 5.23. The O-H and N-H stretches are broad, suggesting some form of constraint, probably by hydrogen bonding, in the solid. The C=O stretch at 1570cm^{-1}. closely resembles that shown by metal acetates, indicating coordination through the C=O group, probably with chelation.

The presence of the acetamido group is indicated in the samples since their mass spectra show major mass peaks at 58, 43 and 42 mass units. A parent ion peak could not be found. Since the blue material does not melt, but decomposes above 250^{o}C, this is not surprising.

The material is not particularly soluble in common organic solvents. The only feature of the n.m.r. spectrum,

in deuterated dimethylsulphoxide, is a singlet at 6.6 Tau, which is exceptionally low for a methyl group[119]. However, a structure involving the acetamido group chelated to platinum(IV) would presumably result in considerable deshielding of the methyl protons and might explain the unusually low resonance. No evidence of an N-H proton resonance could be found, but since these are usually broad and the solution quite dilute the resonance of a single N-H proton would be difficult to distinguish above a noisy baseline. A low-field scan did not reveal an enolic O-H proton resonance.

The visible spectrum of the material in water exhibits a very broad absorption centred at 632nm. and thus differs from the original solution from which the solid was isolated. It seems likely that the concentration of such solutions causes a degree of polymerization, a possibility suggested by Brown et al[53]. Although polymerization is indicated in concentrated solution, Beer's law is obeyed for the blau prepared in dilute solution, implying the presence of monomeric species. The peak maximum of such solutions, at ca. 612nm., corresponds to that observed by Wilkinson et al[54] for the species dihydroxybis(acetamido)platinum(IV). However, it should be mentioned that the visible spectrum of this latter complex comprises a very broad absorption, which is sensitive to substantial changes in the pH. These factors may account for the disparity between the various determinations of the peak maximum reported for this complex.

Table 5.24. summarizes the visible spectroscopic data for these species and includes that of the related complex dichlorobis(acetamido)platinum(IV), for comparison.

Table 5.24.

Species	Peak max. (nm.)	M.ext.coeff.	Ref.
$PtCl_2(CH_3CONH)_2$	598	ca. 4000	53
	578		Within
$Pt(OH)_2(CH_3CONH)_2$	690	ca. 4000	53
	664		54
	614		54
	598		54
	578		54
	655 (pH 7)		Within
	643 (pH 4)		Within
Blau	612 (pH 7)		Within
(dilute soln.)	599 (pH 4)		Within
Blau			
(isolated solid)	632 (pH 7)		Within

The physical data discussed here shows that the blau is closely related to dihydroxybis(acetamido)platinum(IV) and suggests that it may contain this complex as a major component. This is supported by the kinetic studies in that complex equilibria are indicated for the final species in solution.

5.4.6. Interpretation of the results.

The dependence of α_c and α_d upon the acetonitrile concentration, revealed by table 5.20., may both, in principle, be explained by the scheme 5.48.

$$A \xrightarrow{k_s} \text{side reaction path}$$

$$A + xL \underset{}{\overset{K_x}{\rightleftharpoons}} B$$

$$B \xrightarrow{k_m} \text{main reaction path} \qquad 5.48.$$

for which it may be shown that

$$k_{obs} = \frac{(k_s + k_m K_x L^x)}{(1 + K_x L^x)} \qquad 5.49.$$

As the concentration of acetonitrile is increased k_{obs} will tend to the constant value of k_m.

However, since it is quite possible that α_d, in fact, continually decreases with increasing acetonitrile concentration and does not approach a constant value, the scheme 5.50. must be considered as an alternative.

$$A + yL \overset{K_y}{\rightleftharpoons} B$$

$$A \xrightarrow{k_m} \text{main reaction path} \qquad 5.50.$$

for which

$$k_{obs} = \frac{k_m}{(1 + K_y L^y)} \qquad 5.51.$$

The dependence of α_d upon the hydrogen ion concentration, exhibited in table 5.19., may be considered to arise from a rate determining direct attack of hydroxide ion, followed by a rapid protonation, according to the scheme 5.52.

$$A + nOH^- \xrightarrow{k_m} B^{n-}$$

$$B^{n-} + nH^+ \overset{K_n}{\rightleftharpoons} BH_n$$

$$BH_n \longrightarrow \text{main reaction path} \qquad 5.52.$$

for which

$$k_{obs} = k_m[OH^-]^n \qquad 5.53.$$

Alternatively, the dependence may, in principle, be explained in terms of the scheme 5.54.

$$A + nH^+ \overset{K_n}{\rightleftharpoons} AH_n^{n+}$$

$$A \xrightarrow{k_m} \text{main reaction path} \qquad 5.54.$$

for which

$$k_{obs} = \frac{k_m}{(1 + K_n H^n)} \qquad 5.55.$$

Once the release of acid is complete in these reactions no further pH change is observed. This fact demonstrates that there can be no permanent loss or capture of hydrogen ion during the remainder of the reaction sequence. Moreover, it militates strongly against the scheme 5.54., since in order to account for the substantial dependence shown by α_d upon the pH (table 5.19.) the proposed acid-base equilibrium must operate strongly in favour of the protonated species at pH 6. This would necessitate a significant temporary increase in the pH.

The dependence of D_{inf}, at high acetonitrile concentration, may be considered to arise from the equilibrium 5.56. of the product.

$$\text{Blau} + zL \overset{K_z}{\rightleftharpoons} \text{Not blau} \qquad 5.56.$$

for which

$$D_{inf} = \frac{D_{max}}{(1 + K_z L^z)} \qquad 5.57.$$

where D_{max} is the theoretical optical density at infinite time for 100% reaction.

The function that describes the variation of D_{inf} over all acetonitrile concentrations must take account of the proposed parallel reaction of the scheme 5.48. and may be shown to be of the form

$$D_{inf} = \left(\frac{k_m K_x L^x}{(k_s + k_m K_x L^x)} \right)^p \frac{D_{max}}{(1 + K_z L^z)} \qquad 5.58$$

where p=2, if both consecutive steps involve a parallel reaction.

Presumably the small variation of D_{inf} with chloride ion concentration may be explained in terms of a similar process to that of the equilibrium 5.56., although no realistic plot can be obtained.

5.4.7. Discussion.

It is impossible, from the data available, to assign an unambiguous mechanism for the production of the blau during the stages of reaction after the release of acid is complete. However, on the basis of the general alternatives advanced in section 5.4.6., the implications of section 5.3., several important observations on the system and the accepted chemistry of platinum(II) and platinum(IV), a plausible scheme may be suggested.

Table 5.19. reveals the independence of D_{inf} upon the pH. Therefore, the two species of the equilibrium 5.39. (section 5.3.6.) must both be on the direct route to the blau.

$$PtCl(H_2O)(OH)_2^- \overset{K_6}{\rightleftharpoons} PtCl(OH)_3^{2-} + H^+ \qquad 5.39.$$

The infrared data reported in section 5.4.5. shows the blau to contain no coordinated chloride ion. Therefore, the removal of the final chloride ion would seem a necessary prerequisite to blau formation. The results of section 5.3. imply that the most probable attacking reagent, in the case of the species of the equilibrium 5.39., would be water. Moreover, inspection of table 5.15. (section 5.3.8.) strongly suggests that such a replacement would be relatively slow. However, the dependences of α_c and α_d preclude their association with such a reaction. Therefore, it seems likely that the replacement of the final chloride ion does not occur on platinum(II), but relatively rapidly by some other process.

Table 5.20. reveals the yield of the blau to decrease with decreasing acetonitrile concentration, below 0.1M in this reagent. In fact, experiments performed at 0.02M in acetonitrile produced a grey precipitate and almost no blau. The analytical data reported in section 2.3.6. shows the blau to contain two nitrogen atoms per platinum atom and taken in conjunction with the results of section 5.4.5. indicate that these are derived from the acetamido group. Therefore, it appears that ultimately two acetonitrile ligands must coordinate to platinum and undergo hydrolysis, prior to the formation of the blau.

As previously mentioned, the data of tables 5.5., 5.6. and 5.7. for $\emptyset$ (section 5.3.) may only be rationalized if the species of the equilibrium 5.39. are not involved in further equilibria with acetonitrile. The data of table 5.9. suggests a similar criterion to operate in the case of molecular oxygen. However, these limitations need only apply, in principle, to those strongly bound equatorial ligands on platinum(II). Thus

it is permissible to consider suitable equilibria involving the replacement of loosely bound axial ligands.

The results of sections 5.3.5. and 5.4.4. reveal the oxidation step to occur after the stepwise hydrolysis of the tetrachloroplatinite(II) ion. The work in phosphate buffer (section 5.2.3.) implies that a four-electron transfer does not occur since this would require the production of the blau to show a dependence upon the platinum(II) concentration. Another point of interest is that the oxidation of transition metal ions is reported to be enhanced by the coordination of oxygen donor ligands, especially the hydroxide ion[24]. It seems reasonable to propose, therefore, that the stepwise hydrolysis of the tetrachloroplatinite(II) ion reduces the value of $E^{o}(Pt^{4+}/Pt^{2+})$, such that the oxidation of platinum(II) by molecular oxygen, in a two-electron step, becomes favourable.

It seems probable that the hydrolysis of coordinated acetonitrile would occur on platinum(IV), following the oxidation step. Arguably, the superior ability of platinum(IV) to polarize the nitrile bond would facilitate nucleophilic attack at the electron deficient carbon atom. Reference to section 5.1. suggests that the attacking reagent would be the hydroxide ion. Moreover, the dependence of α_d, revealed at high hydrogen ion concentration by table 5.19., is certainly consistent with the hydrolysis of one acetonitrile ligand, by such a process.

The points made so far form the basis upon which a plausible mechanism may be proposed. Since the major component of the equilibrium 5.39., over the pH range of study, is the dihydroxy species, it is the pathway from this species that is considered for simplicity. The pathway from the trihydroxy

species is presumed to be essentially identical.

The oxidation step may be considered in terms of the scheme 5.59., which is also in accord with the general dependence shown by α_c upon the acetonitrile concentration and molecular oxygen.

$$\begin{array}{l} Pt^{II}Cl(H_2O)(OH)_2(H_2O)_2^- \\ \quad H_2O \uparrow\downarrow O_2 \\ Pt^{II}Cl(H_2O)(OH)_2(H_2O)(O_2)^- \xrightarrow{k_s} Pt^{IV}Cl(OH)_3(H_2O)(O_2H)^- \\ \quad H_2O \uparrow\downarrow CH_3CN \\ Pt^{II}Cl(H_2O)(OH)_2(CH_3CN)(O_2)^- \xrightarrow{k_c} Pt^{IV}Cl(OH)_3(CH_3CN)(O_2H)^- \end{array} \qquad 5.59.$$

The preequilibrium processes are suggested to involve the replacement of the loosely coordinated axial ligands on platinum(II). Table 5.19. reveals α_c to be independent of the hydrogen ion concentration at an acetonitrile concentration of 0.1M. Therefore, it is necessary to propose that the rate constant for the oxidation of the platinum(II)-acetonitrile species derived from the trihydroxy species of the equilibrium 5.39. is similar to k_c.

The subsequent mechanistic discussion must of necessity be highly speculative. For instance, the general dependence of α_d, revealed at high acetonitrile concentration by table 5.20., may reasonably be explained by any one of several preequilibrium schemes. Moreover, each of these involves substitution reactions of platinum(IV) and would therefore be expected to be relatively slow. It is possible, however, to circumvent this latter problem by postulating such substitution reactions to occur rapidly by either S_N1CB (substitution nucleophilic unimolecular conjugate base) mechanisms[120], or

platinum(II) catalysis[121].

It is noted, in this context, that the course of the reaction is most probably subtly dictated by the cis and trans effects of the various ligands on platinum(IV)[122].

In view of the inherent complexity of the system the subsequent mechanistic proposals will be confined to one plausible scheme, in which the acetamido anion is considered to play an important role.

It is possible to explain the dependence of α_d in terms of the scheme 5.60., in which the proposed preequilibrium is suggested to be platinum(II) catalysed.

$$\begin{array}{lll} Pt^{IV}Cl(OH)_3(H_2O)(O_2H)^- & & \text{side reaction path} \\ \quad H_2O \uparrow\downarrow CH_3CN & & \\ Pt^{IV}Cl(OH)_3(CH_3CN)(O_2H)^- & \xrightarrow[+OH^-]{k_d} & Pt^{IV}Cl(OH)_3L'(O_2H)^{2-} \\ & & \quad H_2O \uparrow\downarrow H^+ \\ & & Pt^{IV}Cl(OH)_2L''(O_2H)^- \end{array} \qquad 5.60.$$

Here, L' refers to the monodentate and L'' to the chelated acetamido anion. Both species may be considered as conjugate bases and might therefore be anticipated to labilize those ligands situated trans to them[120]. Thus, once the chelation of the acetamido anion occurs, it is possible to envisage a series of rapid equilibria, involving those ligands situated in a trans position. Consequently, it is feasible to propose the rapid hydrolysis of a second acetonitrile ligand, according to the scheme 5.61.

It is understood that, in principle, there are a great number of preequilibria, that can operate, for the schemes 5.60. and 5.61. It seems reasonable to propose, however, that

only those species involving one or two nitrogen containing ligands can be on the direct route to the blau.

$$\begin{array}{l} Pt^{IV}Cl(OH)_2L''(O_2H)^- \\ H_2O_2 + Cl^- \rightleftharpoons H_2O + CH_3CN \\ Pt^{IV}(OH)_3L''(CH_3CN) \end{array} \xrightarrow[+OH^-]{\text{fast}} \begin{array}{l} Pt^{IV}(OH)_3L''L'^- \\ H_2O \rightleftharpoons H^+ \\ Pt^{IV}(OH)_2(L'')_2 \end{array} \qquad 5.61.$$

The equilibria of the final product, indicated by the dependence of D_{inf} upon the acetonitrile and possibly the chloride ion concentration, might be explained in terms of schemes such as 5.62.

$$Pt^{IV}(OH)_2(L'')_2 \xrightleftharpoons{2CH_3CN} Pt^{IV}(OH)_2(L')_2(CH_3CN)_2 \qquad 5.62.$$

This idea finds some support in the observations of Brown et al[53], who reported their isomers of their blau to undergo a slow tautomerism. Thus the yellow, monodentate species XIX was found to isomerize to the blue, chelated species XX (section 5.1.).

Finally, it should be mentioned that the lack of further pH changes, after the release of acid is complete, shows that the blau must consist of two basic species, involved in an acid-base equilibrium, the ionization constant for which is effectively equal to K_6, for the equilibrium 5.39.

Figure 5.11.

Visible spectrum of the blau produced at concentrations of 0.0004M potassium tetrachloroplatinite, 0.1M acetonitrile and at pH 7.

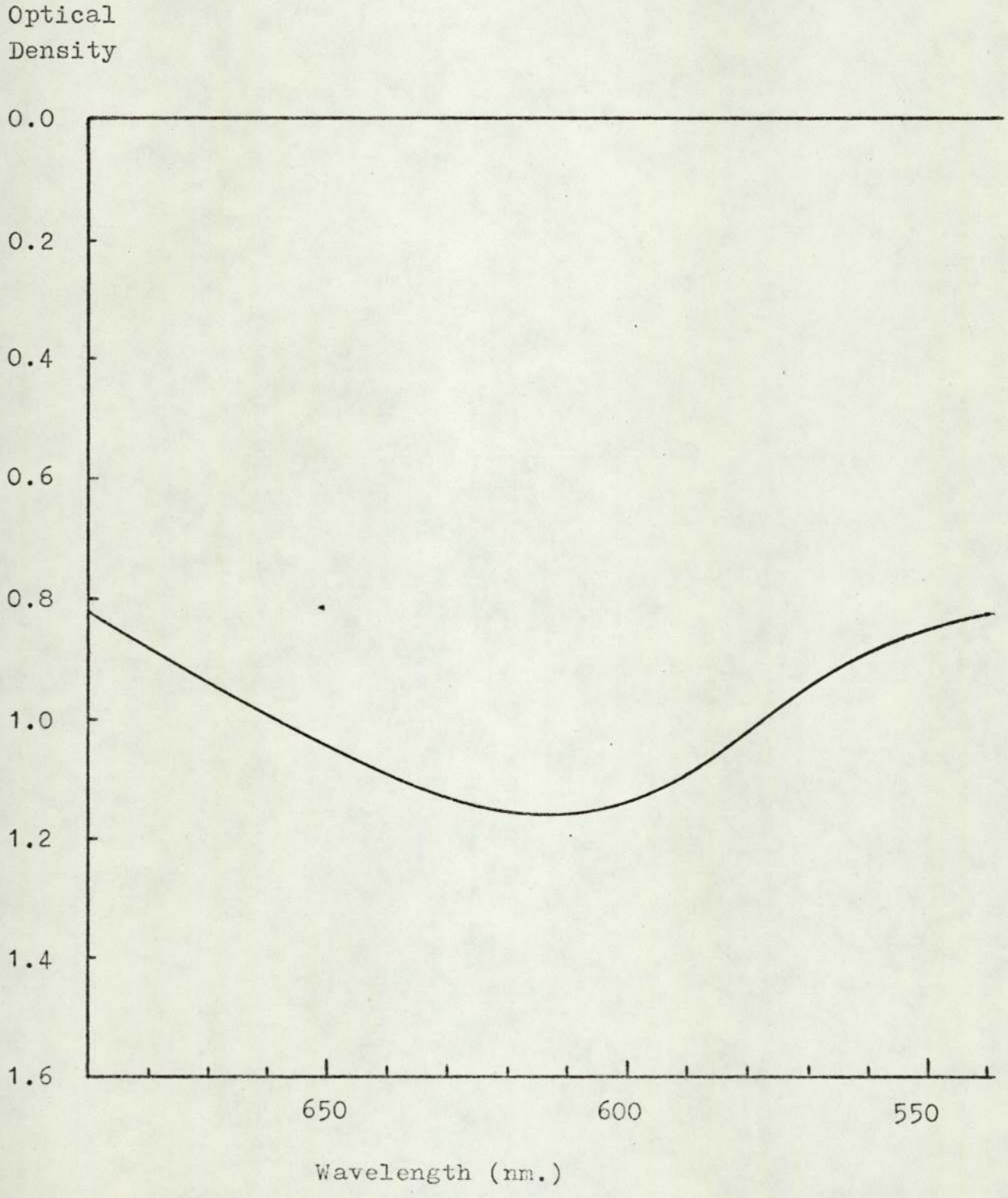

Figure 5.12.

Plot of the optical density at 612nm. against the initial concentration of potassium tetrachloroplatinite, for blau solutions produced at a concentration of 0.1M acetonitrile and at pH 7.

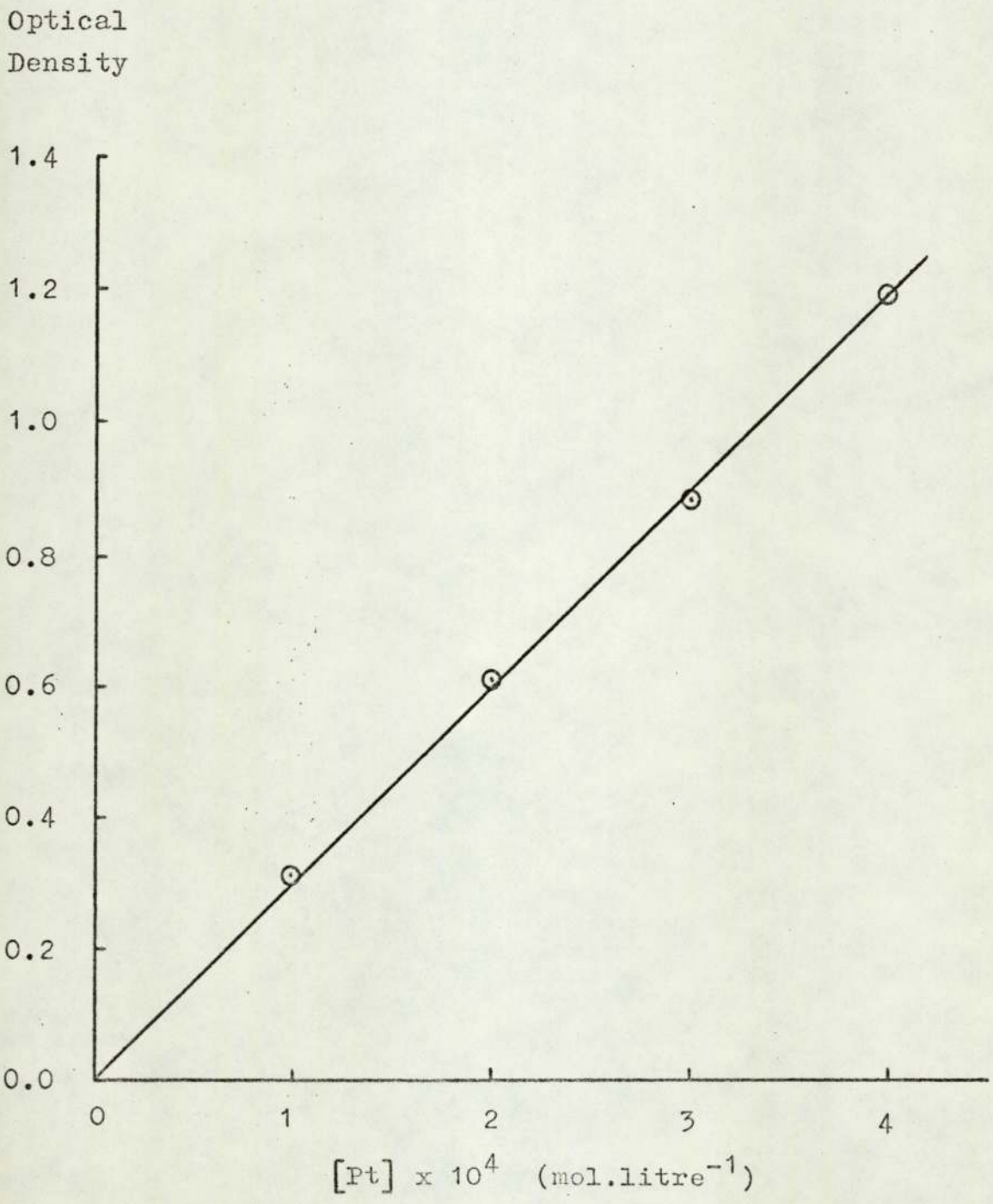

Figure 5.13.

Two plots of the optical density at 612nm. against time at concentrations of 0.0004M potassium tetrachloroplatinite, 0.1M acetonitrile, pH 7 and 64°C.

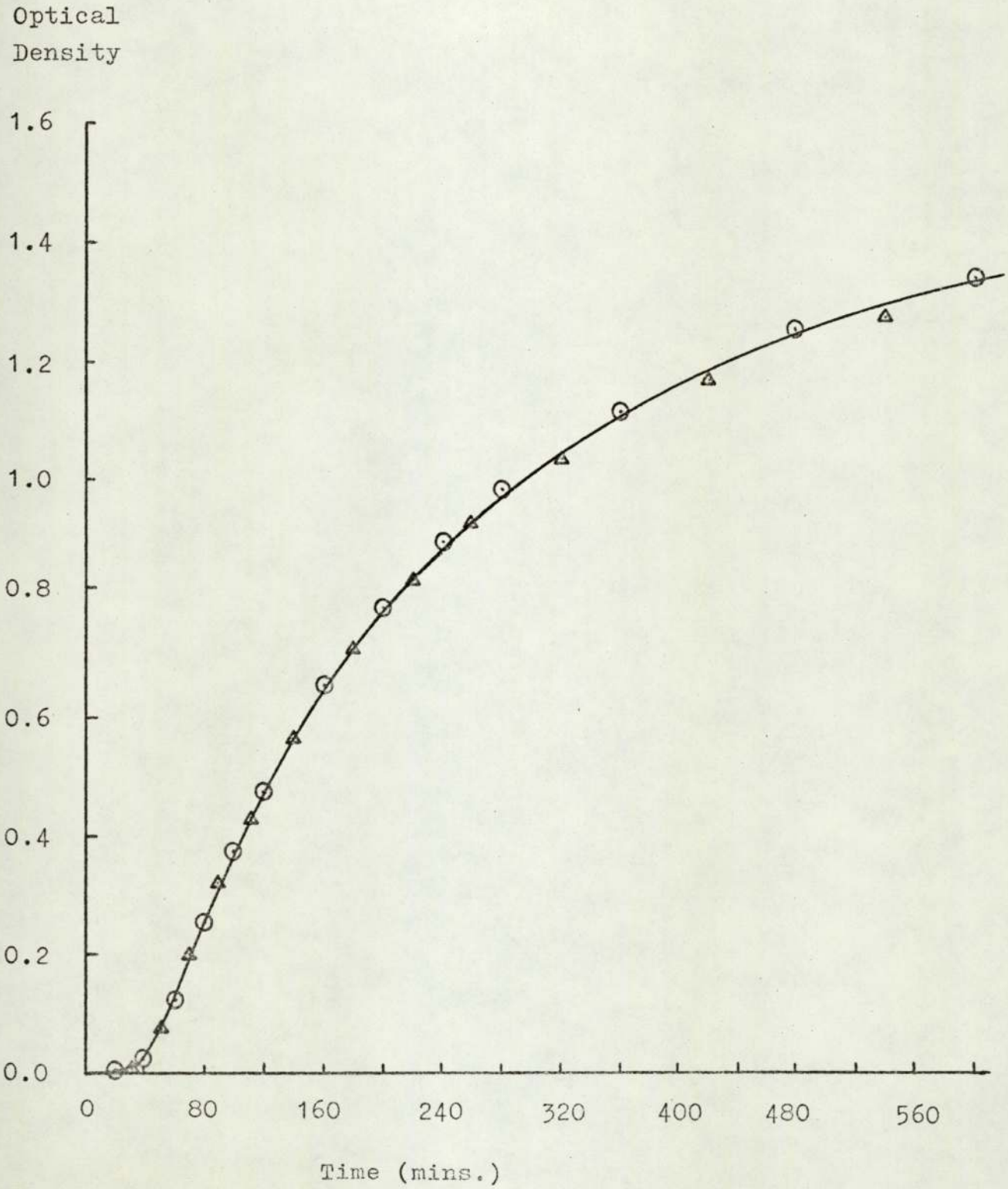

Figure 5.14.

Plot of $\log_{10}\alpha_c$ against 1/T at a concentration of 0.1M acetonitrile and pH 7.

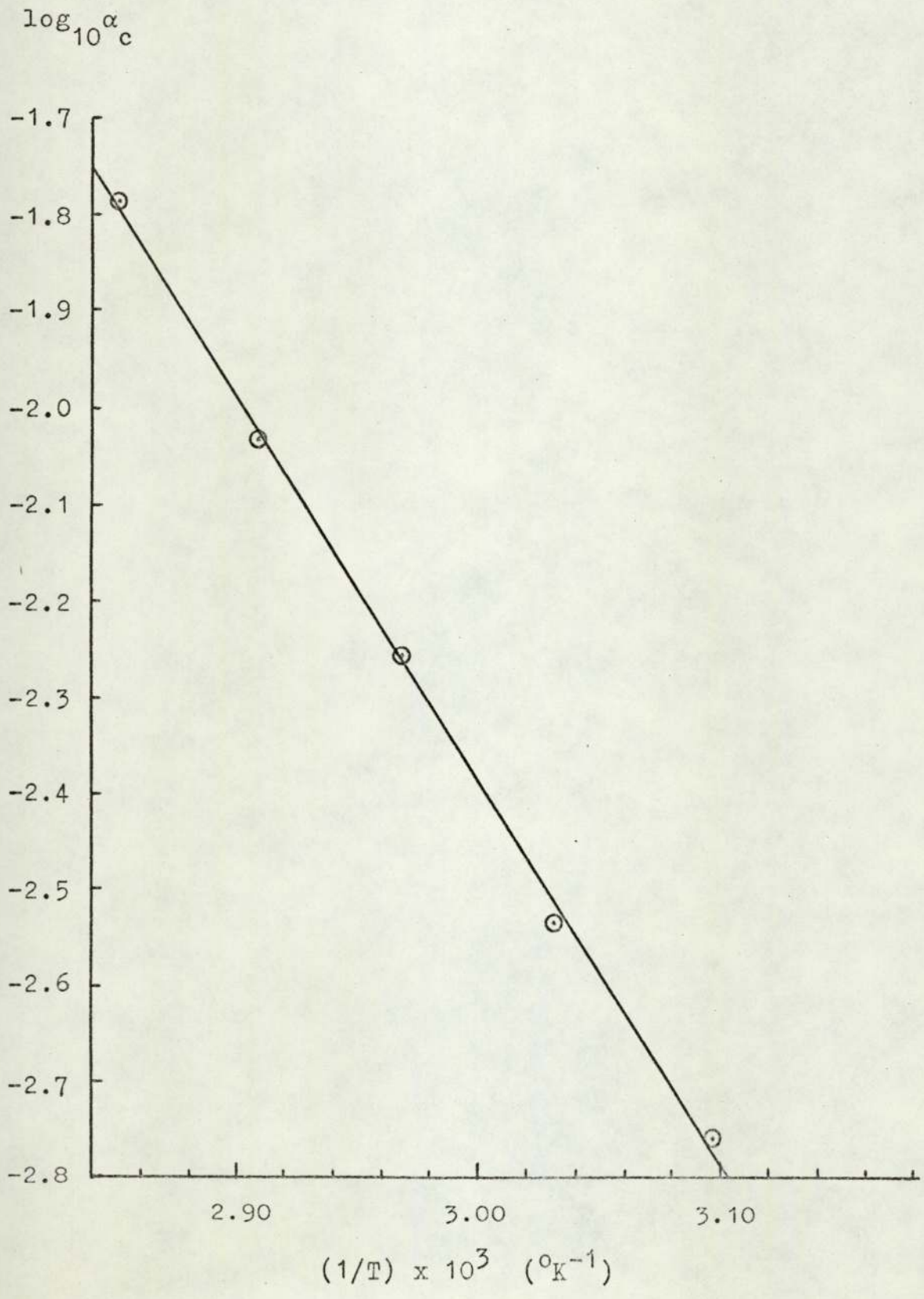

5.5. Proposed reaction mechanism.

The following overall reaction mechanism is postulated for the production of the blau from the tetrachloroplatinite(II) ion and excess acetonitrile.

Initially the stepwise replacement of chloride ion from the coordination sphere of platinum(II) is proposed. The principle attacking reagent is suggested to be water and the release of between two and three protons per platinum atom are observed. The mechanism advanced to account for this is shown schematically in figure 5.15., in which attacking species are assumed and the major species are underlined.

Figure 5.15.

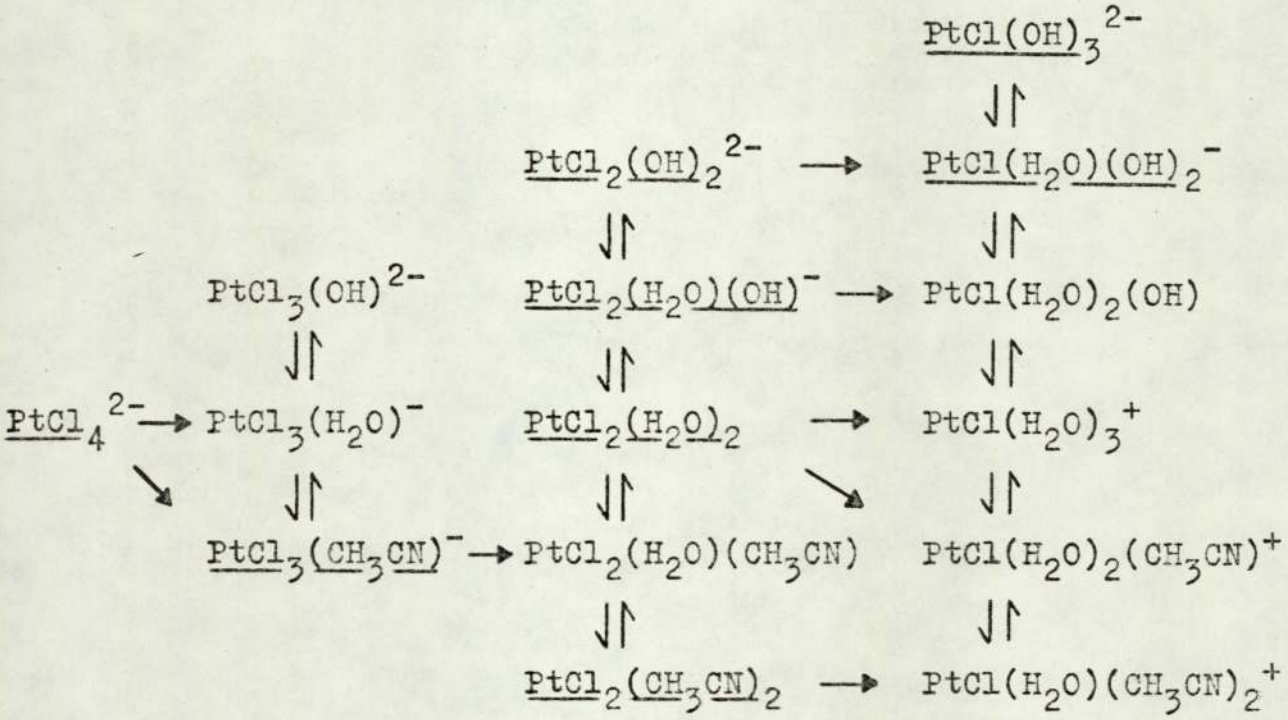

The latter stages of the reaction remain unconfirmed. It seems feasible that the oxidation of the two monochloro species of platinum(II), underlined above, occurs via a two-electron transfer from platinum(II) to coordinated molecular oxygen and subsequently that the hydrolysis of acetonitrile takes place on platinum(IV). The hydrolysis step may involve

the attack of hydroxide ion upon the electron deficient carbon atom of the nitrile group. Using the data of table 5.19. and equation 5.53., for n=1, an estimate of 2000 $mol^{-1}.sec^{-1}$. may be made for the second order rate constant of such a base hydrolysis, at 64°C. This may be compared to the value of ca. 500 $mol^{-1}.sec^{-1}$. for the base hydrolysis of benzonitrile on cobalt(III), calculated from the data of Pinnel et al[104], at 64°C. A similar comparison for the base hydrolysis of acetonitrile on cobalt(III) is prevented, since no parameters of activation were reported for this reaction[105].

The blau is suggested to comprise two components, both containing the chelated acetamido anion and involved in an acid-base equilibrium. One of these species is thought to be dihydroxybis(acetamido)platinum(IV) and the other a deprotonated form.

6. A report of some incomplete investigations.

In addition to the two principle research topics presented in this thesis a number of incidental studies were undertaken. These are reported primarily as interesting areas, in which further research may prove profitable.

6.1. Differential scanning calorimetric (D.S.C.) studies of several nickel(II)-aldoxime complexes.

Four complexes of the general formula NiL_4X_2, where L represents benzaldoxime or p-methoxybenzaldoxime and X represents chloride or iodide, were investigated.

Each sample was crimped into an aluminium sample pan and scanned at $8^{o}C.min^{-1}$. under a nitrogen atmosphere. Each scan was corrected for thermal lag. The various endothermic and exothermic processes observed for each complex are compared to their melting point characteristics in table 6.1.

Table 6.1.

Complex	M.pt. characteristics		D.S.C. scan	
	Temp. ^{o}K	Observations	Temp. ^{o}K	Observations
$Ni(PhCHNOH)_4Cl_2$	441-448	Green:melts	447-450	Endotherm
	478-488	Yellow:boils	485-495	Exotherm
	488	Brown solid		
$Ni(PhCHNOH)_4I_2$	410-418	Green to red: melts	ca. 423	Endotherm
	428-435	Black:boils	427-444	Exotherm
$Ni(pMeOPhCHNOH)_4Cl_2$	418-425	Green:melts	425-432	Endotherm
	477-488	Yellow:boils	482-494	Exotherm
	488	Brown solid		
$Ni(pMeOPhCHNOH)_4I_2$	407-413	Green to red: melts	ca. 411	Endotherm
	416-420	Black:boils	414-426	Exotherm

Table 6.1. reveals the principle thermal characteristics of these complexes to be as follows. As the temperature of each complex is raised, initially an endothermic process occurs, which corresponds closely to its observed melting point. Subsequently, an exothermic process arises, often accompanied by substantial physical changes within the sample. In the case of the iodide complexes the endotherms were partially masked by the large exotherms.

The exotherms are presumably due to the nickel(II) catalysed rearrangement of the aldoxime. The thermal stabilities of the complexes are seen to obey the following relationships. Benzaldoxime $>$ p-methoxybenzaldoxime, for a given halide ligand, and chloride $>$ iodide, for a given aldoxime ligand. The latter observation is consistent with the implications of section 3.4.1. (chapter 3), namely that iodide compounds are superior to their chloride analogues as catalysts for the rearrangement of benzaldoxime to benzamide.

6.2. A study of the behaviour of cyanoacetamide in the presence of several transition metal ions.

The hydrolysis of malononitrile, in aqueous alkaline solution at 25°C, has been reported to occur in two consecutive pseudo-first order steps, initially to produce cyanoacetamide and subsequently to yield cyanoacetic acid[123], according to the scheme 6.1.

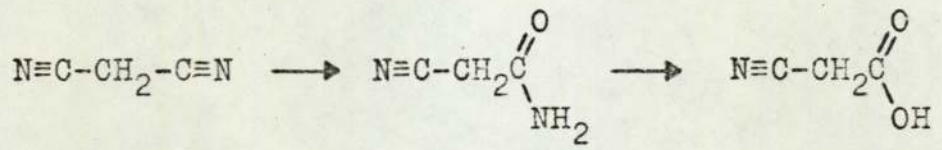

6.1.

The second nitrile group of malononitrile was observed to be singularly resistant to hydrolysis under these conditions.

It was suggested that this was due to the formation of the carbanion of malononitrile, presumably as a result of the somewhat stringent conditions employed.

It was of interest to determine, therefore, whether the hydrolysis of the nitrile group of cyanoacetamide could be achieved under more gentle conditions, in the presence of a suitable metal ion.

The structure of cyanoacetamide suggests that hydrolysis could, in principle, be facilitated by coordination to a metal ion in two different ways. Firstly, by the direct N-coordination of the nitrile group (XXV), and secondly, by coordination of the amide group through either oxygen or nitrogen (XXVI).

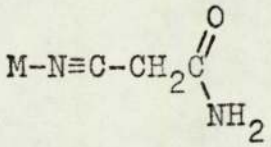

XXV

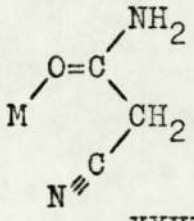

(or via N)

XXVI

Both these structures have literature parallels in the metal ion assisted hydrolysis of nitriles[87,104,105,106] (section 5.1.).

The simple expedient of gently refluxing an excess of cyanoacetamide, in aqueous solutions containing catalytic amounts of certain first-row transition metal ions, produced no malonamide, as determined by melting point analysis. The potential catalysts studied by this means included chromium(III), iron(III), cobalt(II), nickel(II) and copper(II). The latter metal ion seemed the most promising, since a colour change from blue to green was observed during refluxing.

A further investigation revealed several transition metal ions to show a tendency to interact with cyanoacetamide. The

most promising systems studied are summarized in table 6.2.

Table 6.2.

Reagents	Conditions	Observations (hrs.)
$Cu(OAc)_2H_2O$(1mmol) +$NCCH_2CONH_2$(2mmol)	Butanol(25mls.): reflux.	Blue to green solution: dirty green ppt. (ca.1)
$RhCl_3xH_2O$(1mmol) +$NCCH_2CONH_2$(2mmol)	Ethanol/water(6:1) (35mls.):reflux.	Red to orange solution: orange ppt. (ca.6)
K_2PdCl_4(1mmol) +$NCCH_2CONH_2$(2mmol)	Water(10mls.): stand at R.T.	Orange ppt. (ca.8)
K_2PtCl_4(1mmol) +$NCCH_2CONH_2$(2mmol)	Water(10mls.) stand at R.T.	Brown ppt. (ca.72)

The precipitates of table 6.2. were filtered at the pump, washed thoroughly with fresh solvent, ethanol and diethylether and dried under vacuum, over silica gel.

The compound $RuCl_3xH_2O$ was treated in a similar manner to that of its rhodium analogue (table 6.2.). However, a small excess of zinc dust was added during refluxing, to reduce the ruthenium(III) to ruthenium(II). After ca. 1hr. the suspension was filtered at the pump and an excess of diethylether added to the yellow filtrate. The yellow, flocculent precipitate, thus produced, was observed to decompose rapidly, to yield a green, spongy mass. In addition, the yellow filtrate was seen to darken more gradually, to produce a green solution.

These observations suggest that the atmospheric oxidation of ruthenium(II) to ruthenium(III) is involved in this system.

The infrared spectra of the materials isolated from the systems of table 6.2. and that of cyanoacetamide were recorded in the solid state as potassium bromide discs. The salient

features of the spectra are compared in table 6.3.

Table 6.3.

Origin of compound	Absorption (cm^{-1})	Assignment
Free ligand	3410,3220 (medium)	N-H (stretch:primary)
	2275 (medium)	C≡N (stretch)
	1690 (strong)	C=O (stretch)
	1620 (strong)	N-H (bend)
Cu(II) system	3270 (medium)	N-H (stretch:secondary)
	2170 (medium)	C≡N (stretch)
	1640 (strong)	C=O (stretch)
	1600 (strong)	N-H (bend)
Rh(III) system	3320,3180 (strong)	N-H (stretch:primary)
	1650 (strong)	C=O (stretch)
	1605 (medium)	N-H (bend)
Pd(II) system	3430,3320 (medium)	N-H (stretch:primary)
	2220 (medium)	C≡N (stretch)
	1650 (strong)	C=O (stretch)
	1585 (medium)	N-H (bend)
Pt(II) system	3300,3190 (medium)	N-H (stretch:primary)
	1685 (strong)	C=O (stretch)
	1600 (medium)	N-H (bend)

The assignments of table 6.3. are somewhat tentative, however, the spectra clearly demonstrate that the nitrile group of cyanoacetamide has undergone substantial modification. The C≡N stretch is lowered by $105cm^{-1}$. in the copper(II) system, by $55cm^{-1}$. in the palladium(II) system, and is absent altogether in the rhodium(III) and platinum(II) systems.

The infrared spectrum of the material isolated from the copper(II) system would seem to indicate a structure of the type XXVI, in which coordination is achieved through the deprotonated nitrogen atom of the amide group and a degree of

pi interaction between the metal ion and the nitrile group occurs.

The copper(II) system was somewhat irreproducible. Replacement of butanol by ethanol yielded a much darker material, with the C≡N stretch at 2170cm^{-1}. much reduced in intensity. Attempts to undertake the reaction in water produced copper metal.

7. Conclusions and suggestions for further work.

The ability of nickel(II) to catalyse the rearrangement of benzaldoxime to benzamide is suggested to be due principally to two factors. Firstly, the N-coordination of β-benzaldoxime to nickel(II) is believed to cause a degree of polarization of the C=N bond and to facilitate nucleophilic attack, at the electron deficient carbon atom, by a suitable oxygen containing nucleophile in solution. Secondly, the intermediate, thus produced, postulated to be a benzimidate, is suggested to exhibit a low affinity for nickel(II) and to enable the regeneration of the catalytic species.

Although the essential inorganic features of this rearrangement have been resolved, there remains further scope in some of the organic aspects of the reaction. Primarily, the isolation and unambiguous identification of both the intermediate and the side product(s) are required.

The kinetic studies were performed under somewhat fierce conditions. An investigation of the rearrangement of the water soluble compound, acetaldoxime, in aqueous solutions containing the nickel(II) ion, at lower temperatures, might be experimentally easier.

Preliminary studies with zinc(II) suggest that an investigation of the catalytic function of this metal ion would be of interest. The diamagnetism of zinc(II) would enable nuclear magnetic resonance spectroscopy to be used as an additional technique in such a study.

The Lossen and Curtius reactions are closely related to the Beckmann rearrangement[127,128]. All three processes involve the migration of a suitable group from a carbon atom to an electron deficient nitrogen atom. It would be of interest,

therefore, to determine whether nickel(II) or zinc(II) have any catalytic influence upon these reactions.

The production of the blau, in aqueous solutions of potassium tetrachloroplatinite and acetonitrile, has proved to be dependent upon a complicated sequence of processes.

The initial stages of the reaction are suggested to mainly involve the stepwise aquation of the tetrachloroplatinite(II) ion. The release of acid, observed during this process, is proposed to arise from the deprotonation of coordinated water. The behaviour of acetonitrile, towards the various species of platinum(II), appears somewhat enigmatic. It is suggested that acetonitrile may be required to function initially as a pi acid towards platinum(II). This theory implies that the substitution of chloride ion, by acetonitrile, should depend both on the pi donor ability and the actual size of the other ligands on the platinum(II) substrate.

It might prove illuminating, therefore, to compare the rates of chloride ion substitution, by acetonitrile, for a suitable range of substrates, differing essentially in the pi donor ability of their ligands. In addition, a comparison of the rates of chloride ion substitution, for a series of nitriles of increasing bulk, with a single substrate containing other bulky ligands might be worthwhile. It would probably be necessary to undertake such studies in non-aqueous media.

The latter stages of the reaction remain obscure and the principle objective of the study, namely the elucidation of the mechanism of acetonitrile hydrolysis, has not been satisfactorily concluded. Nevertheless, the problem should not prove insoluble, although further experimentation is required.

In addition to the two steps involved in the release of acid, two further rate determining steps are suggested to govern the production of the blau. Unfortunately, the majority of experiments were performed under conditions at which the faster of these became kinetically unimportant. An investigation of the reaction over the pH range 4.3 to 6.7, using pH 5 as a pivot, should prove more profitable.

Under these conditions a careful kinetic study, over a range of low acetonitrile concentrations, should provide a more detailed insight into the nature of the preequilibria and the side reactions indicated for these steps. Moreover, the dependence of the reaction upon the concentration of molecular oxygen, argon and platinum(II) should be more thoroughly investigated, to enable a clearer understanding of the oxidation step.

In addition, a study of the behaviour of the blau in aqueous solutions containing either acetonitrile or chloride ion is necessary, to establish the nature of the complex equilibria indicated for the final product.

It seems likely that the oxidation of platinum(II) to platinum(IV) is a necessary prerequisite to blau formation. An investigation of aqueous solutions of the hexachloroplatinate(IV) ion and acetonitrile might therefore prove interesting. Since the oxidation step appears to be the slowest in the reaction sequence, such a study could be undertaken at lower temperatures, subject to the rate of the various substitution reactions of platinum(IV), thus obviating the problem of acetonitrile evaporation.

A kinetic investigation of the original reaction of Hoffmann and Bugge[102] (section 5.1.) would presumably be inherently simpler than the system studied here. It should

be feasible to circumvent the problem of silver chloride precipitation (section 5.1.) by the inclusion of an effective filtration unit in the peristaltic flow circuit of the apparatus described in section 2.2.2.2. This reaction might prove interesting since the oxidation of platinum(II) by silver(I) is a possibility.

A kinetic study of the related amminolysis reaction[109] (section 5.1.) should be simpler still since there is no oxidation step involved and the problem of silver chloride precipitation does not arise. It might also be of interest to determine whether a similar reaction occurs between the tetrammineplatinum(II) ion and acetonitrile.

Finally, it is reiterated that there is considerable scope for further investigation into the behaviour of cyanoacetamide, in the presence of copper(II), rhodium(III), palladium(II), platinum(II) and perhaps ruthenium(III).

Appendix 1.

Least squares computer program SEQUEXP.

```
'BEGIN'
'REAL' X,Y,SQ;
'INTEGER' D,E,I,J,K,L,M,N,Ø,P,Q,R,A;
'REAL' 'ARRAY' G,F[1:5],S,V[0:10],B,T[1:99],U,H[1:5,1:10],
W[1:10,1:10],C[1:5,1:10,1:10];
'SWITCH' Z:= ONE,TWO,THREE,FOUR,FIVE,SIX,SEVEN,EIGHT,NINE,
TEN,ELEVEN;
ONE: A:= READ;
'IF' A=-1 'THEN' 'GOTO' TEN;
WRITETEXT ('('''('2C')'RUN')');
PRINT (A,2,0); NEWLINE (1);
WRITETEXT ('('''('2C')''('3S')'L.SQ'('9S')'INFT'('9S')'K[1]'
('9S')'K[2]'('9S')'K[3]'('9S')'K[4]'('2C')'')');
Ø:= READ; P:= READ;
'FOR' I:=1 'STEP' 1 'UNTIL' Ø 'DO' V[1]:= READ; N:=0;
TWO: B[N+1]:= READ;
'IF' B[N+1]=-1 'THEN' 'GOTO' THREE;
T[N+1]:= READ;
'IF' B[N+1]'LE' 0.05 'THEN' 'GOTO' TWO;
'IF' B[N+1]/V[1]'GE' 0.90 'THEN' 'GOTO' TWO; N:=N+1;
'GOTO' TWO;
THREE: H[1,1]:=0;
'FOR' R:=1 'STEP' 1 'UNTIL' 9 'DO' 'BEGIN'
'FOR' J:=1 'STEP' 1 'UNTIL' (Ø-P) 'DO' 'BEGIN' S[J]:=0;
'FOR' K:=1 'STEP' 1 'UNTIL' (Ø-P) 'DO' W[J,K]:=0;
'END';
'FOR' I:=(Ø+1) 'STEP' 1 'UNTIL' (2*Ø) 'DO' V[I]:=V[I+1-Ø];
SQ:=0;
'FOR' I:=1 'STEP' 1 'UNTIL' N 'DO' 'BEGIN'
'FOR' J:=2 'STEP' 1 'UNTIL' Ø 'DO' 'BEGIN'
'IF' V[J]*T[I] 'LE' 50 'THEN' 'GOTO' NINE;
F[J]:=0; 'GOTO' ELEVEN;
NINE: F[J]:=-EXP(-V[J]*T[I]);
'FOR' K:=(J+1) 'STEP' 1 'UNTIL' (J+Ø-2) 'DO'
F[J]:=F[J]*V[K]/(V[K]-V[J]);
ELEVEN: 'END';
G[1]:=1;
```

```
'FOR' J:=2 'STEP' 1 'UNTIL' Ø 'DO' 'BEGIN'
G[1]:=G[1]+F[J]; U[J,10]:=-T[I]; C[J,J,J]:=0;
'FOR' K:=(J+1) 'STEP' 1 'UNTIL' (J+Ø-2) 'DO' 'BEGIN'
X:=V[K]-V[J]; U[J,10]:=U[J,10]+1/X;
U[J,K]:=-V[J]*F[J]/(V[K]*X);
C[J,J,J]:=C[J,J,J]+F[J]/(X*X);
'END';
U[J,J]:=F[J]*U[J,10];
C[J,J,J]:=C[J,J,J]+U[J,J]*U[J,10];
'END';
'FOR' J:=2 'STEP' 1 'UNTIL' Ø 'DO' 'BEGIN'
'FOR' K:=(J+1) 'STEP' 1 'UNTIL' (J+Ø-2) 'DO' 'BEGIN'
X:=V[K]-V[J];
C[J,J,K]:=U[J,10]*U[J,K]-F[J]/(X*X);
C[J,K,J]:=C[J,J,K];
C[J,K,K]:=2*V[J]*F[J]/(V[K]*X*X);
'END';
'FOR' K:=2 'STEP' 1 'UNTIL' Ø 'DO' 'BEGIN'
'IF' K=J 'THEN' 'GOTO' FIVE;
'FOR' L:=2 'STEP' 1 'UNTIL' Ø 'DO' 'BEGIN'
'IF' L=J 'THEN' 'GOTO' FOUR; 'IF' L=K 'THEN' 'GOTO' FOUR;
C[J,K,L]:=V[J]*V[J]*F[J]/(V[K]*V[L]*(V[K]-V[J])*(V[L]-V[J]));
FOUR: 'END';
FIVE: 'END';
'END';
'FOR' J:=3 'STEP' 1 'UNTIL' Ø 'DO' 'BEGIN'
'FOR' K:=2 'STEP' 1 'UNTIL' (J-1) 'DO' 'BEGIN'
M:=K+Ø-1; C[J,K,K]:=C[J,M,M]; U[J,K]:=U[J,M];
C[J,J,K]:=C[J,J,M]; C[J,K,J]:=C[J,M,J];
'END';
'END';
'FOR' J:=2 'STEP' 1 'UNTIL' Ø 'DO' 'BEGIN'
G[J]:=0; H[J,J]:=0;
'FOR' K:=2 'STEP' 1 'UNTIL' Ø 'DO' 'BEGIN'
G[J]:=G[J]+U[K,J]*V[1]; H[J,K]:=0;
'FOR' L:=2 'STEP' 1 'UNTIL' Ø 'DO'
H[J,K]:=H[J,K]+C[L,J,K]*V[1];
'END';
'END';
'FOR' J:=2 'STEP' 1 'UNTIL' Ø 'DO' 'BEGIN'
```

```
H[1,J]:=G[J]/V[1]; H[J,1]:=H[1,J];
'END';
X:=V[1]*G[1]-B[I]; SQ:=SQ+X*X;
'FOR' J:=1 'STEP' 1 'UNTIL' (Ø-P) 'DO' 'BEGIN'
S[J]:=S[J]+X*G[J];
'FOR' K:=1 'STEP' 1 'UNTIL' (Ø-P) 'DO'
W[J,K]:=W[J,K]+X*H[J,K]+G[J]*G[K];
'END';
'END';
PRINT (SQ,0,4);
'FOR' I:=1 'STEP' 1 'UNTIL' (Ø-P-1) 'DO' 'BEGIN'
D:=Ø-P-I; E:=Ø-P-I+1;
'FOR' J:=1 'STEP' 1 'UNTIL' D 'DO' 'BEGIN'
S[J]:=S[J]*W[E,E]-S[E]*W[J,E];
'FOR' K:=1 'STEP' 1 'UNTIL' D 'DO'
W[J,K]:=W[J,K]*W[E,E]-W[J,E]*W[E,K];
'END';
'END';
S[1]:=S[1]/W[1,1]; V[1]:=V[1]-S[1]/2;
'FOR' I:=2 'STEP' 1 'UNTIL' (Ø-P) 'DO' 'BEGIN' X:=0;
'FOR' J:=1 'STEP' 1 'UNTIL' (I-1) 'DO'
X:=X+S[J]*W[I,J]; S[I]:=(S[I]-X)/W[I,I];
'IF' S[I]/2 'GE' V[I] 'THEN' 'GOTO' EIGHT;
V[I]:=V[I]-S[I]/2;
'END';
'FOR' I:=1 'STEP' 1 'UNTIL' Ø 'DO'
PRINT (V[I],0,4); NEWLINE (1);
'END';
SIX: NEWLINE (1);
WRITETEXT ('('''('2C')''('3S')'TIME'('9S')'DATA'('9S')'CALC'
('2C')'')');
'FOR' J:=(Ø+1) 'STEP' 1 'UNTIL' (2*Ø) 'DO' V[J]:=V[J+1-Ø];
'FOR' I:=1 'STEP' 1 'UNTIL' N 'DO' 'BEGIN' X:=V[1];
'FOR' J:=2 'STEP' 1 'UNTIL' Ø 'DO' 'BEGIN'
F[J]:=V[1]*(-EXP(-V[J]*T[I]));
'FOR' K:=(J+1) 'STEP' 1 'UNTIL' (J+Ø-2) 'DO' 'BEGIN'
F[J]:=F[J]*V[K]/(V[K]-V[J]);
'END'; X:=X+F[J];
'END'; Y:=ABS(X-B[I]);
PRINT (T[I],0,4); PRINT (B[I],0,4); PRINT (X,0,4);
```

```
'IF' Y 'LE' 0.010 'THEN' 'GOTO' SEVEN;
WRITETEXT ('('''('2S')'POOR')');
SEVEN: NEWLINE (1);
'END'; 'GOTO' ONE;
EIGHT: WRITETEXT ('('''('2S')'CUTOUT')');
'GOTO' SIX;
TEN: 'END';
```

Appendix 2.

Least squares computer program HYDR.

```
'BEGIN'
'REAL' L,M,Q,X,Y;
'INTEGER' A,I,J,K,N,R;
'REAL' 'ARRAY' V,D,E[1:2],B,T[1:50],F,C[1:2,1:2];
'SWITCH' S:=ONE,TWO,THREE,FOUR,FIVE,SIX,SEVEN;
ONE: A:=READ;
'IF' A=-1 'THEN' 'GOTO' SEVEN;
WRITETEXT ('('''('2C')'RUN')');
PRINT (A,2,0); NEWLINE (1);
WRITETEXT ('('''('2C')''('3S')'L.SQ'('9S')'K[1]'('9S')'B.INF'
('2C')'')');
V[1]:=READ; X:=READ; Y:=READ; N:=0;
TWO: L:=READ;
'IF' L=-1 'THEN' 'GOTO' THREE; B[N+1]:=X-L;
M:=READ; T[N+1]:=M-Y; N:=N+1;
'GOTO' TWO;
THREE: V[2]:=1.20*B[N];
C[2,2]:=0;
FOUR: 'FOR' R:=1 'STEP' 1 'UNTIL' 15 'DO' 'BEGIN'
'FOR' I:=1 'STEP' 1 'UNTIL' 2 'DO' 'BEGIN' E[I]:=0;
'FOR' J:=1 'STEP' 1 'UNTIL' 2 'DO' F[I,J]:=0;
'END'; Q:=0;
'FOR' I:=2 'STEP' 1 'UNTIL' N 'DO' 'BEGIN'
X:=EXP(-V[1]*T[I]); D[2]:=1-X;
C[1,2]:=X*T[I]; C[2,1]:=C[1,2];
D[1]:=V[2]*C[1,2]; C[1,1]:=-D[1]*T[I];
Y:=V[2]*D[2]-B[I]; Q:=Q+Y*Y;
'FOR' J:=1 'STEP' 1 'UNTIL' 2 'DO' 'BEGIN'
E[J]:=E[J]+Y*D[J];
'FOR' K:=1 'STEP' 1 'UNTIL' 2 'DO'
F[J,K]:=F[J,K]+Y*C[J,K]+D[J]*D[K];
'END';
'END';
Y:=(E[1]*F[2,2]-E[2]*F[1,2])/(F[1,1]*F[2,2]-F[1,2]*F[2,1]);
V[2]:=V[2]-(E[1]-F[1,1]*Y)/(2*F[1,2]); V[1]:=V[1]-Y/2;
'IF' V[1] 'LE' 0 'THEN' 'GOTO' FIVE;
PRINT (Q,0,4); PRINT (V[1],0,4); PRINT (V[2],0,4);
```

```
'END'; NEWLINE (1);
WRITETEXT ('('''('2C')''('3S')'TIME'('9S')'DATA'('9S')'CALC'
('2C')'')');
'FOR' I:=2 'STEP' 1 'UNTIL' N 'DO' 'BEGIN'
L:=V[2]*(1-EXP(-V[1]*T[I])); M:=ABS(L-B[I]);
PRINT (T[I],0,4); PRINT (B[I],0,4); PRINT (L,0,4);
'IF' M 'LE' 0.005 'THEN' 'GOTO' SIX;
WRITETEXT ('('''('2S')'POOR')'); 'GOTO' SIX;
FIVE: WRITETEXT ('('''('2C')''('3S')'FAILURE')'); 'GOTO' ONE;
SIX: NEWLINE (1);
'END'; 'GOTO' ONE;
SEVEN: 'END';
```

Appendix 3.

Least squares computer program HREL.

```
'BEGIN'
'REAL' C,D,G,H,L,M,Ø,P,Q,X,Y,GG;
'INTEGER'A,I,J,K,N;
'REAL' 'ARRAY' BB,B,E,T[1:99],S,V,W[1:4],U[1:9,1:9],F[1:4,1:99],
R[1:4,1:4,1:99];
'SWITCH' Z:=ONE,TWO,THREE,FOUR,FIVE,SIX,SEVEN;
ONE: A:=READ;
'IF' A=-1 'THEN' 'GOTO' SEVEN;
WRITETEXT ('('''('2C')'RUN')');
PRINT (A,2,0); A:=0; NEWLINE (1);
WRITETEXT ('('''('2C')''('3S')'L.SQ'('9S')'K 1 '('9S')'K 2 '
('9S')'FACTOR'('2C')'')');
'FOR' I:=1 'STEP' 1 'UNTIL' 3 'DO' V I :=READ;
Ø:=READ; GG:=READ; P:=READ; N:=0;
TWO: H:=READ;
'IF' H=-1 'THEN' 'GOTO' THREE;
BB[N+1]:=H;
L:=READ; M:=READ;
T[N+1]:=L+(M-P)/60; N:=N+1;
'GOTO' TWO;
THREE: A:=A+1; G:=V[2]-V[1]; P:=G*G*G; H:=1-V[3];
L:=V[1]*V[3]-V[2];
'FOR' I:=1 'STEP' 1 'UNTIL' N 'DO' 'BEGIN'
B[I]:=(BB[I]-GG*EXP(-V[1]*T[I]))/Ø;
C:=EXP(-V[1]*T[I]); D:=EXP(-V[2]*T[I]);
E[I]:=(1+(L*C+H*V[1]*D)/G);
F[1,I]:=(-C*V[2]*H+T[I]*C*G*L-D*V[2]*H)/(G*G);
F[2,I]:=V[1]*H*(C-D*(1+G*T[I]))/(G*G);
F[3,I]:=V[1]*(C-D)/G;
R[1,1,I]:=-(2*V[2]*H*(C-D)+T[I]*T[I]*C*G*G*L)/P;
R[1,2,I]:=H*((V[1]+V[2])*(C+D)+T[I]*G*(V[1]*C+V[2]*D))/P;
R[1,3,I]:=(C*V[2]+V[1]*T[I]*C*G+V[2]*D)/(G*G);
R[2,1,I]:=H*((V[1]+V[2])*(C-D)-T[I]*G*(V[1]*C+V[2]*D))/P;
R[2,2,I]:=H*V[1]*(2*(D-C)+D*T[I]*G*(T[I]*G+2))/P;
R[2,3,I]:=-V[1]*(C-D*(1+T[I]*G))/(G*G);
R[3,1,I]:=(-G*V[1]*T[I]*C+V[2]*(C-D))/(G*G);
R[3,2,I]:=(-G*V[1]*T[I]*D-V[1]*(C-D))/(G*G);
```

```
R[3,3,I]:=0;
'END';
'FOR' J:=1 'STEP' 1 'UNTIL' 3 'DO' 'BEGIN' S J :=0;
'FOR' K:=1 'STEP' 1 'UNTIL' 3 'DO' U J,K :=0;
'END'; Q:=0;
'FOR' I:=1 'STEP' 1 'UNTIL' N 'DO' 'BEGIN'
G:=E[I]-B[I]; Q:=Q+G*G;
'FOR' J:=1 'STEP' 1 'UNTIL' 3 'DO' 'BEGIN'
S[J]:=S[J]+G*F[J,I];
'FOR' K:=1 'STEP' 1 'UNTIL' 3 'DO'
U[J,K]:=U[J,K]+G*R[J,K,I]+F[J,I]*F[K,I];
'END';
'END'; PRINT (Q,0,4);
'FOR' J:=1 'STEP' 1 'UNTIL' 3 'DO' 'BEGIN'
'IF' U[J,3]=0 'THEN' 'GOTO' FIVE;
S[J]:=S[J]/U[J,3];
'FOR' K:=1 'STEP' 1 'UNTIL' 3 'DO'
U[J,K]:=U[J,K]/U[J,3];
'END';
Q:=S[1]-S[2]; G:=U[1,2]-U[3,2];
H:=U[1,2]-U[2,2]; P:=U[2,2]-U[2,1];
'IF' H=0 'THEN' 'GOTO' FIVE;
L:=P*G-(U[1,1]-U[3,1])*H;
'IF' L=0 'THEN' 'GOTO' FIVE;
W[1]:=(Q*G-(S[1]-S[3])*H)/L;
W[2]:=(Q-W[1]*P)/H;
W[3]:=S[1]-U[1,1]*W[1]-U[1,2]*W[2];
'FOR' I:=1 'STEP' 1 'UNTIL' 3 'DO' 'BEGIN'
V[I]:=V[I]-0.2*W[I]; PRINT (V[I],0,4);
'IF' V[I]'LE' 0 'THEN' 'GOTO' SIX;
'END'; NEWLINE (1);
'IF' V[3]'GE' 1 'THEN' 'GOTO' SIX;
'IF' A 'LE' 9 'THEN' 'GOTO' THREE; NEWLINE (1);
WRITETEXT ('('''('2C')''('3S')'TIME'('9S')'DATA'('9S')'CALC'
('2C')''')');
'FOR' I:=1 'STEP' 1 'UNTIL' N 'DO' 'BEGIN'
X:=Ø*(1+1/(V[2]-V[1])*((V[3]*V[1]-V[2])*EXP(-V[1]*T[I])+
(1-V[3])*V[1]*EXP(-V[2]*T[I])));
B[I]:=B[I]*Ø; Y:=ABS(X-B[I]);
PRINT (T[I],0,4); PRINT (B[I],0,4); PRINT (X,0,4);
```

```
'IF' Y 'LE' 0.080 'THEN' 'GOTO' FOUR;
WRITETEXT ('('''('2S')'POOR')');
FOUR: NEWLINE (1);
'END'; 'GOTO' ONE;
FIVE: WRITETEXT ('('''('2C')'CUTOUT'('2C')''')');
'GOTO' ONE;
SIX: WRITETEXT ('('''('2C')'WILD'('2C')''')');
'GOTO' ONE;
SEVEN: 'END';
```

Appendix 4.

The difficulty in distinguishing the two psuedo-first order rate constants, governing the formation of product in a consecutive reaction, as they approach the same value.

Consider the consecutive process

$$A \xrightarrow{k_1} B \xrightarrow{k_2} C$$

If $k_1 \neq k_2$, we have that

$$c = c_\infty \left(1 - \frac{k_2}{(k_2-k_1)} e^{-k_1 t} + \frac{k_1}{(k_2-k_1)} e^{-k_2 t}\right) \qquad 1$$

where $c = [C]$ at time t, and $c_\infty = [C]$ at infinite time.

Let

$k_1 = k-x$, and $k_2 = k+x$.

Thus, from 1, it follows that

$$c = c_\infty \left(1 - \frac{e^{kt}}{2x} \left((k+x)e^{xt} - (k-x)e^{-xt}\right)\right) \qquad 2$$

If $xt \ll 1$, then to a good approximation equation 2 may be expanded merely to the second power in x and t.

Rearrangement then yields the relation

$$c = c_\infty \left(1 - e^{-kt}(1 + kt + (x^2t^2)/2\right) \qquad 3$$

Now, if $k_1 = k_2 = k$, we have that

$$c = c_\infty \left(1 - e^{-kt}(1 + kt)\right) \qquad 4$$

Equations 3 and 4 are indistinguishable if

$$1 >> (x^2t^2)/2 \qquad 5$$

An upper limit to the criterion 5 may be obtained, in terms of the relationship between k and x, by considering a reaction followed to 90% completion, whence

$$kt \sim 2.3$$

Thus, equations 3 and 4 are indistinguishable, even at the last observed point, if

$$k >> 1.5x \qquad 6$$

More realistically, over a range of study for which there is sufficient experimental data to define the curve, the criterion 6 might be considered to become

$$k > 3x$$

Therefore, equations 3 and 4 approach indistinguishability once the ratio of k_1 and k_2 is within the range

$$1.33 \geq k_1/k_2 \geq 0.75 \qquad 7$$

The precise range in which the criterion 7 falls will clearly depend upon the extent to which the experimental data deviates from perfection.

Appendix 5.

The approximate formula used in the calculation of the standard deviation of the slope of a linear plot.

Consider an experimental plot for which the calculated slope is $\bar{x}$. The standard deviation of $\bar{x}$ is given by the approximate equation

$$S.D. = \frac{5\sum|\bar{x} - x_i|}{4n\sqrt{n}}$$

where x_i refers to the ith calculated slope for n sets of equidistant points.

Appendix 6.

Curve inversion.

Consider the experimental curve (figure 1), depicting the disappearance of the tetrachloroplatinite(II) ion.

Figure 1

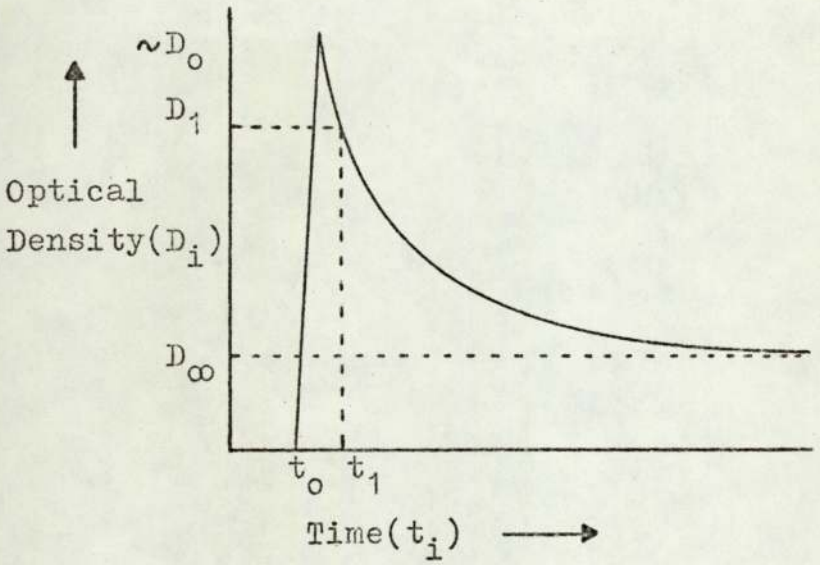

If the curve is defined by the infinite set of points, D_i at t_i, where i = 0 to ∞, then the disappearance of the tetrachloroplatinite(II) ion is governed by the equation

$$\frac{(D_i - D_\infty)}{(D_o - D_\infty)} = e^{-k_{obs} t_i} \qquad 8$$

Inherent in the experimental technique, there is a short delay in the formation of a homogeneous solution, which, in addition to the finite pen response time, causes an uncertainty in the absolute value of D_o. Consequently, the equation 8 cannot be used to obtain an accurate value of k_{obs}.

If a new curve (figure 2) is defined by the infinite set of points, D_i' at t_i', where i = 0 to ∞, such that

$$D_i' = D_1 - D_{(i+1)}$$

and $$t_i' = t_{(i+1)} - t_1$$

then k_{obs} may be obtained from the equation

$$D_i' = D_\infty' (1 - e^{-k_{obs} t_i'}) \qquad 9$$

Figure 2.

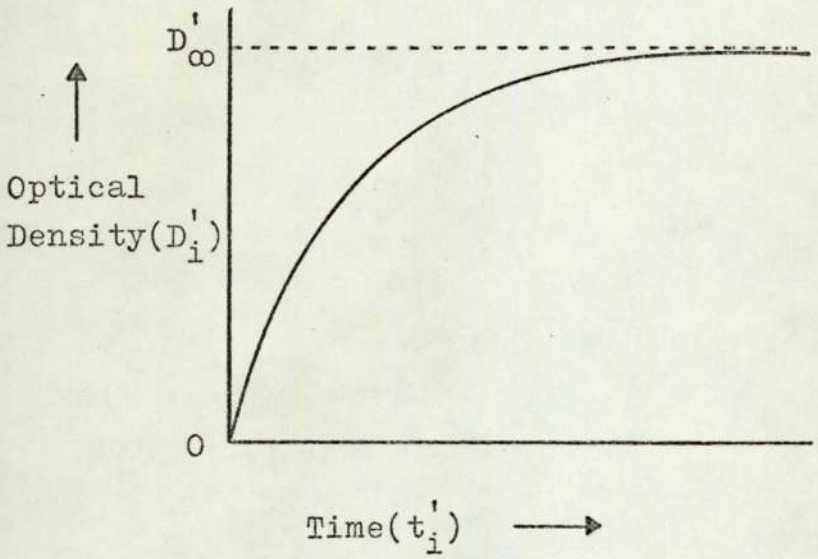

The experimental data, obtained from the curve of figure 1, was modified in this fashion by the "read" instructions of the computer program HYDR (appendix 2). The new data, thus obtained and defining the curve of figure 2, was fitted to equation 9, according to the least squares procedure of HYDR.

Appendix 7.

The initial correction introduced into the experimental data obtained from the release of acid, in aqueous systems of the tetrachloroplatinite(II) ion and acetonitrile.

Typically, it was observed that an extrapolation of the early points of an acid release curve, to zero time, did not proceed smoothly through the origin, but cut the burette reading axis at some positive value. Consequently, the computed fits, for equation 5.17. (chapter 5), were poor over the early portion of the experimental curves.

The small, extra quantity of acid released, in the early stages of reaction, may be considered to arise from the species trichlorohydroxyplatinum(II), during the rapid establishment of the initial equilibrium scheme 10.

$$\begin{array}{l} \qquad\qquad\quad PtCl_3(OH)^{2-} + H^+ \\ \qquad\qquad\quad \downharpoonleft\upharpoonright \\ PtCl_4^{2-} \xrightarrow{k_s} PtCl_3(H_2O)^- \\ \qquad\quad \searrow^{k_L} \quad \downharpoonleft\upharpoonright \\ \qquad\qquad\quad PtCl_3(CH_3CN)^- \end{array} \qquad 10$$

At the acetonitrile concentrations of this study the concentration of trichlorohydroxyplatinum(II) is low, and only a small quantity of acid is produced from the scheme 10. Clearly, however, this quantity will increase with increasing pH and decreasing acetonitrile concentration.

To account for the initial contribution, over the entire curve, a function $\left[OH^-\right]_o.e^{-k_a t}$ was subtracted from each observed point, by the computer program HREL (appendix 3). Here, the observed psuedo-first order rate constant k_a governs the disappearance of the equilibrium species of the

scheme 10.

The quantity $\left[OH^-\right]_o$ was estimated graphically, from those experimental curves obtained at high pH and low acetonitrile concentration, by extrapolation to zero time. These values were then used to calculate $\left[OH^-\right]_o$ over all experimental conditions.

In practice, it was found that this correction procedure was only really necessary above pH 7 and below acetonitrile concentrations of 0.1M.

Bibliography.

1. C.C.Price, Chem.Rev., 1941,29,37.
2. J.Halpern, Pure Appl.Chem., 1969,20,59.
3. E.W.Stern, Cat.Rev., 1967,1,73.
4. J.Halpern, Chem.Eng.News, 1966(Oct.31st.),44,68.
5. P.M.Henry, Adv.Chem.Ser., 1968,70,126.
6. R.G.Schultz, D.E.Gross, Adv.Chem.Ser., 1968,70,97.
7. N.Rosch, R.P.Messmer, K.H.Johnson, J.Amer.Chem.Soc., 1974, 96,3855.
8. Chem.Soc., Spec.Per.Rep., Inorganic Reaction Mechanisms, Vol.1, p.265-310.
9. J.P.Collman, W.R.Roper, Adv.Organomet.Chem., 1968,7,84-90.
10. F.Basolo, R.G.Pearson, Mechanisms of Inorganic Reactions, 2nd.Ed., Wiley, New York, p.31-33.
11. M.M.Jones, Ligand Reactivity and Catalysis, Academic Press, 1968, New York, p.77.
12. N.Ando, K.I.Maruya, T.Mizoroki, A.Ozaki, J.Cat., 1971,20, 299.
13. J.F.Harrod, S.Ciccone, J.Halpern, Can.J.Chem., 1961,39, 1372.
14. J.P.Collman, W.R.Roper, Adv.Organomet.Chem., 1968,7,67-81.
15. J.Halpern, J.F.Harrod, B.R.James, J.Amer.Chem.Soc., 1966, 88,5150.
16. J.A.Osborn, F.H.Jardine, J.F.Young, G.Wilkinson, J.Chem. Soc.A, 1966,1711.
17. I.Jardine, F.J.McQuillin, Chem.Commun., 1969,477.
18. J.P.Collman, W.R.Roper, Adv.Organomet.Chem., 1968,7,54-90.
19. J.Tsuji, K.Ohno, J.Amer.Chem.Soc., 1968,90,99.
20. Chem.Soc., Spec.Per.Rep., Inorganic Reaction Mechanisms, Vol.1, p.30-89.

21. W.Brackman, P.J.Smit, Rec.Trav.Chim., 1963,82,757.

22. W.Brackman, Discuss.Faraday Soc., 1968,46,122.

23. K.B.Harvey, G.B.Porter, Introduction to Physical Inorganic Chemistry, Addison Wesley, 1965, Reading U.S.A., p.362.

24. S.Fallab, Angew.Chem.Internat.Ed., 1967,6,496.

25. Chem.Soc., Spec.Per.Rep., Inorganic Reaction Mechanisms, Vol.1, p.90-103.

26. M.M.Jones, Ligand Reactivity and Catalysis, Academic Press, 1968, New York, p.105.

27. D.Benson, Mechanisms of Inorganic Reactions in Solution, McGraw Hill, 1968, Maidenhead, p.200.

28. H.J.H.Fenton, H.O.Jones, J.Chem.Soc., 1900,77,69.

29. J.C.Taft, M.M.Jones, J.Amer.Chem.Soc., 1960,82,4196.

30. M.M.Jones, Adv.Chem.Ser., 1963,37,116.

31. F.Basolo, R.G.Pearson, Mechanisms of Inorganic Reactions, 2nd.Ed., Wiley, New York, p.608-609.

32. Ibid, p.650-654.

33. A.Chakravorty, Coord.Chem.Rev., 1974,13,11.

34. Chem.Soc., Spec.Per.Rep., Inorganic Reaction Mechanisms, Vol.1, p.240-262.

35. M.M.Jones, Ligand Reactivity and Catalysis, Academic Press, 1968, New York, p.55-61.

36. W.H.Rinkerbach, Ind.Eng.Chem., 1927,19,474.

37. User Manual SP 1700/1800, Pye Unicam Ltd., Cambridge, Pub.No. 299406.

38. D.E.Pearson, J.D.Bruton, J.Org.Chem., 1954,19,957.

39. A.I.Vogel, Practical Organic Chemistry, 2nd.Ed., Longmans Green, 1951, London, p.683.

40. Dictionary of Organic Compounds, Eyre Spottiswoode, 1965, London, a. p.247, b. p.2431, c. p.322.

41. F.Krohnke, H.Leister, Chem.Ber., 1958,91,1295.

42. R.A.Olofson, D.M.Zimmerman, J.Amer.Chem.Soc., 1967,89,5057.

43. W.J.Hickinbottom, Reactions of Organic Compounds, 2nd.Ed., Longmans Green, 1948, London, p.284.

44. G.D.Lander, J.Chem.Soc., 1900,77,736.

45. W.Hieber, F.Leutart, Chem.Ber., 1927,60,2296.

46. Ibid, 1929,62,1839.

47. L.M.Venanzi, J.Chem.Soc., 1958,1,719.

48. B.E.Dawson, Practical Inorganic Chemistry, Methuen, 1963, London, p.172.

49. Handbook of Chemistry and Physics, 48th.Ed., Chemical Rubber Co., 1967, Section B, p.200.

50. P.J.McCarthy, R.J.Hovey, K.Ueno, A.E.Martell, J.Amer.Chem. Soc., 1955,77,5820.

51. L.Malatesta, C.Cariello, J.Chem.Soc., 1958,2,2323.

52. V.A.Golovnaya, Ni Tszya-Tszyan, Russ.J.Inorg.Chem., 1960, 5,716.

53. D.B.Brown, R.D.Burbank, M.B.Robin, J.Amer.Chem.Soc., 1969, 91,2895.

54. R.D.Gillard, G.Wilkinson, J.Chem.Soc., 1964,3,2835.

55. P.Sykes, A Guidebook to Mechanism in Organic Chemistry, 2nd.Ed., Longmans Green, 1967, London, p.95-98.

56. Organic Reactions, Vol.11, Wiley, 1960, New York, p.1-156.

57. Ibid, p.43.

58. W.J.Comstock, Amer.Chem.J., 1897,19,485.

59. S.Yamaguchi, Mem.Coll.Sci.Kyoto Imp.Univ., 1925,9A,33. (Chem.Abs., 1925,19,3261.)

60. S.Yamaguchi, Bull.Chem.Soc.Japan, 1926,1,35. (Chem.Abs., 1927,21,75.)

61. R.Paul, Compt.Rend., 1937,204,363.

62. R.Paul, Bull.Soc.Chim.France, 1937,4,1115.

63. R.Paul, P.Buisson, N.Joseph, Ind.Eng.Chem., 1952,44,1006.

64. A.G.Caldwell, E.R.H.Jones, J.Chem.Soc., 1946,1,599.

65. L.Field, P.B.Hughmark, S.H.Shumaker, W.S.Marshall, J.Amer. Chem.Soc., 1961,83,1983.

66. M.E.Stone, K.E.Johnson, Can.J.Chem., 1973,51,1260.

67. A.Bryson, F.P.Dwyer, J.Proc.Roy.Soc.N.S.W., 1940,74,471.

68. Ibid, p.107.

69. A.Chakravorty, Coord.Chem.Rev., 1974,13,4.

70. D.S.Hoffenberg, C.R.Hauser, J.Org.Chem., 1955,20,1496.

71. E.C.Horning, V.L.Stromberg, J.Amer.Chem.Soc., 1952,74,5151.

72. H.R.Snyder, C.T.Elston, J.Amer.Chem.Soc., 1954,76,3039.

73. J.R.Dyer, Applications of Absorption Spectroscopy of Organic Compounds, Prentice Hall, 1965, New Jersey, p.33-38.

74. K.J.Laidler, Chemical Kinetics, 2nd.Ed., McGraw Hill, 1965, New York, p.323-324.

75. Organic Reactions, Vol.14, Wiley, 1965, New York, p.1-51.

76. Ibid, p.31.

77. I.L.Finar, Organic Chemistry, 6th.Ed., Longmans, 1973, Vol.1, p.349-352.

78. S.M.McElvain, B.E.Tate, J.Amer.Chem.Soc., 1951,73,2233.

79. S.A.Miller, Ethylene and its Industrial Derivatives, Benn, 1969, London, p.605.

80. Semi-Micro Qualitative Inorganic Analysis, 1st.Ed., Stanford Mann, 1963, Birmingham, p.73.

81. A.I.Vogel, Practical Organic Chemistry, 2nd.Ed., Longmans Green, 1951, London, p.924.

82. D.Sutton, Electronic Spectra of Transition Metal Complexes, McGraw Hill, 1968, London, p.15-16.

83. B.R.Panchal, Private Communication.

84. P.Goodwin, Private Communication.

85. S.J.Ashcroft, C.T.Mortimer, Thermochemistry of Transition Metal Complexes, Academic Press, 1970, London, p.227.

86. Ibid, p.90.

87. R.Breslow, R.Fairweather, J.Keana, J.Amer.Chem.Soc., 1967,89,2135.

88. W.R.McWhinnie, J.D.Miller, Adv.Inorg.Radiochem., 1969, 12,135.

89. K.J.Laidler, Chemical Kinetics, 2nd.Ed., McGraw Hill, 1965, New York, p.501 and 506.

90. K.A.Hoffmann, G.Bugge, Chem.Ber., 1907,40,1772.

91. V.V.Lebedinski, V.A.Golovnaya, Izvest.Sekt.Platiny., 1948,21,32. (Chem.Abs., 1950,44,10566.)

92. Y.Y.Kharitonov, Ni Chia-Chiang, A.V.Babaeva, Russ.J.Inorg. Chem., 1962,7,9.

93. L.Cattalini, M.T.P.Internat.Rev.Sci., Reaction Mechanisms in Inorganic Chemistry, Series 1, Vol.9, p.269-302.

94. L.F.Grantham, T.S.Ellemann, D.S.Martin, J.Amer.Chem.Soc., 1955,77,2965.

95. A.A.Grinberg, Y.N.Kukushkin, Zhur.Neorg.Khim., 1957,2,2360.

96. D.Banerjea, F.Basolo, R.G.Pearson, J.Amer.Chem.Soc., 1957,79,4055.

97. L.I.Elding, I.Leden, Acta.Chem.Scand., 1966,20,706.

98. L.Drougge, L.I.Elding, L.Gustafson, Acta.Chem.Scand., 1967,21,1647.

99. D.Benson, Mechanisms of Inorganic Reactions in Solution, McGraw Hill, 1968, Maidenhead, p.60-83.

100. F.Basolo, R.G.Pearson, Mechanisms of Inorganic Reactions, 2nd.Ed., Wiley, New York, p.404-405.

101. W.M.Latimer, W.L.Jolly, J.Amer.Chem.Soc., 1953,75,1548.

102. K.A.Hoffmann, G.Bugge, Chem.Ber., 1908,41,312.

103. S.Komiya, S.Suzuki, K.Watanabe, Bull.Chem.Soc.Japan, 1971,44,1440.

104. D.Pinnel, G.B.Wright, R.B.Jordan, J.Amer.Chem.Soc., 1972,94,6104.

105. D.A.Buckingham, F.R.Keene, A.M.Sargeson, J.Amer.Chem.Soc., 1973,95,5649.

106. D.A.Buckingham, A.M.Sargeson, A.Zanella, J.Amer.Chem.Soc., 1972,94,8246.

107. M.A.Bennet, T.Yoshida, J.Amer.Chem.Soc., 1973,95,3030.

108. P.F.B.Barnard, J.Chem.Soc.A., 1969,2140.

109. L.A.Chugaev, V.K.Lebedinski, Compt.Rend., 1915,161,563.

110. V.V.Lebedinski, V.A.Golovnaya, Izvest.Sekt.Platiny., 1939,16,57. (Chem.Abs., 1940,34,4685.)

111. V.A.Golovnaya, Ni Chia-Chiang, Russ.J.Inorg.Chem., 1961,6,64.

112. N.C.Stephenson, J.Inorg.Nucl.Chem., 1962,24,801.

113. F.A.Cotton, G.Wilkinson, Advanced Inorganic Chemistry, 2nd.Ed., Interscience, 1966, New York, p.1025.

114. S.Komiya, S.Suzuki, K.Watanabe, Bull.Chem.Soc.Japan, 1971,44,1441.

115. P.I.Chamberlain, Diss.Abstr., 1968,29B,521.

116. Ion Exchange Resins, 5th.Ed., B.D.H.Brochure, p.8.

117. H.T.S.Britton, Hydrogen Ions, 4th.Ed., Chapman Hall, 1955, London, Vol.1, p.352-376.

118. K.Nakamoto, Infrared Spectra of Inorganic and Coordination Compounds, 2nd.Ed., Interscience, 1969, New York, p.123.

119. J.R.Dyer, Applications of Absorption Spectroscopy of Organic Compounds, Prentice Hall, 1965, New Jersey, p.84-85.

120. F.Basolo, R.G.Pearson, Mechanisms of Inorganic Reactions, 2nd.Ed., Wiley, New York, p.183-187.

121. Ibid, p.237-238.

122. Ibid, p.170-177.

123. S.Bloch, F.Raulin, G.Toupance, R.Buvet, Compt.Rend., 1973,276,915.

124. M.F.Farona, N.J.Bremer, J.Amer.Chem.Soc., 1966,88,3735.

125. H.C.Clark, L.E.Mauzer, Chem.Commun., 1971,387.

126. W.J.Bland, R.D.W.Kemmit, I.W.Nowell, D.R.Russel, Chem. Commun., 1968,1065.

127. Organic Reactions, Vol.11, Wiley, 1960, New York, p.49-51.

128. P.Sykes, A Guidebook to Mechanism in Organic Chemistry, 2nd.Ed., Longmans Green, 1967, London, p.93-95.